UNIVERSITAT DE BARCELONA

# A Novel role for glycogenin in the regulation of glycogen metabolism

Giorgia Testoni

# A NOVEL ROLE FOR GLYCOGENIN IN THE REGULATION OF GLYCOGEN METABOLISM

Memoria presentada por

GIORGIA TESTONI

Para optar al grado de

**Doctora por la Universidad de Barcelona**

Tesis realizada en el
Institut de Recerca Biomèdica (IRB Barcelona),
Laboratorio de Ingeniería metabólica y terapia de la diabetes
Tesis adscrita al programa de doctorado en Biomedicina

Universidad de Barcelona

El Director de la tesis — La autora

Joan J. Guinovart Cirera — Giorgia Testoni

Noviembre, 2015

# A NOVEL ROLE FOR GLYCOGENIN IN THE REGULATION OF GLYCOGEN METABOLISM

GIORGIA TESTONI

Fulfillment of the requirements for the degree of

**Doctor of Philosophy (Ph.D.)**

At Institute for Research in Biomedicine (IRB Barcelona),
Metabolic Engineering and Diabetes Laboratory
Doctoral program in Biomedicine

University of Barcelona

Thesis director

Joan J. Guinovart Cirera

Author

Giorgia Testoni

November 2015

# Table of Contents

# Abbreviations

| | |
|---|---|
| $^{14}C$ | Carbon-14 or radiocarbon |
| ACN | Acetonitrile |
| ADP | Adenosine diphosphate |
| AGL | Glycogen debranching enzyme (GDE) |
| AMP | Adenosine monophosphate |
| Ant. A. | Antimycin A |
| ATP | Adenosine triphosphate |
| bp | base pair |
| CAs | Corpora Amylacea |
| CK | Creatine Kinase |
| Cre | Cre recombinase |
| Cyt C. | Cytochrome c |
| Del | Deleted /Excised allele |
| dpc | days post coitum |
| EDL | extensor digitorum longus muscle |
| EM | electron microscopy |
| En2A | splice acceptor site |
| FA | formic acid |
| $FADH_2$ | flavin adenine dinucleotide hydroquinone form |
| FASP | Filter Aided Sample Preparation |
| FBS | fetal bovine serum |
| FCCP | protonophore carbonylcyanide-4-(trifluoromethoxy)-phenylhydrazone |
| FRT | Flippase recognition target for site-directed recombination |
| G-6P | glucose-6-phosphate |
| GAPDH | Glyceraldehyde 3-phosphate dehydrogenase |
| GBE | Glycogen branching enzyme |
| GM | glutamate + malate |
| GMD | glutamate+ malate+ ADP |
| GMDS | glutamate+ malate + ADP + succinate |
| GN | glycogenin protein |
| GN2 | glycogenin protein - liver isoform |
| GPa | Glycogen Phosphorylase- active state |
| GPB | Glycogen Phosphorylase-muscle isoform |
| GPb | Glycogen Phosphorylase- inactive de-phosphorylate state |
| GPL/GP2 | Glycogen Phosphorylase-liver isoform |
| GPM | Glycogen Phosphorylase-brain isoform |
| GS | Glycogen Synthase |
| GSDs | Glycogen Storage Diseases |
| GT | glycosyl-transferase |
| GTT | insulin tolerance test |
| Gyg | gene of glycogenin in mus musculus |

| | |
|---|---|
| Gyg Del | gene of glycogenin- excised |
| GYG1 /GYG2 | genes of glycogenin in homo sapiens |
| Gys1 | gene of muscle glycogen synthesis in mus musculus |
| Gys2 | gene of liver glycogen synthesis in mus musculus |
| hbcaP | autonomous promoter |
| HPLC | High performance liquid chromatography |
| IRES | internal ribosome entry site |
| ITT | glucose tolerance tetst |
| Kin | Knock in |
| KO | Knockout |
| lacZ | gene enconding β-galactosidase |
| LBs | Lafora's bodies |
| LC-MS/MS | Liquid chromatography-tandem mass spectrometry |
| LD | Lafora Disease |
| LGS | Liver glycogen synthase |
| loxP | sequence recognized by Cre recombinase |
| MGS | muscle glycogen synthase |
| MHC | Myosin heavy chain |
| MLC1 | Myosin light chain1 |
| MS | mass spectrometry |
| mtDNA | mitochondrial DNA |
| NAD | Nicotinamide adenine dinucleotide |
| NADH | Nicotinamide adenine dinucleotide |
| NADP | Nicotinamide adenine dinucleotide phosphate |
| neo | neomycin resistance |
| OXPHOS | Oxidative phosphorylation |
| pA | polyA tail |
| PAS | Periodic acid–Schiff stain |
| PAS-D | Succinate dehydrogenase |
| PCR | polymerase chain reaction |
| PCr | Phosphocreatine |
| PFA | paraformaldehyde |
| PGB | Polyglucosan Bodies |
| PGC-1 | peroxisome-proliferator-activated receptor-gamma co-activator-1 |
| Pygl | gene of liver glycogen phosphorylase in mus musculus |
| Pygm | gene of muscle glycogen phosphorylase in mus musculus |
| QC | quadriceps-muscle |
| RER | respiratory exchange ratio |
| Rot | rotenone |
| rpm | rotation per minute |
| s.e.m. | standard error of the mean |
| SDH | succinate dehydrogenase |
| SEC | size exclusion chromatography |
| Sol | Soleus muscle |
| STBD1 | Starch-binding domain-containing protein 1 |

| | |
|---|---|
| TCA cycle | tricarboxylic acid or Krebs cycle |
| Tib | Tibialis - muscle |
| U | enzymatic unit |
| Ub | Ubiquitin |
| UDP | Uridine diphosphate |
| V | volume |
| WB | western blot |
| WT | Wild type |

# Introduction

## Glycogen

Glycogen is a branched polysaccharide that serves as a glucose store. The majority of glycogen is stored in the liver, and to a lesser extent in the skeletal muscle. The heart, brain and adipose tissue have also been described to accumulate small amounts of glycogen (Roach 2002). Polymerization of the glucose chains occurs by the formation of α-1,4-glycosidic linkages between the residues, creating a linear polymer. In addition, periodic insertions of α-1,6-glycosidic linkages generate branching points on the molecule creating a spherical structure with protruding branches. The main difference between glycogen and glucose storage in plants lies in the branching levels of the polysaccharides. The frequency of branch points in glycogen is every ~8 to 12 glucose residues. Starch, on the other hand, is a mixture of amylopectin with branching points every 30 residues, and amylose, a linear chain. Branching degree determines the topology, structure and solubility of the polysaccharide, and more branching points allow for faster degradation due to the increased number of out chains. Glycogen does not have defined weight and size due to the fact that the chain can elongate until steric impediment (Melendez, Melendez-Hevia, and Canela 1999). The biggest particle has a a MW ~$10^6$-$10^7$ Da, a diameter of ~20 nm and contains about 55000 glucose residues (Gunja-Smith et al. 1970). This is known as β particle. In liver, granules with a diameter between 40 and 300nm and a MW over $10^8$ are generated by the aggregation of β particles into the so-called α particles (Sullivan et al. 2011; Drochmans 1962). Many proteins interact with glycogen and favor interaction between particles.

Another characteristic of glycogen is its level of phosphorylation. Since the 1980's, there are evidences of phosphate, of uncertain origin and function, which is covalently linked to glycogen (Fontana 1980; Alonso et al. 1994; Lomako et al. 1993). For example, muscle glycogen contains one phosphate per 600-1500 glucose residues, depending on the species (Tagliabracci et al.

2007; Tagliabracci et al. 2008)). Covalently bound phosphate has been proposed to be a catalytic error during glycogen synthesis, and recent studies show that a specific phosphatase (Laforin) acts to remove it (Tagliabracci et al. 2011). Indeed, higher phosphate levels have been associated to both lower polymer solubility and increased glycogen levels, as is the case in the onset of specific pathologies such as Lafora Disease.

## Glycogen metabolism

In addition to the polyglucosan chain, the glycogen granule contains many proteins, many of which take part in the glycogen metabolism, including glycogen synthase (GS), glycogen phosphorylase (GP) and debranching enzyme (AGL or DBE).

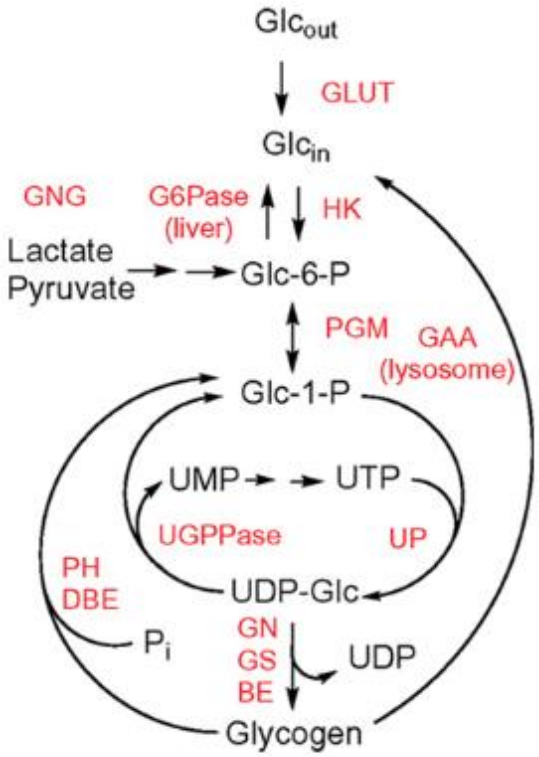


**Figure 1. Overview of glycogen metabolism-** Glcout, extracellular glucose; Glcin, intracellular glucose; HK, hexokinase; G6Pase, glucose- 6-phosphatase; PGM, phosphoglucomutase; UP, UDP-glucose pyrophosphorylase; UGPPase, UDP-glucose pyrophosphatase; GN, glycogenin; GS, glycogen synthase; BE, branching enzyme; PH, glycogen phosphorylase; DBE, debranching enzyme; GAA, lysosomal α-glucosidase; GNG, gluconeogenesis (Font. Roach, 2012)

The general routes of glycogenesis and glycogenolysis are identical in all tissues, but the enzymes and their regulation are adapted to the specific requirements of each tissue. Glucose enters the cell by glucose transporters, which permits the passage of glucose across the cell membrane **(Figure 1).** These transporters vary according to the tissue and differ in their affinity for glucose (Arbuckle et al. 1994; Bell et al. 1993; Gould and Holman 1993). Once inside, glucose is phosphorylated by tissue specific hexokinases, and is converted into glucose 6-phosphate (G-6P) (Katzen, Soderman, and Nitowsky 1965).

If the G-6P is destined for glycogen synthesis, it is isomerized to glucose 1-phosphate (G-1P) by the action of phosphoglucomutase. The direct conversion of G-1P to glycogen and phosphate is thermodynamically unfavorable, consequently an additional step is required. UDP glucose pyrophosphorylase catalyzes the reaction between G-1P and UTP in order to produce UDP glucose and PP1, then converted to 2 inorganic phosphate (Pi) by pyrophosphatase. UDP glucose is the donor of all glycosyl residues that are added to the growing glycogen molecule. It is generally accepted that glycogenin initiates glycogen synthesis by transferring glucose from UDP glucose to a specific tyrosine residue (Tyr 195) on its side chain. It catalyzes its own glycosylation in order to form an oligomer of 8 to 10 glucose residues that serves as a primer for elongating the polymer. Chain elongation ensues by the formation of α-1,4-glycosidic bonds between the C-1 of the glycosyl group of a new UDPglucose and the C-4 glycosyl of the acceptor residue in the growing glycogen chain **(Figure 2).** Glycogen synthase (GS), which interacts with glycogenin (GN), catalyzes this reaction in acceptor chains. Branches are introduced by the action of the branching enzyme (GBE), a α-1,4-glycosyltransferase, which transfers 4 to 7 glycosidic units from the non-reducing end of the chain to a hydroxyl group on the C-6 of glucose residue within the polymer. The enzymes involved in the glycogen breakdown differ from those of its synthesis, which provides greater control over total glycogen levels.

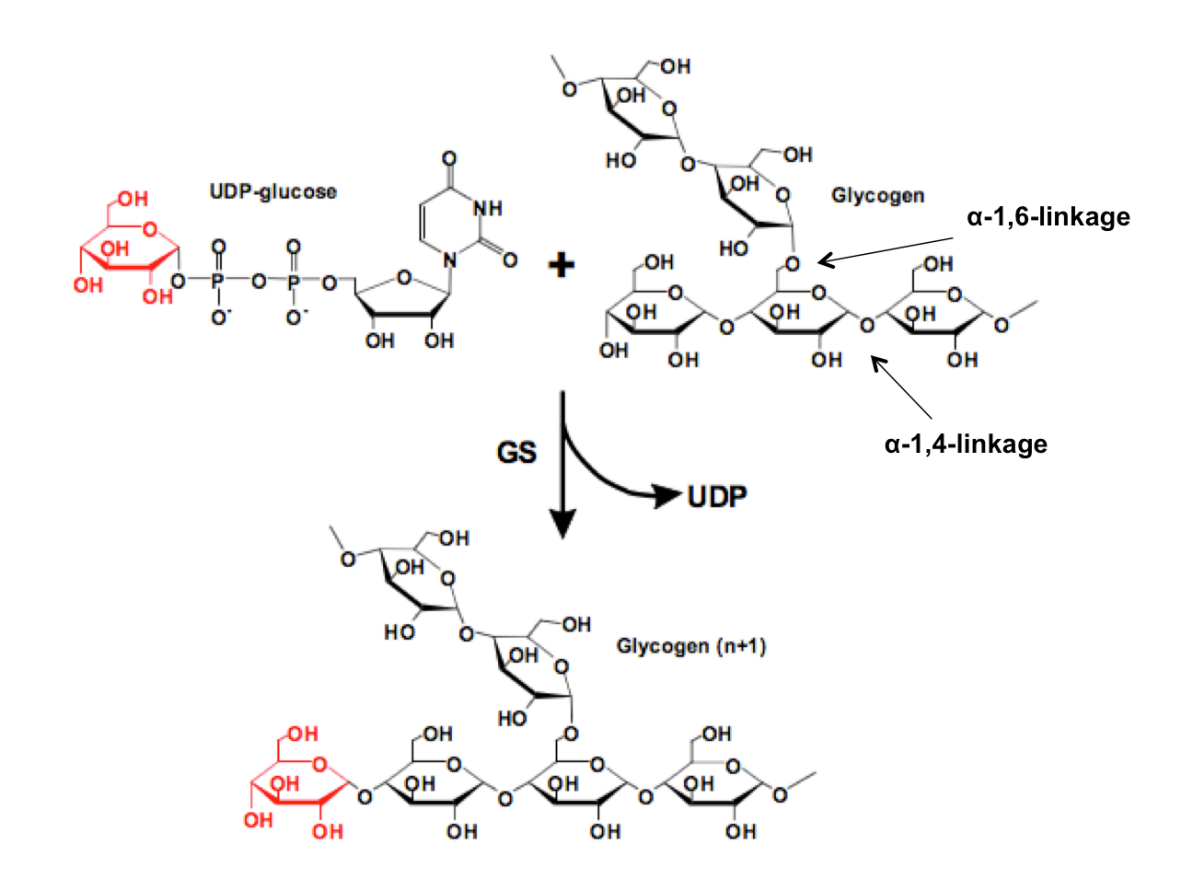


**Figure 2. The glycogen synthase reaction.** Glycogen synthase transfers a glucosyl moiety (red) from UDP-glucose to the non-reducing end (C4-OH) of a glycogen particle. (Modified from Roach, 2012)

The product of glycogen breakdown is primarily G-1P, which is subsequently converted to G-6P by the action of phosphoglucomutase, and glucose. The proportion of G-1P and glucose depends on the number of glycosyl residues between branch points. The metabolic fate of G-6P is tissue specific and depends on the presence of glucose 6-phosphatase. Glycogen phosphorylase (GP), cleaves α-1,4 glycosidic bonds, effectively releasing G-1P residues, until only 4 residues remain until the branch point. At this point, GP activity stops and the debranching enzyme (AGL or DBE) takes over. First, AGL glucotransferase activity removes three glycosyl residues from the outermost branch point, and adds them to a non-reducing end of the molecule, which can then be readily degraded by GP. The remaining glycosyl residue, attached to glycogen by α-1,6 bond, is cleaved by AGL, which releases a glucose. The G-1P generated by GP functions in the muscle as fuel for contraction, and in liver it is released as

glucose into the bloodstream. Another pathway for glycogen degradation is mediated by the action of lysosomal α-glucosidase, also known as GAA (acid α-glucosidase) or acid maltase. In this case, glycogen is transferred to the lysosome and hydrolyzed by this enzyme into glucose.

In 2007, two new proteins, Laforin and Malin, were identified as part of the glycogen metabolism pathway. These two proteins have been described to play an important role in neuronal cells, however they can also have a significant impact in other tissues. Laforin is a protein phosphatase la (Wang et al. 2002; Ganesh et al. 2000) with a carbohydrate-binding domain, which promotes binding to glycogen, and is responsible for the removal of glycogen phosphate that is added as a catalytic error during synthesis. Malin ubiquitinates glycogen granules and promotes proteasomal degradation of various proteins related to glycogen metabolism, such as MGS, PTG (Vilchez et al. 2007), or laforin itself (Worby, Gentry, and Dixon 2006). STBD1 is the last protein which as been described in relation to glycogen metabolism (Jiang et al. 2010). It binds glycogen and anchors it to membranes, thereby affecting its cellular localization and its intracellular trafficking to lysosomes.

Many groups have attempted to identify all the proteins involved with glycogen metabolism and interacting with glycogen. These studies confirm the presence of proteins involved in the glycogen metabolism pathway. Glycogenin, GS, GP, glycogen debranching enzyme (AGL) and STBD-1 were consistently found in all samples (Stapleton et al. 2010; Murphy et al. 2012). An interesting result, however, was the observation that GBE is present only in non-stringent purification conditions, indicating that it is not directly bound to the polysaccharide, but is rather only briefly bound to the short glucose chains during the creation of a new branching point.

## The need for a primer in the glycogen initiation

Many groups have tried to study whether GP or GS were able to start *de novo* glycogen synthesis. Only in 1975, Salsa and Larner were able to show that GS is able to synthesize glycogen from UDPG and glycogen in non-physiological conditions (Salsas and Larner 1975). Moreover there are some systems in which no glycogenin-like protein has been identified, supposing that another initiation way should occur. For example in *Agrobacterium tumefaciens* it was demonstrated that *de novo* synthesis is initiated by glycogen synthase without the need of a priming protein (Ugalde, Parodi, and Ugalde 2003). The same was shown by Torija (Torija et al. 2005) in the *glg1glg2* strain of Saccharomyces cerevisiae yeast, mutated on both genes encoding for glycogenin. This mutant resulted to have increased GS activity and retained the ability to synthesize glycogen. Another example is given by plants. In plant very little is known about the biochemical and physics underlying the initiation of starch. Synthesis is catalyzed by many isoforms of the SS gene (starch synthase) acting in a complex, and it is thought that the precursor of amylopectin is derived from simple sugars such as glucose, maltose, maltotriose via dextrins and glucans. In 2009, it has been shown that mutations on multiple isoforms of SS abolish starch synthesis, and that SSIII and SSIV are sufficient to catalyze starch synthesis. However, no priming protein or enzyme has been described to self-glycosylate in order to initiate chain elongation (Szydlowski et al. 2009).

Due to the observation in mammal tissues that the initiation process of glycogen synthesis was occurring only in presence of residual polymer, Cori was the first to hypothesize the presence of a primer in polysaccharide synthesis (Cori, Schmidt, and Cori 1939). Krisman and her team (Krisman and Barengo 1975) postulated the existence of an initiator protein is able to self-glycosylate, but it was Whelan that identified the protein responsible for self-glycosylation in the liver: glycogenin (Whelan 1986). Simultaneously, Cohen described the same primer in skeletal muscle (Pitcher et al. 1987).

## Glycogenin

Glycogenin is a 37KDa protein present in two isoforms in many species. In

humans the gene GYG1 encodes for the isoform widely expressed in the whole body and predominant in the muscle. The second isoform Glycogenin-2 is only expressed in liver, heart and in a minor degree in pancreas (Skurat, Lim, and Roach 1997). However, rodents carry only one isoform of the gene identified (Gyg).

Glycogenin is a member of the GT8 family (glycosyl-transferase), which is structurally characterized by a Rossmann-fold domain with the function of donor and acceptor site for UDP-glucose **(Figure 3A and 3B).** A metal ion ($Mn^{2+}$) coordinates UDP-glucose binding to a β-sheet structure. Next it retains the UDP group, releasing the glucose toward the acceptor site, creating a C1-O linkage with the Tyr195 amino acid. The subsequent glucose residues are attached to the growing chain by α-1,4-glycosidic linkages. GS can then continue to elongate a short chain of minimum 8 to 10 residues. GN has an unusual, if not unique, characteristic which allows it to act as both the catalyst and substrate of the reaction. A crystal structure of GN, isolated from rabbit muscle, was solved and shows that it is found as a homodimer, and that the glycosylation reaction most likely occurs intermolecularly (Gibbons, Roach, and Hurley 2002). Apparently glycogenin remains linked to the polymer through the entire elongation process (Alonso et al. 1995). It has been demonstrated that in skeletal muscle, no apo-glycogenin is found (free of glycogen), but all molecules are covalently bound to carbohydrate (Lomako, Lomako, and Whelan 1990; Smythe, Watt, and Cohen 1990).

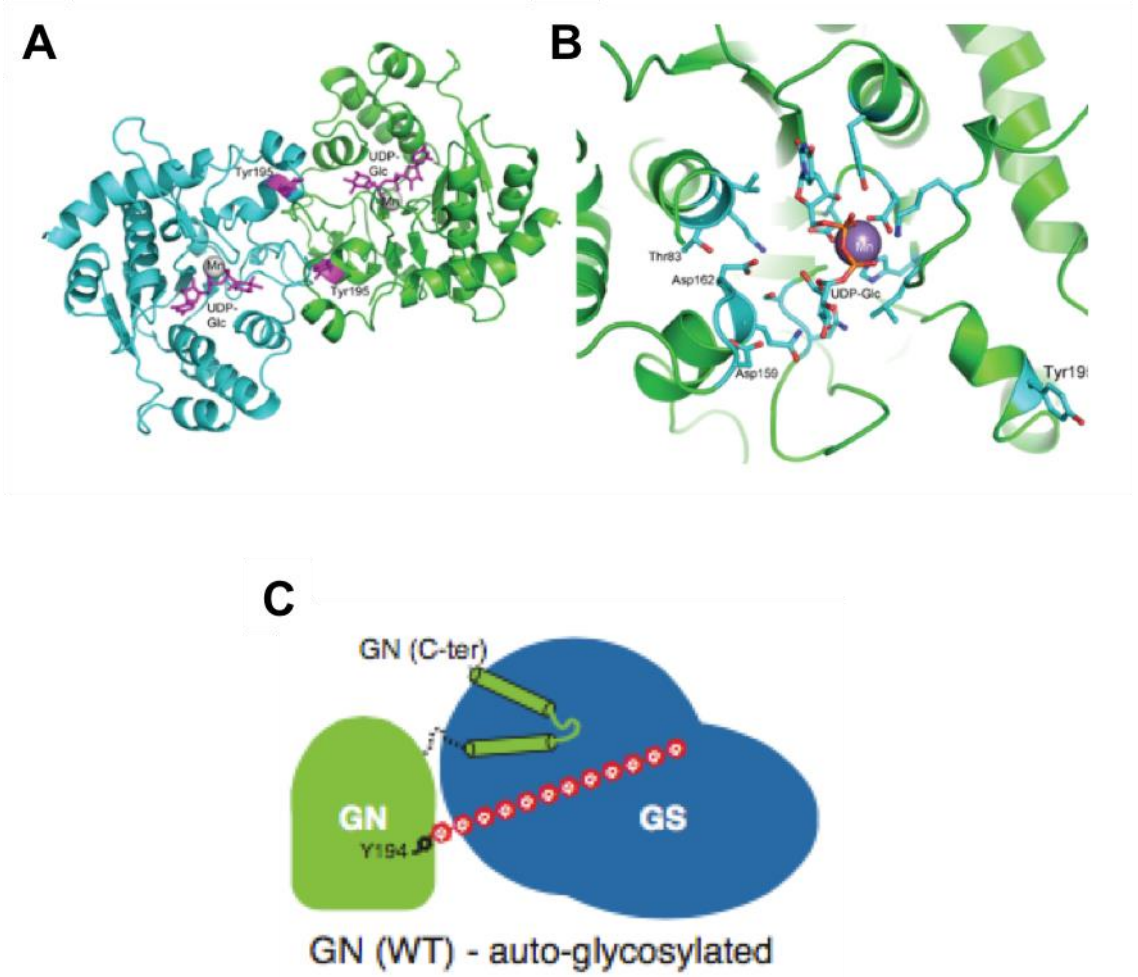


**Figure 3.** A) Ribbon representation of the glycogenin dimer. The active sites are denoted by the bound substrate UDP-glucose (magenta). The location of Tyr195 near the dimer interface is indicated using magenta color of the residue. B) The active site of glycogenin. Position of the catalytically essential $Mn^{2+}$ ion is shown using a purple sphere. (Gibbon, 2002). C) Glycogen Synthase- glycogenin interaction by the 35 amino acids linker. In red the growing glycogen polymer. (Font. Dr. Sakamoto K.)

A partial x-ray crystal structure has been solved for C. Elegans GN in complex with GS (Zeqiraj et al. 2014). The study reveals that the interaction between the two proteins is mediated by a 35 amino acid tail of GN, which is necessary for the in vitro activity of GS **(Figure 3C)**. This linker region, that separates the core catalytic domain of GN from the GS binding motif, differs between the two glycogenin isoforms (long 170 amino acids in human GN2). It is shown that the interaction of GS with GN by this linker can regulate the activity of the protein

GS, besides G-6P allosteric activation and de-phosphorylation (Zeqiraj et al. 2014).

No study has been able to show regulation of the activity of GN (Skurat, Dietrich, and Roach 2000). The only insight belongs from changes in Gyg mRNA level that duplicates after exercise in muscle (Kraniou et al. 2000). Another work (Hansen et al. 2000)found that there is no correlation between increased glycogen level and glycogenin protein. This is consistent with the observation that glycogenin-overexpressing rat fibroblasts that do not accumulate more glycogen even though all glycogenin is found linked to polymer chains (Skurat, Dietrich, and Roach 2006).

Rabbit glycogenin contains a motif similar to an actin-binding domain found in cofilin, a protein responsible for the disassembly of actin filament. The motif $^{321}$DNIKKKL$^{327}$ is located at the C-terminal end of glycogenin. Baqué et al (Baqué, Guinovart, and Ferrer 1997), show by disrupting the actin cytoskeleton the distribution of GN is altered within the cell. They suggest that the interaction between GN and the cytoskeleton plays a role in controlling granule localization, as well as the localization of the regulatory enzymes involved in glycogen metabolism.

The gene glycogenin-2 was described in human by Mu in 1997 (Mu, Skurat, and Roach 1997). It acts with the same mechanism of its homolog gene and it is mostly expressed in liver, and in minor part in heart and pancreas. Its molecular weight is 66Kda and it keeps 72% homology with glycogenin-1. The difference in the sequence is found in C-terminal linker tail, site of interaction with GS.

## Glycogen Synthase

Glycogen synthase is the enzyme responsible for linear chain elongation by creating α,1-4, glycosidic linkages. GS is part of the GT 3 family and mammals encode two isoform of the gene: Gys1, expressed in all tissues but the liver, and a liver-specific isoform: Gys2. As mentioned above, the enzyme is regulated by

multiple mechanisms: (i) Allosteric activation by G-6P; (ii) protein kinases which phosphorylate to inactivate (Roach, Rosell-Perez, and Larner 1977); (iii) Laforin and Malin which negatively regulate GS levels by a proteasome-dependent manner . Numerous protein kinases act on GS, including glycogen synthase kinase-3 (GSK3) (Picton et al. 1982; DePaoli-Roach et al. 1983), phosphorylase kinase (PhK) (Roach, DePaoli-Roach, and Larner 1978), cAMP dependent protein kinase (PKA)(Huang and Cabib 1972), casein kinase 1 (CK1) (Flotow and Roach 1989), casein kinase 2 (CK2) (Fiol et al. 1987), AMP activated protein kinase (AMPK) (Carling and Hardie 1989), PAS kinase (Wilson et al. 2005), DYRK1A (Skurat and Dietrich 2004) and p38 MAPK (Kuma, Campbell, and Cuenda 2004). These enzymes act on the serine 9 residues located at the C and N terminus of GS. Glycogen associated phosphatases (PP1G) have the ability to restore GS activation by removing phosphates.

## Skeletal muscle

Skeletal muscle is striated tissue which functions under voluntary control by the peripheral nervous system. Single units of the skeletal muscle are represented by myocites, also known as muscle fibers. These are cylindrical, multinucleated single cells. Muscle cells are composed of myofibrils, which in turn consist of highly organized and repetitive filaments of actin and myosin, called sarcomeres. Sarcomeres constitute the necessary machinery for muscle contraction and give muscles the typical striated aspect.
Skeletal muscle fibers can be classified based on various characteristics (Schiaffino and Reggiani 2011):

- Myosin ATPase activity (Type I, IIa, IIb)
- Myosin Heavy chain isoforms (MHC I, MHC IIa, MHC IIb) which are closely related to ATPase activity, as MHC type is the primary determinant of ATPase activity.
- Fiber color depends on the myoglobin content. Type I fibers are red

(high myoglobin) and have more mitochondria. Type II fibers are white (low myoglobin) and rely on glycolytic enzymes.

- Twitch speed (fast and slow twitch) is based on the speed by which myosin can split ATP. This characteristic overlaps with MHC type
- Metabolism (oxidative and glycolytic)

Fast twitch fibers include ATPase type II and MHC type II fibers, which are based on glycolytic metabolism for energy transfer, thus leads to faster contractions. These fibers are characterized by high strength in a short time, so these fatigue faster (i.e. Extensor Digitorum Longus). Slow twitch fibers, which include ATPase type I and MHC I, generate long term energy for the scission of ATP molecule by the aerobic energy transfer. Due to their oxidative metabolism, mitochondria content is high and the high myoglobin levels impart a red coloration. Due to the slow activity, these fibers are able to resist to longer before fatigue, but do not resist to high force stimuli.

Type II fibers can be divided in two main subtypes: type IIa and type IIb (or IIx in humans). Although type IIa fibers are fast twitch, they exhibit intermediate characteristics between type IIb and type I, such as color, mitochondria content and mixed metabolism. For the aim of this study, we have only considered differences between types I and IIb.

## Skeletal muscle metabolism

Energy in skeletal muscle can rapidly vary due to sudden consumption when contraction begins. ATP provides all energy required by hydrolysis to ADP and $P_i$. To maintain constant energy availability, fast and efficient methods of ATP re-synthesis are needed. The three main mechanisms to supply energy are:

1) **ATP generation by Creatine kinase (CK) and adenylate-kinase activities**. Phosphocreatine (PCr) uses its high-energy phosphate reservoir for the rapid regeneration of ATP by CK, thus avoiding ADP accumulation. It provides the fastest and most effective way to regenerate ATP that lasts only few seconds. PCr has also the ability to transport ATP from the site of synthesis to the site of

utilization (mitochondria). Its content is slightly higher in fast than slow fibers.

To lower degree ATP can also be resynthesized by the action of adenylate-kinase starting from two ADP molecules and obtaining one ATP and one AMP.

2) **Glycolytic ATP regeneration**. The second source of ATP production belongs from glucose and glycogen breakdown leading to the production of pyruvate or lactate by glycolysis. This mechanism generates 2–3 mol ATP/mol glucose. This metabolism is more efficient in fast-twitch than is slow-twitch fibers due to higher level of glycolytic enzymes.

3) **Mitochondrial ATP regeneration**. The third way of ATP re-synthesis starts from pyruvate or from fatty acids via β-oxidation, towards TCA cycle and it ends with mitochondrial oxidative phosphorylation. It can provide 18 ATP per acetate. This mechanism is more efficient in slow-twitch fibers due to the higher mitochondria density.

Slow and fast muscles differ in the proportion of oxidative and glycolytic metabolisms **(Figure 4).** Slow fibers can provide al the energy they need by oxidative metabolism, in fact ATP consumption is quite slow and this contribute to maintain a contractile activity prolonged in time. On the contrary, fast muscles are able to generate ATP very rapid by glycolytic metabolism, but this does not allow to last long in time.

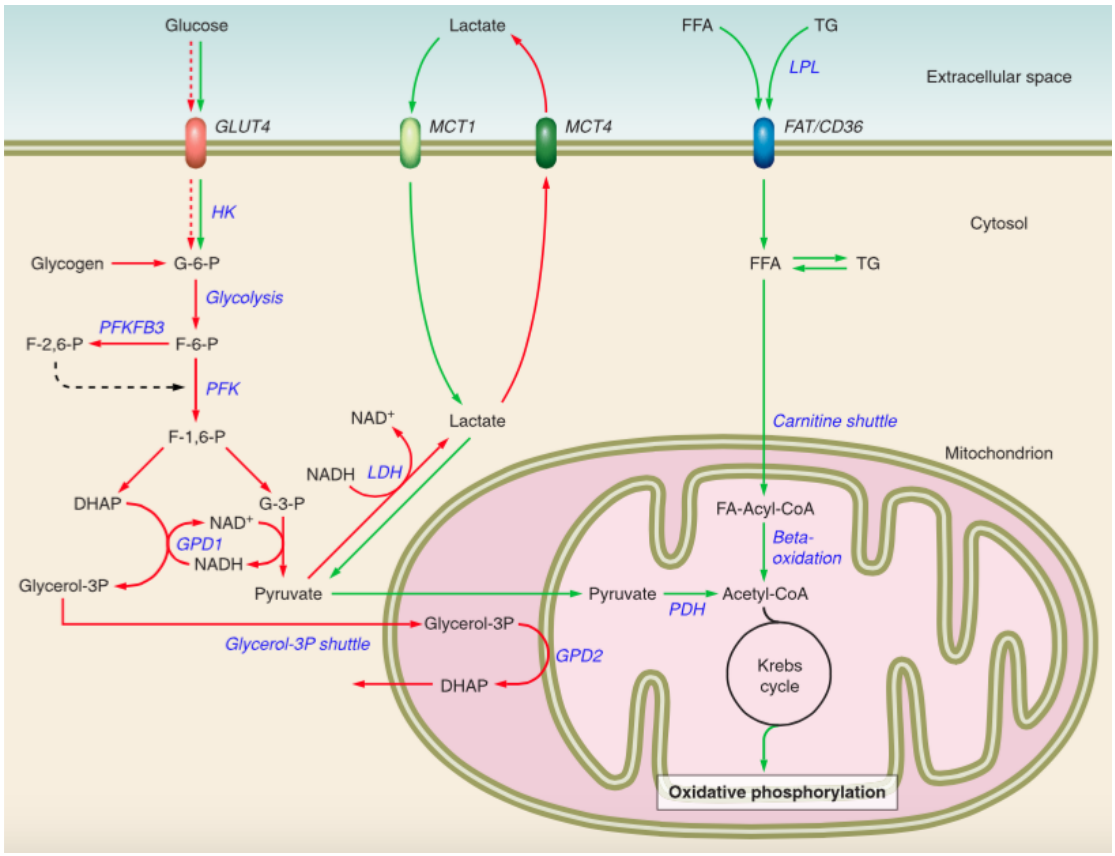


**Figure 4. Scheme showing some differences in glucose, lactate, and fatty acid metabolism between fast and slow muscle fibers.** Pathways prevalent in fast or slow muscle fibers are shown as red or green arrows, respectively. DHAP, dihydroxyacetone phosphate; GLUT4, glucose transporter 4; F-6-P, fructose-6-phos- phate; FAT/CD36, fatty acid translocase; FFA, free fatty acids; F-1,6-P, fructose-1,6-bisphosphate; F-2,6-P, fructose-2,6-bisphosphate; G-3-P, glyceraldehyde-3-phosphate; G-6-P, glucose-6-phosphate; GPD1, glycerol- phosphate dehydrogenase 1 (cytoplasmic); GPD2, glycerolphosphate dehydrogenase 2 (mitochondrial); HK, hexokinase; LDH, lactate dehydrogenase; MCT1, monocarboxilic acid transporter 1; MCT4, monocarboxilic acid transporter 4; PDH, pyruvate dehydrogenase; PFK, phosphofructokinase; PFKFB3, phosphofructokinase- fructose bisphosphatase 3; TG, triglycerides. (Font. Schiaffino and Reggiani, 2011)

Muscle metabolism is greatly influenced by the substrates provided to the fibers, entering by trans-sarcolemmal transport. This is a main reason for the great difference between the fiber types. The substrates entering the cells and utilized as energy sources are:

A) LACTATE. Fast glycolytic fibers produce and eliminate lactate that is transported via blood circulation to other muscles or to the liver where lactate is converted to pyruvate and then into glucose by gluconeogenesis.

B) GLUCOSE. Skeletal muscle consumes most of the circulating glucose and

its main source of energy. For this reason, this tissue also participates in the regulation of glycemia, uptaking glucose by GLUT transporters after the effect of insulin or contractile activity.

C) FATTY ACID. By protein- mediated transport and by passive membrane diffusion, fatty acids enter in the muscle fiber to serve as energy substrate. The presence of different intracellular lipases contributes to make fatty acids available as a substrate. These enzymes show a fiber-type-dependent distribution, being more expressed in slow oxidative than in fast glycolytic muscles.

D) MYOGLOBIN AND OXYGEN TRANSPORT. Myoglobins are proteins that facilitate oxygen transport and diffusion. Large amounts of oxygen are required by mitochondria during sustained contractile activity. Myoglobin levels are high slow-twitch fibers and determine their red coloration.

**Mitochondria**

Mitochondria are cytoplasmic organelles present in most eukaryotic cells. These organelles produce most of the ATP needed by cells as an energy source. Also taking part in the substrate oxidation and ATP production, mitochondria play a key role in many biological processes such as cell signaling, apoptosis, aging, cell cycle control and calcium homeostasis (Rutter and Rizzuto 2000; Chomyn and Attardi 2003; Kujoth et al. 2005). Cells that have an increased demand for ATP, such as muscle, contain a greater number of mitochondria. Several metabolic pathways take place in the mitochondrial matrix, such as the Krebs cycle and β-oxidation of fatty acids; as well as oxidation of the amino acids and synthesis of urea and heme groups. Mitochondria have their own genetic material, organized as a circular chromosome located in the mitochondrial matrix. Mitochondrial DNA (mtDNA) encodes 13 subunits of the respiratory chain complexes, as well as others. (Legros et al. 2004).

Mitochondria oxidation takes place starting from different substrates such as pyruvate from glycolysis, fatty acids or amino acids. These substrates enter the mitochondria via specific transporters generating acetyl-CoA that enters the

Krebs cycle or tricarboxylic acid cycle (TCA cycle). The acetyl-CoA is oxidized to $CO_2$ during the process, producing reduced cofactors NADH and $FADH_2$. The main function of mitochondria is to produce energy in the form of ATP by oxidative phosphorylation (OXPHOS)**.** In this process, electrons from the oxidation of NADH and $FADH_2$ pass through a series of complex enzyme located in the inner mitochondrial membrane, called respiratory chain or electron transport chain. The flow of electrons in these complexes liberates energy used to pump protons, from the matrix to the intermembrane space. This creates an electrochemical proton gradient, which is used by ATP synthase to synthesize ATP from ADP and Pi. Thus, oxygen consumption by the respiratory chain is coupled to ATP synthesis. The ATP produced is exported to the in exchange of ADP.

The system includes OXPHOS enzyme complex of the respiratory chain (complex I-IV), ATP synthase (also called complex V) and two mobile electron carriers: ubiquinone or coenzyme Q and cytochrome c. NADH dehydrogenase or complex I is the main entry point of the electrons in the respiratory chain. Catalyzes the transfer of electrons from NADH to ubiquinone. The complex II or succinate dehydrogenase (SDH) consists of four subunits and represents an entry point to alternative electron respiratory chain. The central component of the system OXPHOS the complex III or Cytochrome c reductase transfers electrons from ubiquinol to cytochrome c, which is a soluble electron transporter found in the intermembrane space. The complex IV or Cytochrome c oxidase is the last enzyme of the electron transport chain. ATP synthase complex or V is an ion channel through which protons go back into the mitochondrial matrix.

## Fiber switch

Skeletal muscle is generally composed by high heterogeneity of fiber types. It has a remarkable capacity to undergo adaptive changes in response to use and disuse, including fiber type (e.g., fast-to-slow fiber type switch), and correlated changes in muscle force and resistance to fatigue (Pette 1997). Constant elevated neuromuscular activity (low-frequency stimulation and prolonged

endurance training) induces a switch from fast to slow-twitch fibers in mammals. The fiber type transition is gradual and it is best represented by the MHC isoforms expression (Pette 1998). The opposite situation is observed in case of high-intensity intermittent training in human. After this kind of exercise in fact, the number of type IIb fast-twitch fibers decreased, in favor of oxidative type I fibers (Simoneau et al. 1985).

Spiegelman's laboratory discovered that increasing the expression of a gene called PGC-1α muscles composed of mixed fiber-type could transform into predominantly slow-twitch types (Lin et al. 2002). PGC-1α (peroxisome-proliferator-activated receptor-gamma co-activator-1) is a transcriptional regulator, which is expressed preferentially in muscle, enriched in type I fibers. It activates oxidative metabolism regulating at transcriptional level genes involved in mitochondrial biogenesis. When PGC-1 α is expressed by a muscle creatine kinase (MCK) promoter in transgenic mice, a fiber type conversion from fast to slow is observed: muscles are redder and activate genes of mitochondrial oxidative metabolism and show a much greater resistance to electrically stimulated fatigue. Conversely, skeletal muscle-specific PGC-1α KO animals report a moderate reduction in the number of oxidative type I and type IIa muscle fibers and lower exercise capacity (Handschin et al. 2007). These data indicate that PGC-1 α is a principal factor regulating muscle fiber type determination required for the maintenance of a normal number of oxidative type I and type IIa muscle fibers. Furthermore a similar mechanism is applied by the transcriptional coactivator PGC-1β that drives the formation of oxidative type IIX fibers in skeletal muscle (Arany et al. 2007). It has been shown that increased muscle mitochondrial fatty acid oxidation capacity leads to muscle remodeling toward an oxidative phenotype. Regulation of the fiber conversion goes through the PGC-1 transcription factors. The enhanced fatty acid oxidation capacity is associates by an increase in muscular glycogen, explained as a consequence of glycolysis inhibition. It is suggested that fatty acids not only provides energy, but also act as metabolic sensor facilitating its adaptation to environmental changes.

## Glycogen in skeletal muscle

Many studies show that muscle glycogen storage correlates with increased endurance during physical exercise (Bergstrom et al. 1967), and that the levels during resting periods is proportional with the time of exhaustion and vice versa (Hermansen, Hultman, and Saltin 1967). This evidence provides insight into the role of muscle glycogen during exercise. However, the link between glycogen and impaired muscle function during fatigue is demonstrated. The rational is that through glycogenolysis, muscle glycogen provides G-6P for glycolysis and the TCA cycle. *In vitro* intermittent stimulation protocols of whole muscles and single fibers indicate that glycogen depletion impairs excitation-contraction (E–C) coupling leading to fatigue (Chin and Allen 1997; Helander, Westerblad, and Katz 2002). The link between glycogen and muscle performance has traditionally been considered as being closely related to impaired energy metabolism when glycogen levels are low.

When muscle contracts, the increase in cytoplasmic $Ca^{++}$ produces glycogen depletion. It has been shown that fast-twitch fibers have higher glycogen content, breaks down more glycogen and after intense exercise resynthesized glycogen at a higher rate than slow-twitch muscle (Etgen et al. 1996; Maier and Pette 1987). On the other hand, slow-twitch muscle has a lower glycogen content and low glycogen phosphorylase activity (Bengtsson, Henriksson, and Larsson 1986), and contraction produces slow glycogen degradation without complete depletion. The different regulation of the first stages of glycogen degradation and glycogen biogenesis in fast- and slow-twitch muscle elucidates a fiber type- specific glucose–glycogen mechanism (Cusso et al. 2003).

## Mechanism of glycogen synthase control by exercise

The drop of glycogen levels in muscle during exercise must be rapidly replenished, which requires glycogen synthesis activation. Depending on

conditions, GS has been found active during exercise and once the activity has stopped (Nielsen and Richter 2003; Nielsen and Wojtaszewski 2004). Several studies have tried to explain the paradox of glycogen turnover: why is glycogen synthesized during a period when it is heavily utilized? There are several possible explanations: (i) to allow glycogen storage usage once the exercise ends; (ii) signaling factors prevent GS phosphorylation and/or favor the glycogen "futile cycle"; and (iii) glycogen is synthesized to be used during exercise (possible unknown energetic advantage). The exact mechanism is still unknown, but it seems that GS activation is not due to insulin signaling, rather PKA pathway activation decreases GS phosphorylation (Hubbards, 1989).

## Glycogen storage diseases (GSDs)

The importance of glycogen metabolism is reflected by the considerable deregulation of the mechanism whenever a mediator is mutated **(Table 1)**. Gain or loss-of-function mutations in the enzymes lead to impaired glycogen storage: over-accumulation (Lafora, Andersen, Pompe, Cori, McArdle diseases and GSD XV) or absence of the polysaccharide (GSD 0). Symptoms vary depending on the gene affected, and their intensity or onset can change based on the mutation affecting the specific gene involved.

**Table 1. Glycogen storage diseases list and features.**

| Number | Enzyme deficiency | Eponym | Organ affected | Glycogen in the affected organ |
|---|---|---|---|---|
| GSD type 0 | Glycogen synthase | - | Liver (LGS), Muscle and heart (MGS) | Null/Low level |
| GSD type I | Glucose-6-phosphatase | Von Gierke's disease | Liver and kidney | Increased amount; normal structure |
| GSD type II | Acid alpha-glucosidase | Pompe's disease | All organs | Massive increase in amount; normal structure |
| GSD type III | Glycogen debranching enzyme | Cori's disease | Muscle and liver | Increased amount; short outer branches |

| | | | | |
|---|---|---|---|---|
| GSD type IV | Glycogen branching enzyme | Andersen disease, APBD | Liver, spleen and nervous system | Increased amount; very long unbranched chains |
| GSD type V | Muscle glycogen phosphorylase | McArdle disease | Muscle | Moderately increased; normal structure |
| GSD type VI | Liver glycogen phosphorylase | Hers' disease | Liver | Increased amount |
| GSD type VII | Muscle phosphofructokinase | Tarui's disease | Muscle | Increased amount; normal structure |
| GSD type VIII | Liver phosphofructokinase | - | Liver | Increased amount; normal structure |
| GSD type X | Phosphorylase kinase, PHKA2 | | Liver and muscle | Increased amount |
| GSD type IX | Phosphoglycerate mutase | | Muscle | Increased amount |
| GSD type XI | Lactate dehydrogenase | | Muscle, blood | |
| GSD type XII | Aldolase A | Red cell aldolase deficiency | Blood | |
| GSD type XIII | β-enolase | | Muscle | Increased amount |
| | Laforin or Malin | Lafora Disease | Nervous system, muscle, heart | Increased amount, LBs |
| GSD type XV | Glycogenin | | Muscle, heart | Increased amount |

**Polyglucosan bodies-accumulating GSDs**

Some GSDs are characterized by the accumulation of abnormal glycogen or the so-called Polyglucosan bodies (PGBs), which occurs in cells of patients affected by Adult Polyglucosan Body Disease or Andersen Disease (APBD, GBE mutation) and Lafora Disease (LD, Laforin or Malin mutations). PGBs are aggregates of glycogen and proteins and are characterized as being insoluble due to the low branching degree and high glycogen phosphate content. These accumulations increase with the age and become toxic for cells. No currently available treatments are able to prevent PGB formation or stimulate

degradation. GS is responsible for PGB formation, and current studies aim to reduce GS activity as a possible cure for these pathologies.

## GSD type 0

Glycogen storage disease type 0 (GSD 0) is a rare autosomal recessive pathology caused by mutations in the glycogen synthase genes, resulting in an almost complete loss of glycogen, specifically in the tissues encoding for the mutated isoform. Patients affected by GYS2 loss of function have a 95% reduction in liver glycogen content, and the same phenotype has also been described in Gys2 KO mice. However, both patients and mice can survive the disease. Only one clinical case described a mutation in the GYS1 gene that resulted in sudden cardiac death of an 8-year-old patient after collapsing during a bout of exercise (Cameron et al. 2009). Similarly, Gys1 null mice suffer of high lethality dying soon after birth due to impaired cardiac function. Those that do survive develop severe muscle weakness and cardiomyopathy (Pederson et al. 2004).

## GSD type XV

Shortly after we generated the Gyg KO mouse model, the first clinical case of a patient affected by a mutation in glycogenin 1's catalytic site was reported by Moslemi (Moslemi et al. 2010). This patient showed complete glycogen depletion in the skeletal muscle as well as severe myopathy, consistent with GSD 0 and opposite to our observations. This study supported the theory that both GS and glycogenin are necessary for glycogen synthesis. On the other hand, cardiac tissue specimens showed hypertrophic cardiomyocytes with abnormal PAS-positive material, which the authors explained as a compensatory mechanism by the GYG2 gene in humans. Recently, ten new cases of the newly described GSD XV (Malfatti et al. 2014; Colombo et al. 2015; Luo et al. 2015) have been reported, in which patients, carried different missense, nonsense, or frameshift GYG1 pathogenic variants, distributed all over the gene. There was either reduced or complete absence of glyogenin-1

protein, in accordance with the deleterious effects of the variants. All patients have adulthood onset of the disease, starting with symptomatic muscle weakness and worsening with the age: hip girdle, shoulder girdle, and/or hand and leg muscle weakness. Glycogen from some patients muscle biopsies showed PAS-positive accumulations in 30-40% of muscle fibers, partially amylase-resistant, but in lower degree compared to PGBs (Colombo et al. 2015; Luo et al. 2015). Frequently found fibers retain various amount of normal glycogen. No data regarding the mechanism behind the regulation of glycogen synthesis are provided. The difference found between these patients and the one described in 2010 is explained by the amount of glycogenin-1, accumulated in the first case and depleted in the others. This observation hypothesize that the interaction between glycogenin and GS is important for the regulation of glycogenin synthesis.

# Objectives

The glycogen initiation complex, formed by glycogenin and GS, is considered crucial for glycogen synthesis. In order to understand the impact of glycogenin on glycogen metabolism, we generated a constitutive Gyg KO mouse model. Unexpectedly, Gyg KO mice are able to synthesize glycogen and, in fact, accumulate high levels of the polysaccharide, specifically in the skeletal and cardiac muscles.

The present work sought to fulfill the following objectives:

1. To characterize Gyg KO embryos and adult mice.
2. To characterize the glycogen metabolic pathway in the absence of glycogenin.
3. To characterize the glycogen particles synthesized in Gyg KO mice.
4. To identify a putative substitute protein that functions as a glycogen primer.
5. To determine the systemic consequences of higher glycogen accumulation and the physiology of skeletal muscle in Gyg KO mice.

# Results

## 1. Generation of the Gyg KO animal model

### 1.1 Introduction

The priming role of glycogenin (GN) is considered crucial for the functioning of the glycogen initiation complex, which also includes GS. Accordingly, it is generally accepted that the lack of one of the two key players would impair glycogen synthesis.
To study the role of glycogenin in glycogen synthesis, we generated the Gyg KO animal model.

### 1.2 Generation of the animal model and survival analysis

Unlikely other species, rodents present only one isoform of the glycogenin gene and for this reason *mus musculus* is a convenient model to study the impact of glycogenin on glycogen metabolism. We generated a constitutive Gyg KO mouse using knockout first technology that allows complete Gyg ablation. To this end, a selection cassette was inserted flanking exons 3 and 4, effectively creating a KO allele by disrupting the expression of the gene **(Figure 5)**.


**Figure 5. Disruption of the Gyg1 gene**. *FRT*, Flippase Recognition Target sites by Flp recombinase; lacZ, report gene encoding for β-galactosidase; *loxP*, site-specific sequence recognized by Cre recombinase; pA, polyadenylation sequence; SA, splice acceptor sequence.

This insertion cassette is located before exon 5, which is where the sequence encoding for the Gyg active site (Tyr195) is located. In order to obtain Gyg KO

mice, we bred heterozygous animals. The number of pups per litter was lower than expected: ± 5 compared to an average litter size of 8 in animals with the same C57/B6 background. Only about 2.5% of the newborn pups were Gyg KO, which is significantly lower than the expected Mendelian ratio **(Table 2)**.

**Table 2. Survival of mutant embryos**

| Developmental stage | | WT | Gyg +/- | Gyg KO | Total |
|---|---|---|---|---|---|
| **Pups** | **nº** | 118 | 359 | 13 | 490 |
| | **%** | 24 | 73.3 | 2.7 | 100 |
| **Embryos** | **nº** | 40 | 64 | 36 | 140 |
| | **%** | 28,6 | 45,7 | 25,7 | 100 |
| **Mendelian ratio** | **%** | 25 | 50 | 25 | 100 |

## 1.3 Morphology at different embryonic stages and causes of death

To confirm that Gyg depletion was causing embryonic lethality and to determine at which developmental stage this was occurring, we set up timed matings and genotyped the embryos at developmental stages 14.5 and 18.5 dpc. Analyses of embryos at developmental stage E14.5 did not reveal lethality at early embryonic stages, and the body weight and crown-to rump length was not altered in Gyg KO individuals **(Figure 6)**. At 18.5 dpc, which corresponds to the last developmental stage *in utero*, the expected Mendelian ratio of the Gyg KO embryos was maintained. It is for this reason we concluded that Gyg KO embryos die perinatally **(Table 2)**. Again, at 18.5 dpc, no differences in body weight and crown-to rump length were observed. To further analyze possible morphological impairments, tibial length was compared between WT, heterozygous and Gyg KO embryos, but no significant differences were observed **(Figure 7).**

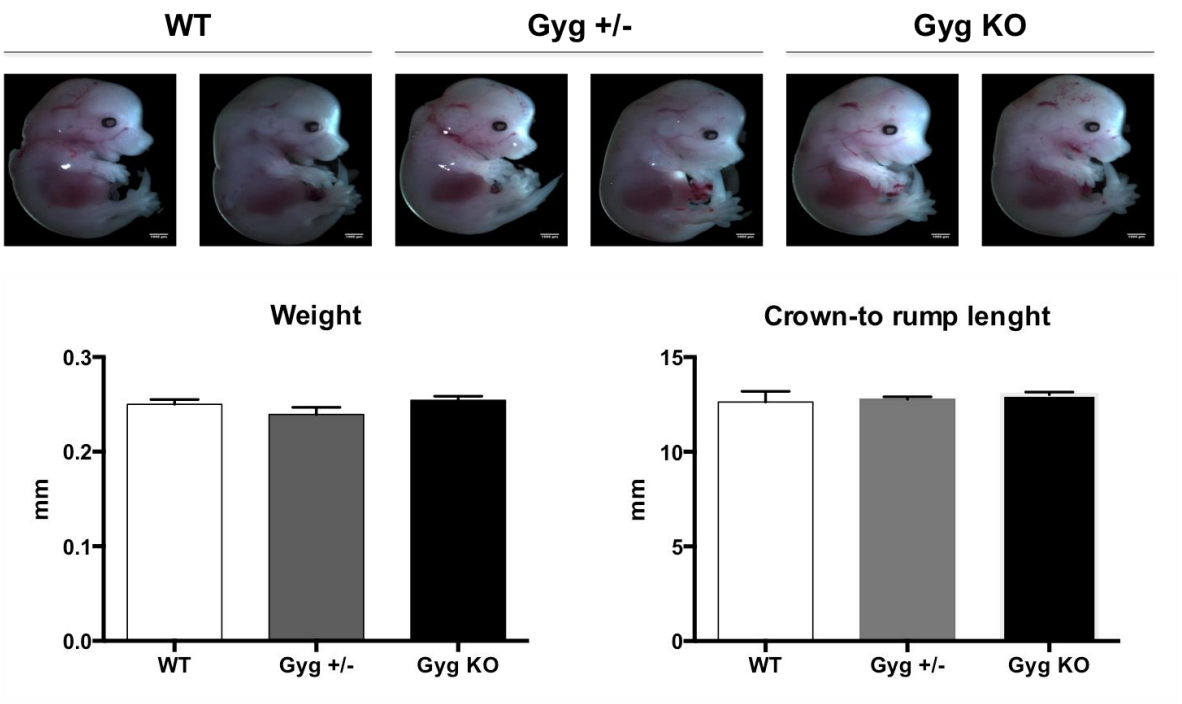


**Figure 6. Embryos at 14.5 dpc –** Top panel: morphology of embryos; Bottom panel: mean of 14.5 dpc embryos' weight and measurement of the length of the embryos from the top of the head (crown) to the bottom of the buttocks (rump).

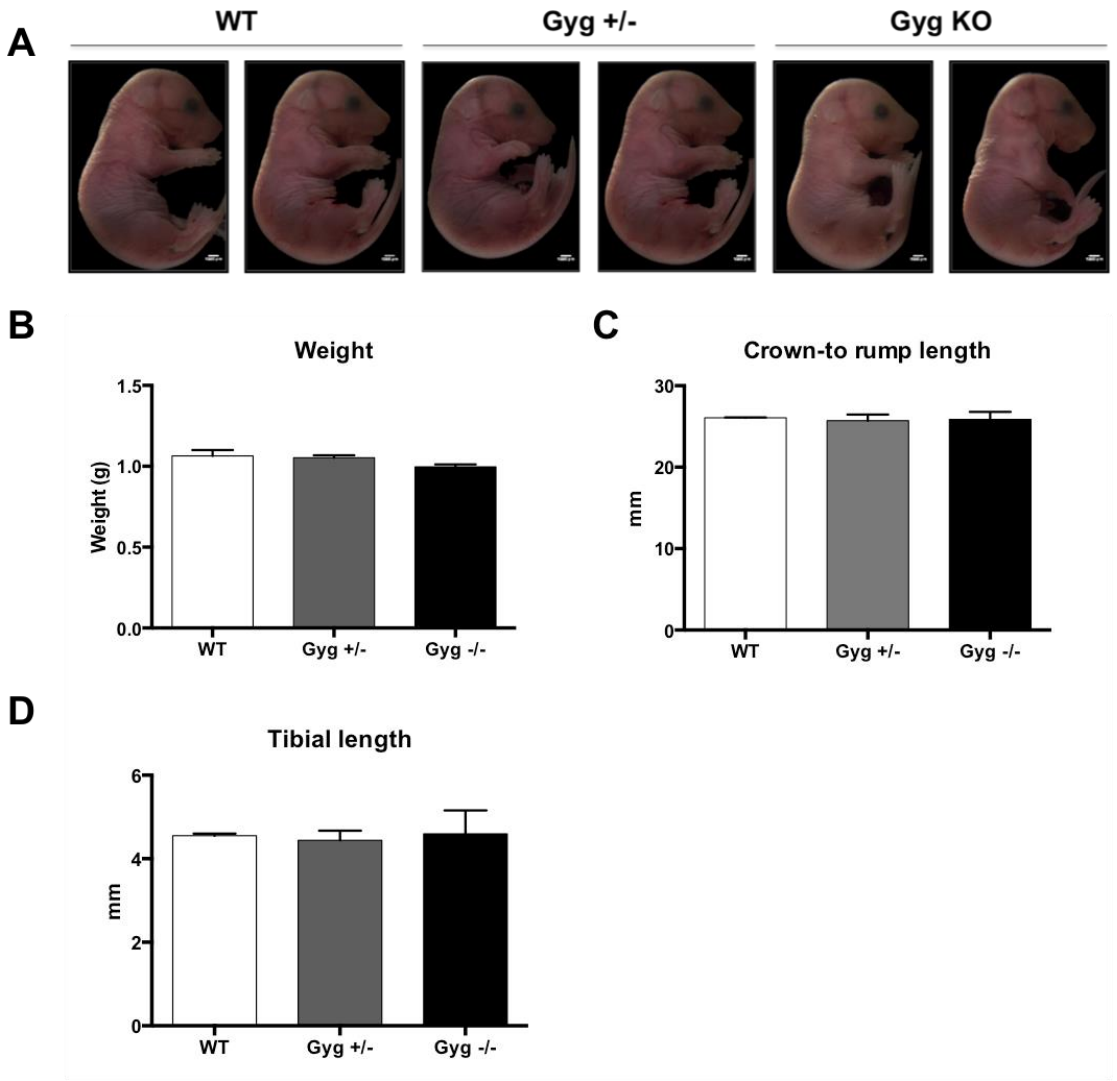


**Figure 7. Embryos 18.5 dpc-** A) Embryo morphology; B and C) Weight and body length measurements; D) Measurement of the lower portion of the leg, which corresponds to the tibia.

Neonatal death can stem from a variety of defects, therefore we obtained full-term E19.5 mice by Caesarean section and monitored them after removing them from the breeding cage. Gyg KO pups were born with breathing difficulties, and died after a few seconds without being able to take a full breath (the parameter was crying). We further confirmed their inability to breathe by performing the Lung Float Test by extracting the lungs of the pups and submerging them in water. We confirmed that GYG KO did not breathe after birth as their lungs sunk to the bottom of the beaker, whereas the lungs of control pups floated **(Figure 8)**.

**SURVIVING TIME AFTER BIRTH**

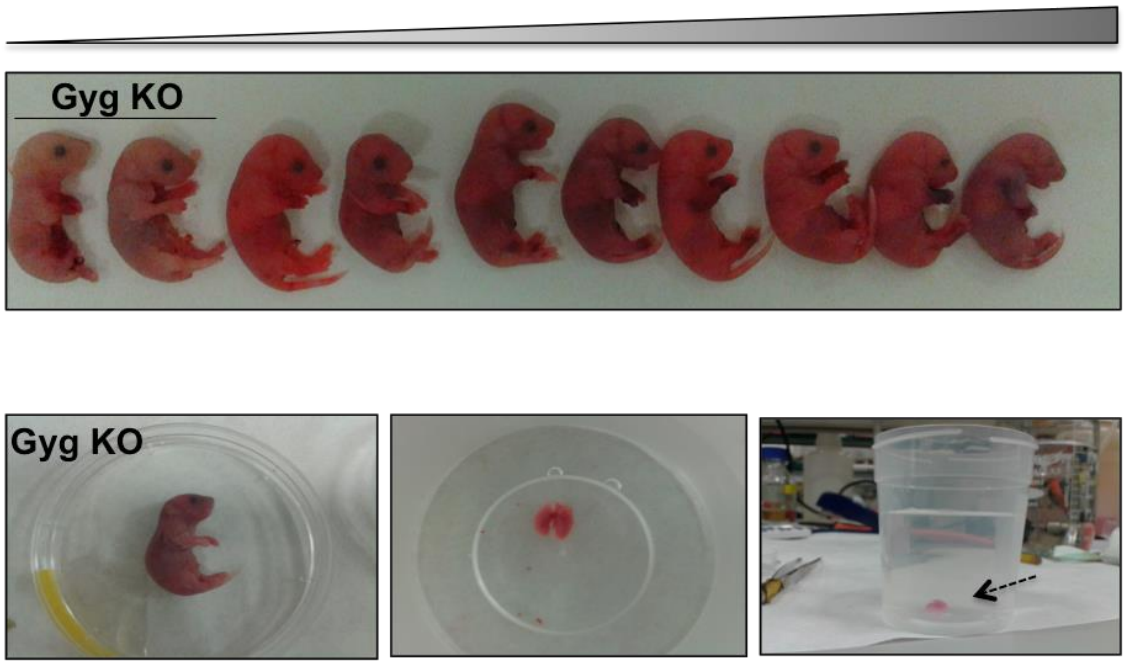


**Figure 8. Gyg KO embryos die perinatally-** Top panel: Survival of 19.5 dpc pups; the bar above the pictures indicates the order in which pups died. Bottom panel: Lung Float Test: dissection of the lungs from the pup and immersion in water.

Histological examination of 18.5 dpc Gyg KO pups revealed defects in cardiac development such as discontinuities in the interventricular septum and a dilated left ventricle. In addition, we observed defects in the lungs, namely hypoplastic right caudal and accessory lobes **(Figure 9)**. By staining the heart and liver with Masson's trichrome stain, we ruled out fibrosis that could impair the function of these tissues (this was previously identified in adult MGS KO mice hearts) **(Figure 10).**

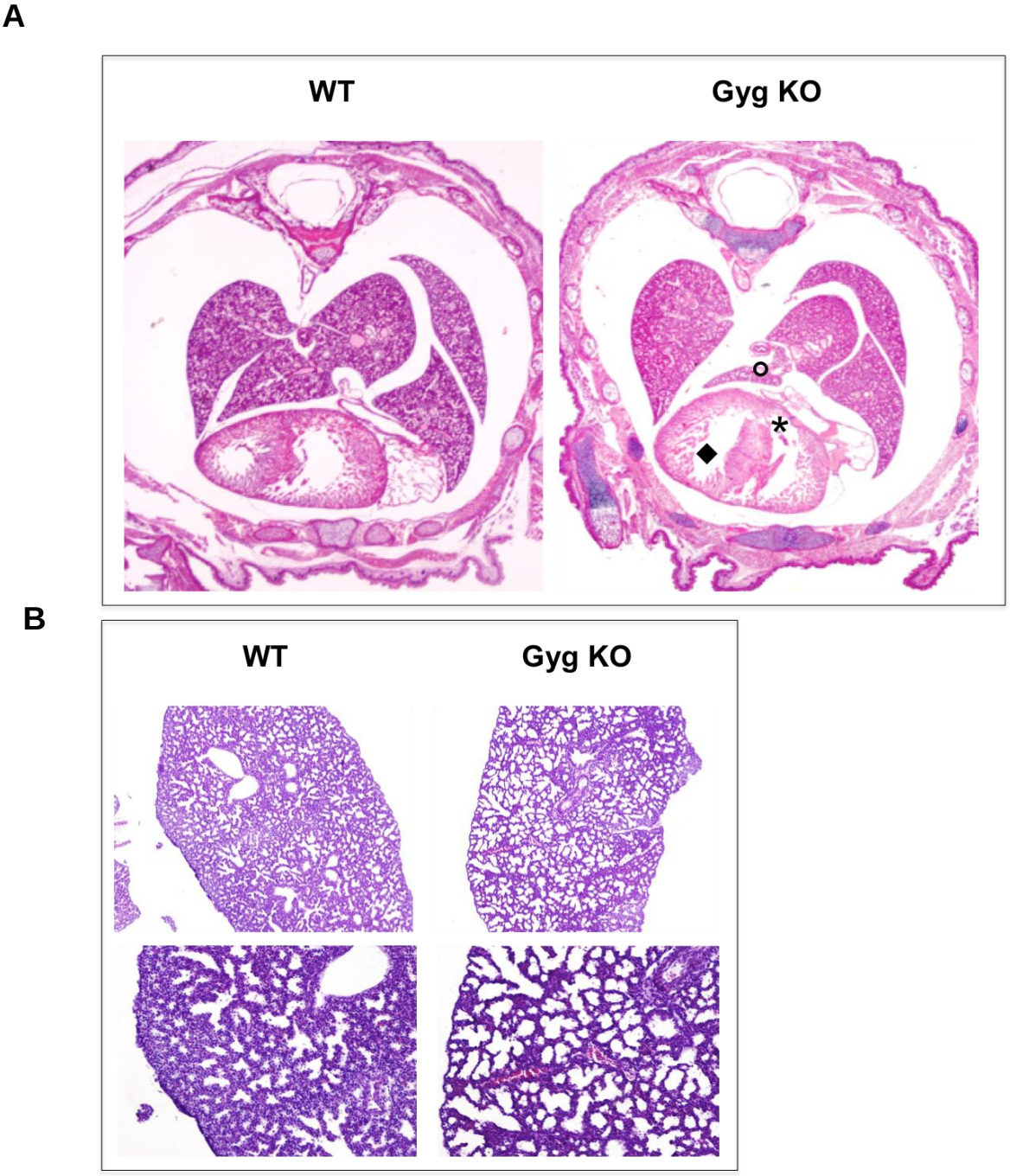


**Figure 9. Histological analyses of Gyg-deficient embryos-** HE A) Transverse section of embryos at 18.5 dpc. (made by Dr. Ruberte J., UAB); B) sagittal section of pulmonary lobe

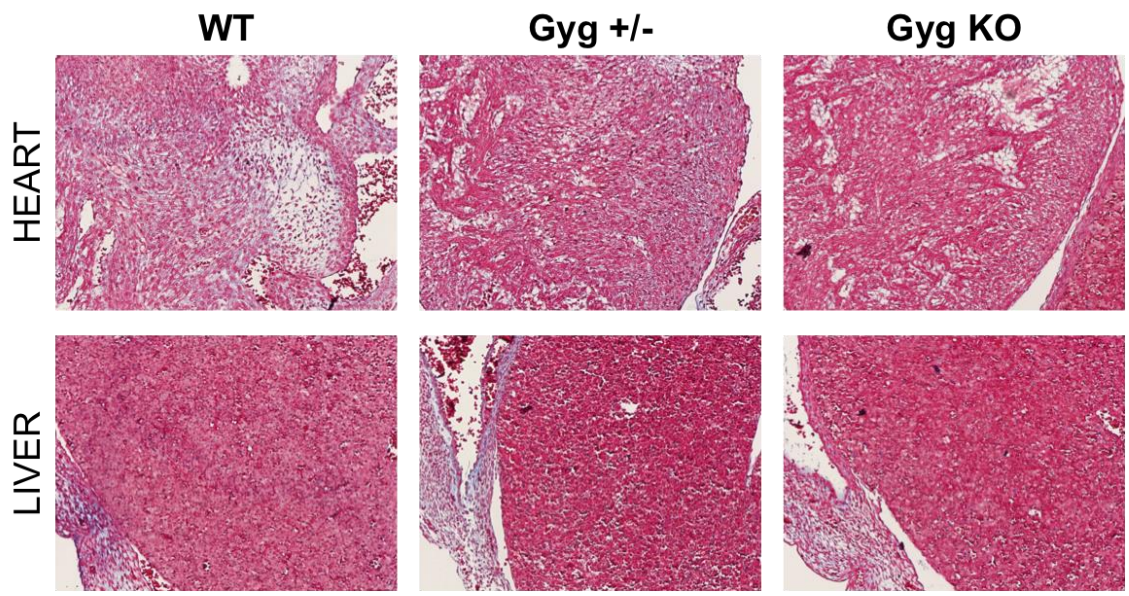


**Figure 10. Masson's trichrome stain-** Analysis of fibrotic tissue. Fibrosis is identified by blue coloration

## 1.4 Conclusions

We conclude that Gyg KO die shortly after birth due to physical abnormalities in the heart and lungs. Of note, these findings show great similarities with previous observations of perinatal lethality in MGS KO pups, which also present cardiac abnormalities such as smaller ventricles with thinner walls, dilated atria, abnormal ventricular septum, reduced trabecular structure and, in some cases, increased pericardial space (Pederson, 2004).

# 2. Gyg KO embryos accumulate glycogen

## 2.1 Detection of glycogen in Gyg KO embryos

Our hypothesis was that the lack of glycogenin gene would impair viability, and that Gyg KO mice die due to severe heart defects caused by the total absence of glycogen, as was the case in MGS KO embryos. Therefore, we performed PAS staining of the hearts. To our surprise, Gyg transgenic mice revealed an unexpected PAS staining. From the first analysis of sagittal sections of 14.5 dpc embryos, PAS staining revealed that Gyg KO mice presented glycogen, particularly visible in cardiac and muscular tissue **(Figure 11)**. Presence of glycogen was confirmed by diastase treatment, which is able to specifically degrade glycogen. After amylase treatment there was a clear reduction in the polysaccharide.

The results were confirmed by electron microscopy analysis of 18.5 dpc hearts: cardiomyocytes revealed abundant glycogen deposits in the cytoplasmic area surrounding the nucleus **(Figure 12)**.

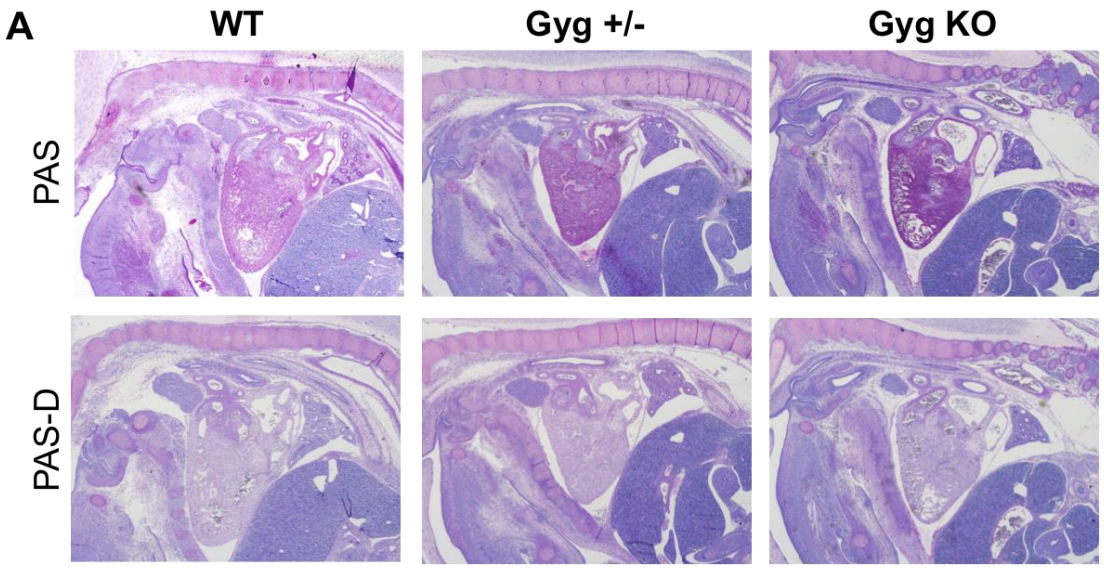

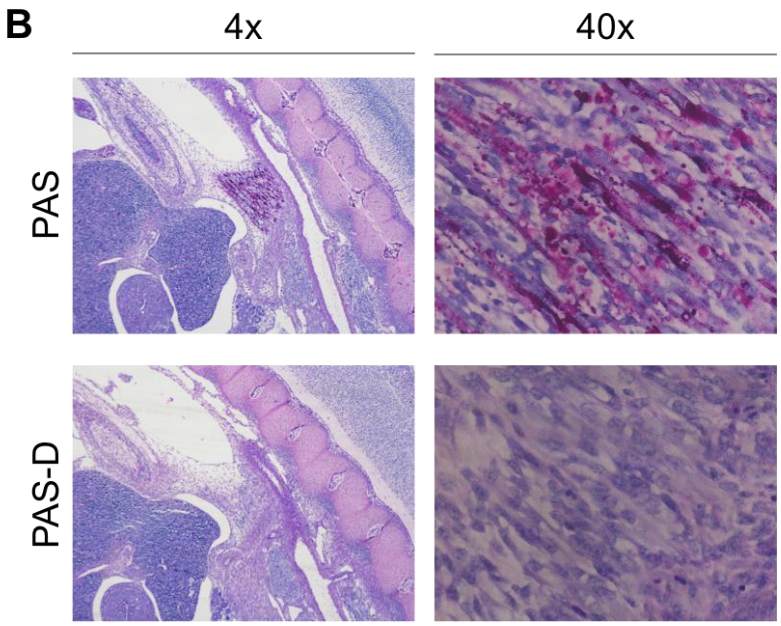


**Figure 11. PAS and hematoxylin stain-** A) Serial section of 18.5 dpc embryo heart stained with PAS, with or without diastase. B) PAS staining and diastase treatment in skeletal muscle.

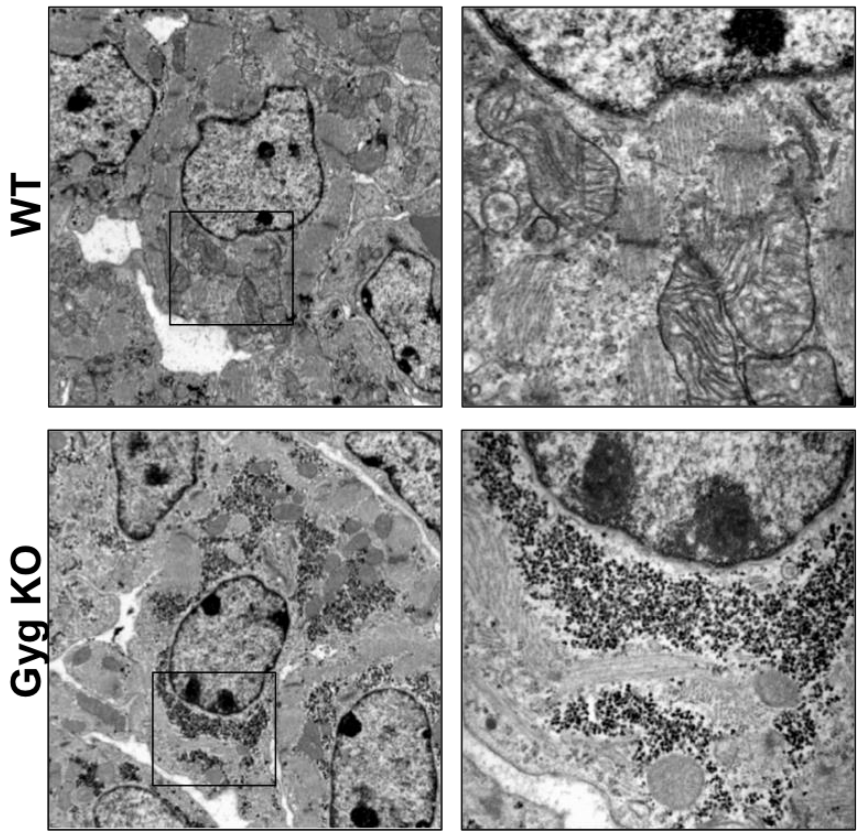


**Figure 12. Magnification of glycogen in Gyg embryo-** EM images of cardiomyocytes from 18.5 dpc embryos.

The conclusion that Gyg KO mice not only maintain the ability to synthesize glycogen, but also accumulate high levels of the polysaccharide was unexpected. To confirm glycogen levels in Gyg KO embryos, we performed a biochemical measurement of glycogen in different tissues. All of the tissues we tested (heart, muscle, liver and brain) presented glycogen accumulation **(Figure 13)**. This observation confirms that glycogen can be synthesized in the absence of glycogenin. Interestingly, the liver and brain of Gyg KO embryos contain about a third of the glycogen content in the same tissues of Gyg heterozygous mice.

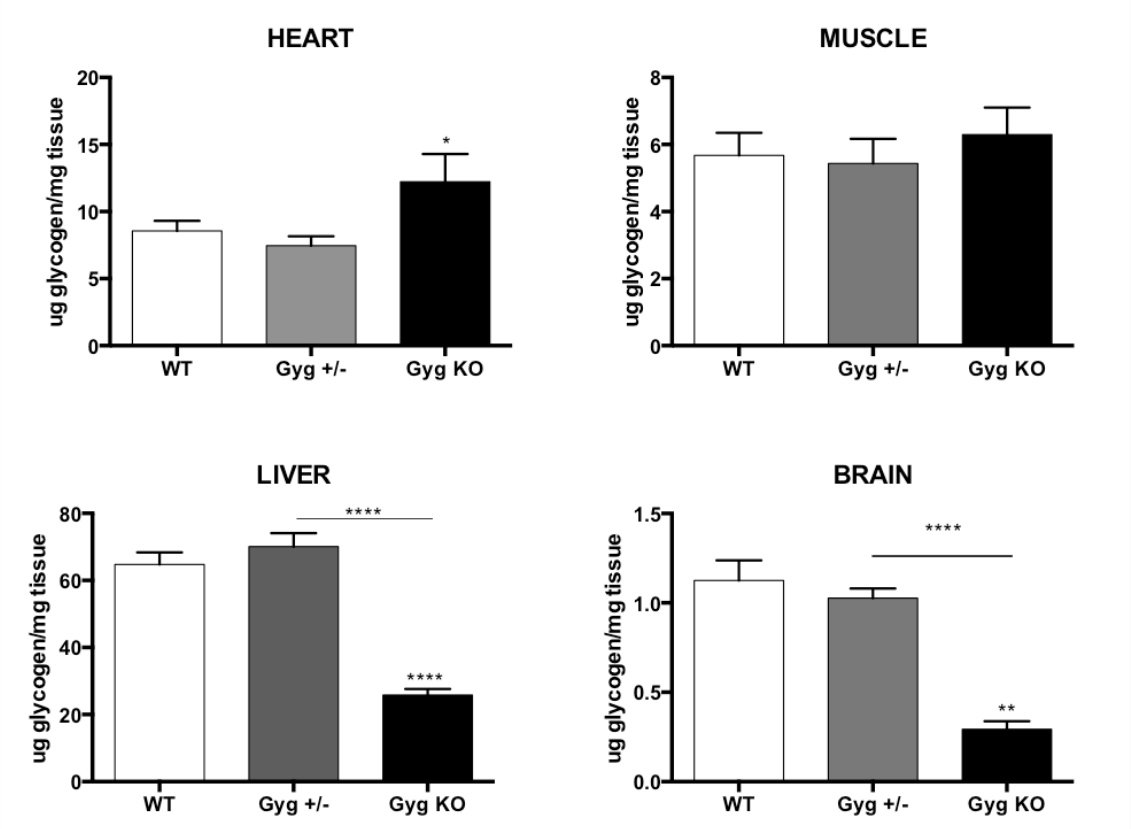


**Figure 13. Glycogen measurement in 18.5 dpc embryos-** Biochemical measurement of glycogen in embryos (n=6)

## 2.2 Generation of Gyg Del animal model

The observation that glycogen is generated in Gyg KO animals is unexpected and challenges the bases upon which the biochemistry of glycogen synthesis is

built. The Gyg KO mouse model was based on an insertion cassette that contains two poly(A)-signals to interrupt protein translation. However, in order to discard the possibility that the gene was partially expressed, we generated a new mouse (Gyg Del), crossing our previous mouse carrying the Gyg KO allele, with a Ub-Cre recombinase expressing mouse (UBC-cre-ESR1). The constitutive expression of the recombinase acts on the *loxP* sites of the insertion cassette, surrounding the exons 3 and 4, and removing them from the allele (Gyg Del) **(Figure 14)**. The excised allele is compromised and no possible translation can occur. To study this mouse model, we analyzed 18.5 dpc embryos and we confirmed the same glycogen accumulation we previously observed **(Figure 15)**.

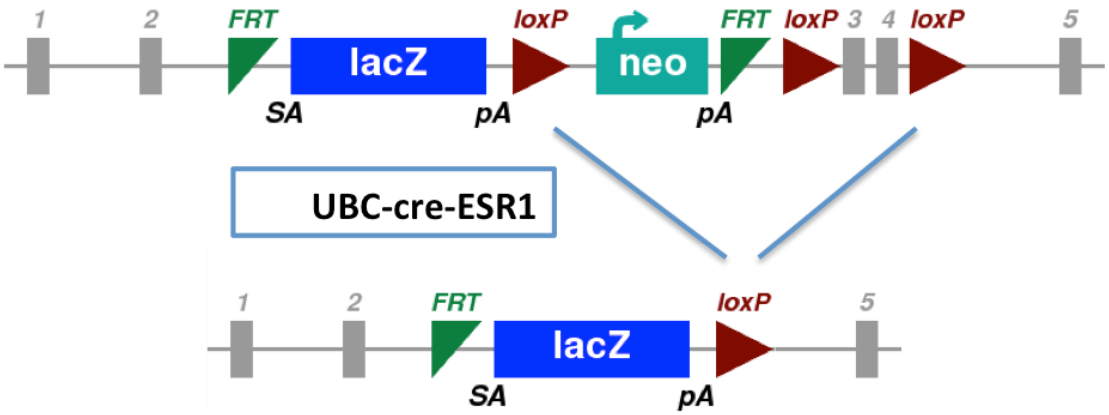


**Figure 14 Excision of the Gyg KO allele-** Ubiquitously expressed Cre recombinase act on loxP sites of the cassette allowing recombination and excision of the exons 3 and 4. All mice are genotyped with specific probes to identify the presence or absence of the exons.

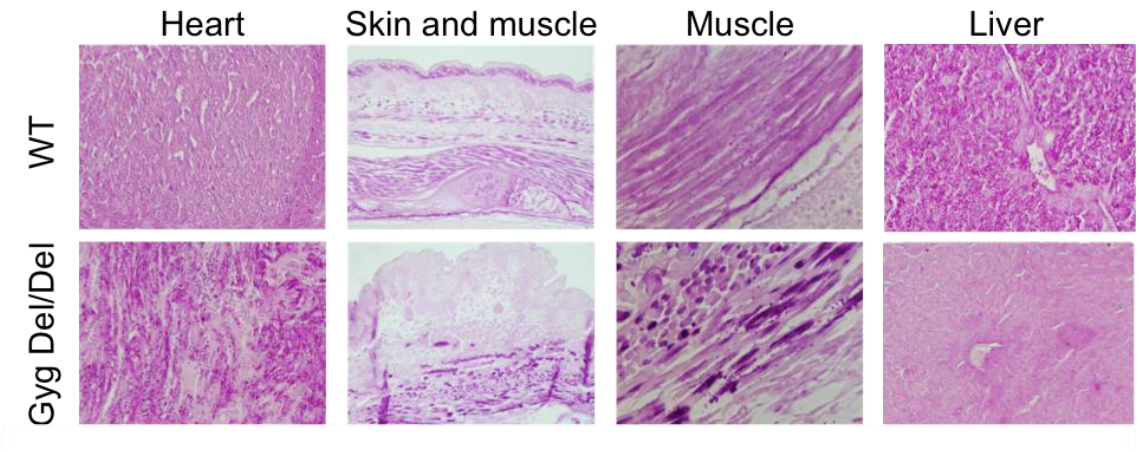


**Figure 15. PAS staining of Gyg Del embryos at 18.5 dpc-** Observation of different tissues stained with PAS.

# 3. Characterization of adult Gyg KO animals

## 3.1 Glycogenin depletion does not impair weight and size of the mice

Gyg KO pups that are able to survive past birth, about 10% of total pups, can reach adulthood and longevity is not compromised (up to 2 years old, as in WT littermates). Surviving Gyg KO mice do not show an overt phenotype or defect in standard conditions. Moreover, size and weight increase during the aging process in the same way as their control counterparts, and no differences between genders are observed **(Figure 16).**

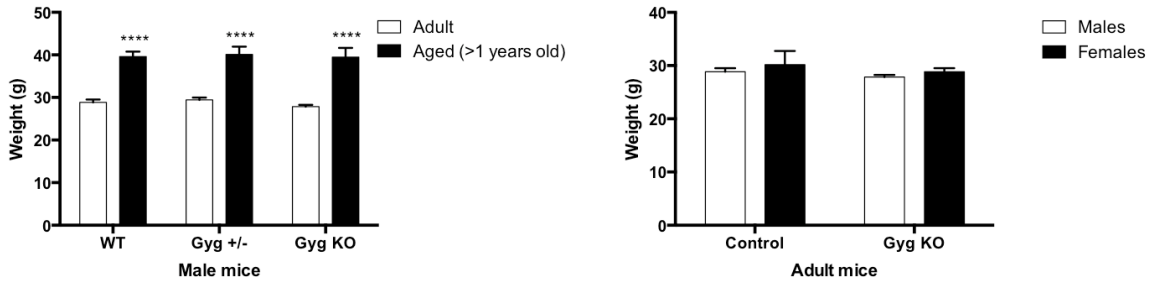


**Figure 16. Body weight of Gyg KO mice** – Left panel: comparison during aging; right panel: comparison between genders. Adult = 18 weeks old. Right panel: animals are 18 weeks old

## 3.2 Glycogenin mRNA and protein detection

To proceed the characterization of Gyg KO animals, we first analyzed RNA and protein levels in 18 week old mice. Relative gene expression clearly shows the absence of the Gyg transcript in the KO animals, while Gyg heterozygous mice express half the levels of WT animals **(Figure 17)**.

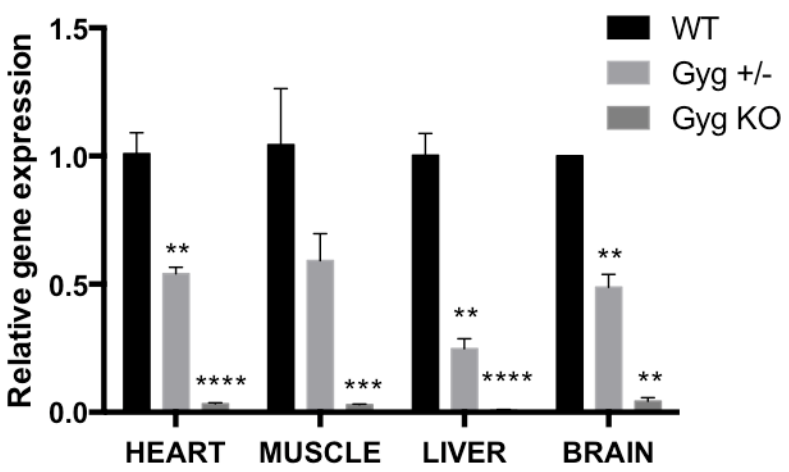


**Figure 17. Relative level of glycogenin transcript**- Quantitative determination of mRNA by SYBR-green of Gyg in different tissues and normalized to 18S expression levels

Western Blot analysis was performed to confirm the lack of glycogenin at the protein level. The sample is digested with amylase in order to liberate glycogenin from glycogen, thus facilitating the entry of the protein into the gel. **Figure 18** shows that muscle, heart, liver and brain are depleted of glycogenin in Gyg KO animals. Moreover, Gyg heterozygous animals retain only half of the protein levels in the tissues analyzed, when compared to WT animals.

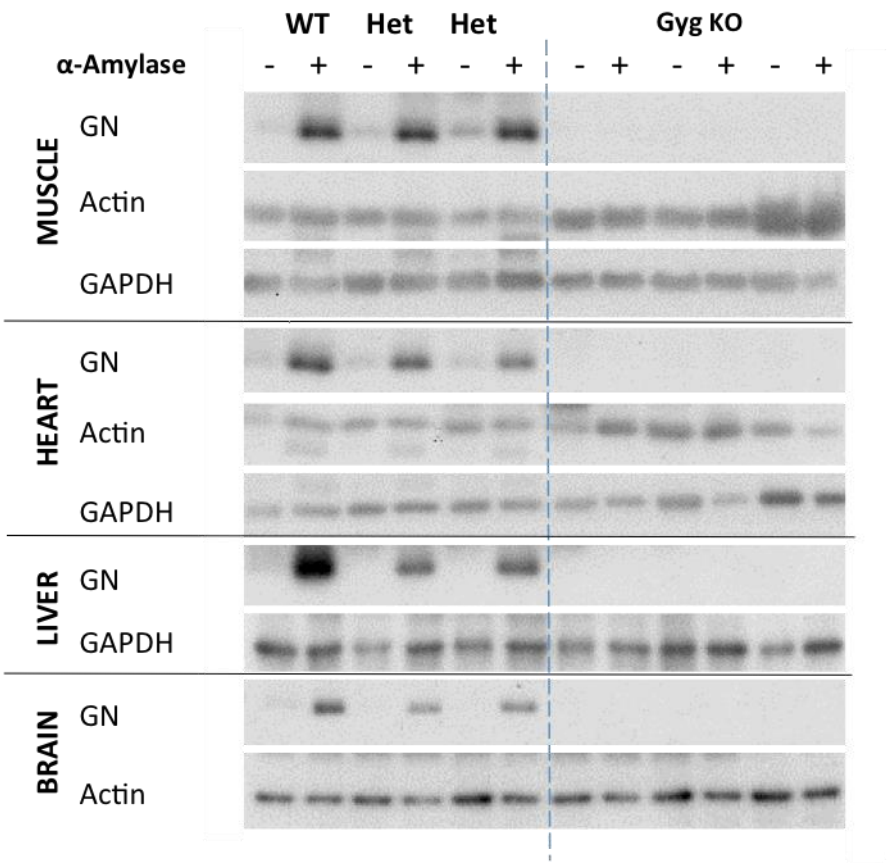


**Figure 18. Detection of GN levels in different tissues.** Gyg KO show complete depletion of the protein, whereas Gyg heterozygous show a decreased amount when compared to WTs**.** β - actin and GAPDH were used as loading controls.

## 3.3 Glycogen measurement in surviving Gyg KO mice

To rule out the possibility that surviving Gyg KO pups made it through birth because of normal glycogen storage, we measured the glycogen levels of four different tissues in adult Gyg KO male mice (18 weeks old) and their WT and Gyg +/- littermates **(Figure 19)**. Gyg KO adult mouse hearts accumulate an average of 6 times more glycogen than in WTs, and 3 times more than in heterozygotes. Gyg KO skeletal muscle shows about an 8-fold and 3-fold increase in glycogen compared to WT and Gyg +/-, respectively. On the other hand, glycogen in the liver and brain is not differently accumulated in terms of quantity. Nevertheless, it is important to note that both of these tissues retain the ability to synthesize glycogen in Gyg KOs.

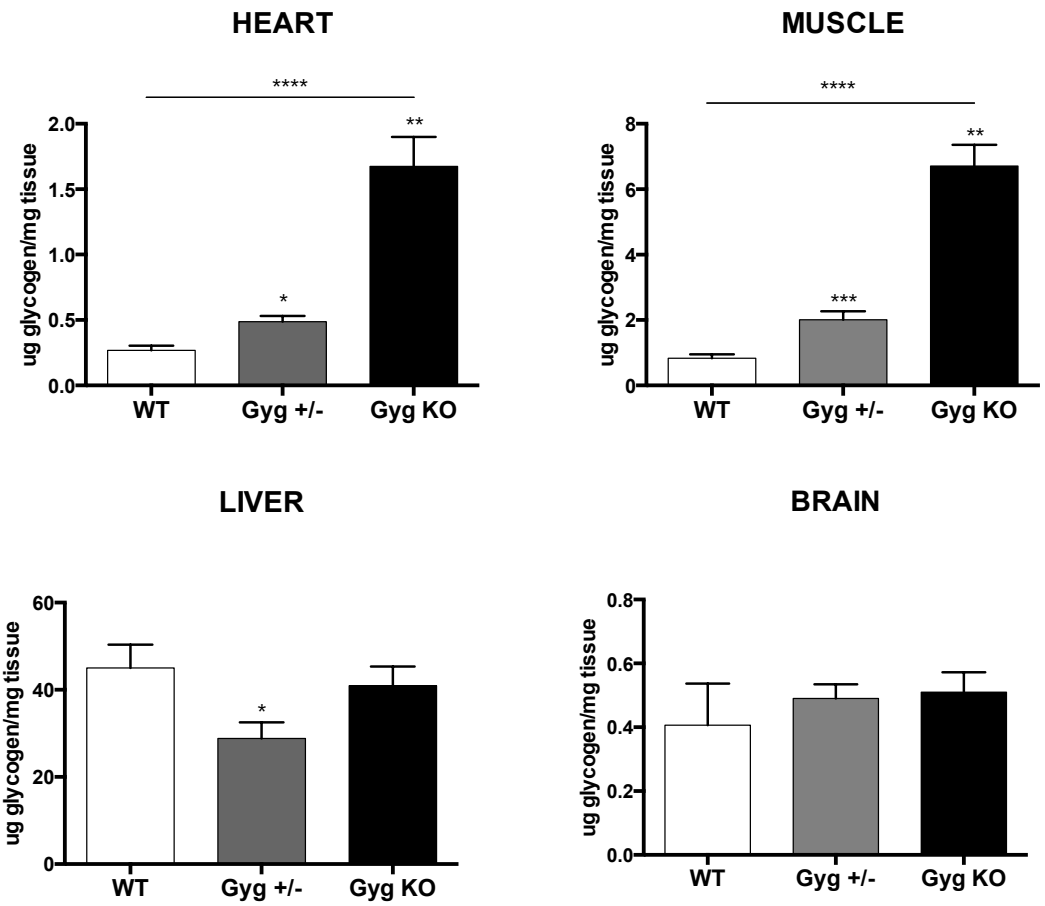


**Figure 19. Glycogen measurement in adult males**- Comparison of glycogen content in different tissues and among littermates of the genotypes: WT, Gyg +/- and Gyg KO. Animals were 18 weeks old (n=6).

By staining adult tissue with PAS, we confirmed the biochemical measurements of glycogen content in the muscle and heart. On the other hand, in brain we corroborate that no glycogen accumulation is observed **(Figure 20)**.

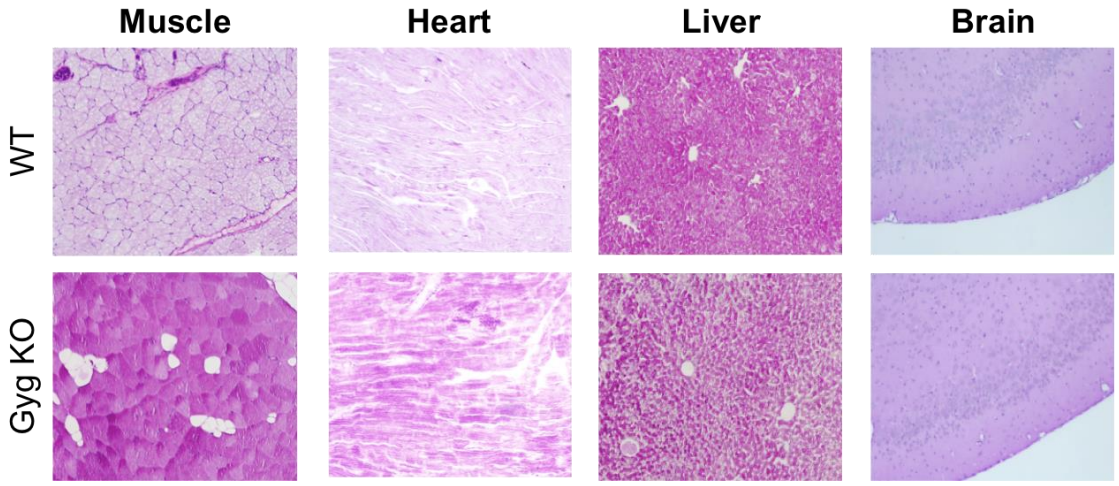


**Figure 20. PAS staining in adult male mice**- Comparison between WT and Gyg KO. Muscle was snap frozen in OCT blocks. Heart, Liver and Brain sections were embedded in paraffin blocks after perfusion of the animal with 4% PFA.

We also analyzed possible gender-dependent differences in glycogen amounts, however none of the tissues analyzed revealed a difference between genders **(Figure 21).**

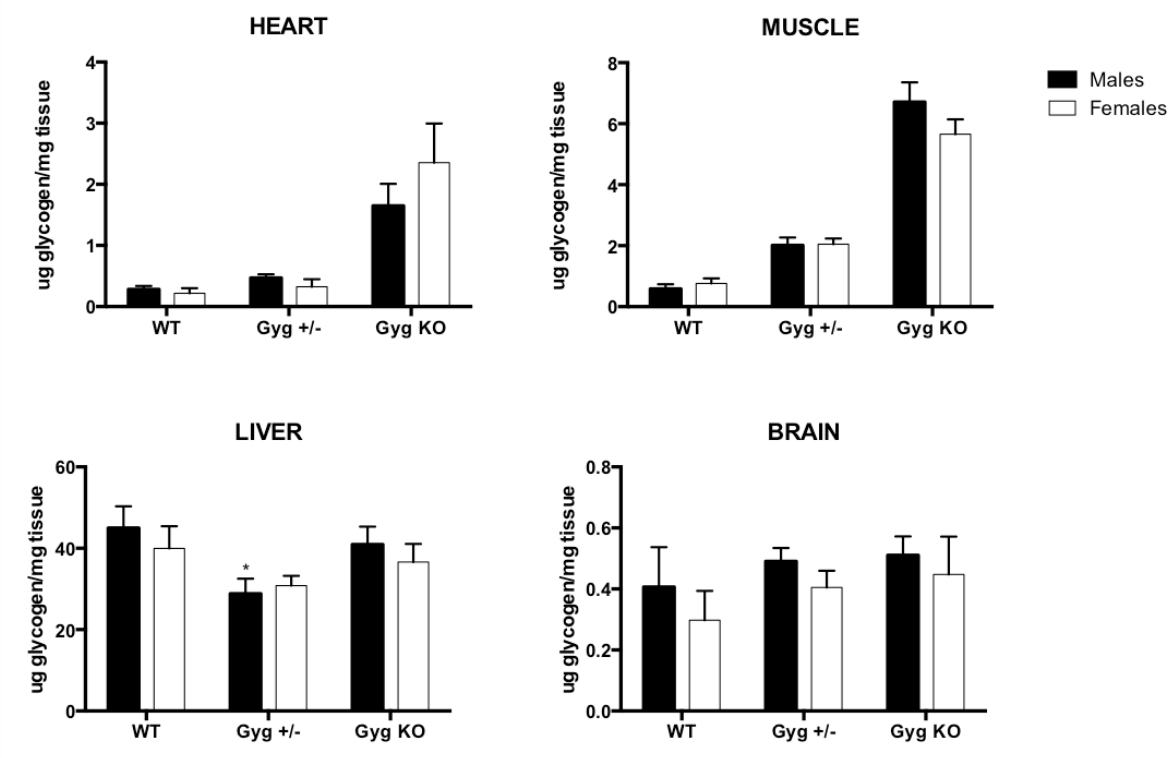


**Figure 21. Glycogen measurement: comparison between genders**- Males and females of 18 weeks of age were compared based on the tissue type (n=6)

Furthermore, we studied whether the accumulation of the polysaccharide progressively increases with age. We compared different age groups: adults between 18 and 25 weeks old, 1 and 2 year old mice **(Figure 22)**. We confirm that glycogen levels are maintained with age in the liver and brain. Gyg heterozygous muscle samples, however, show comparable glycogen content to the muscles of 2 year old Gyg KO animals.

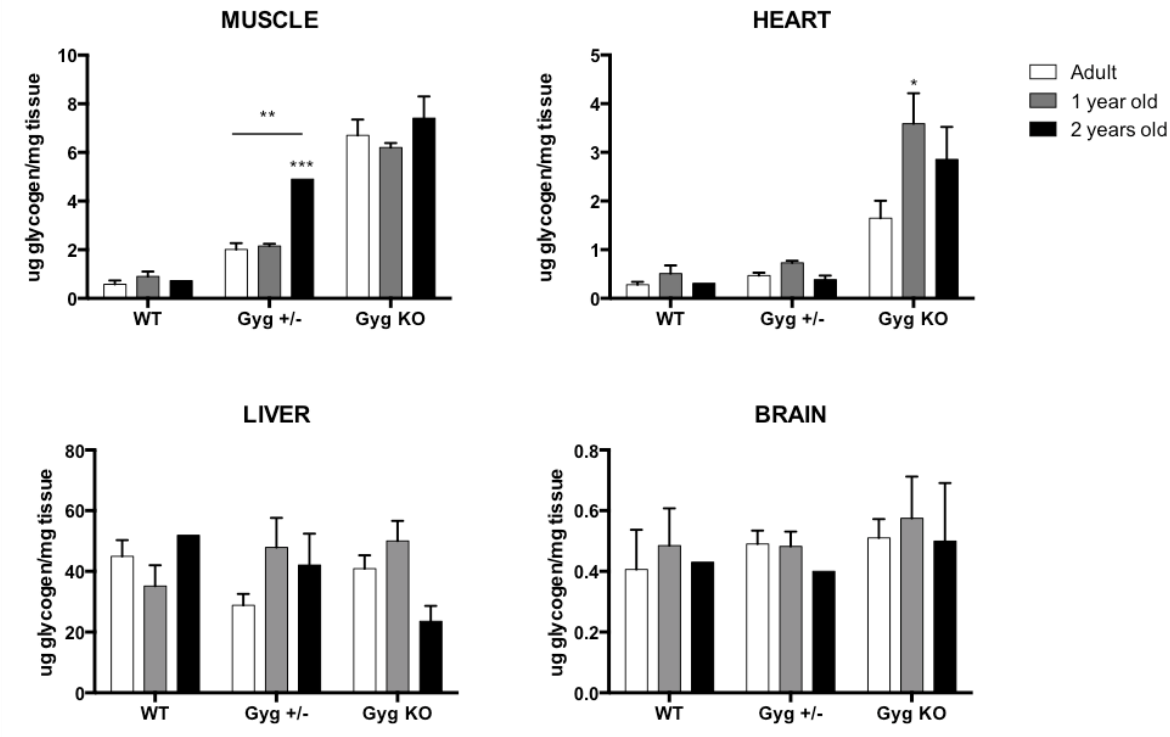


**Figure 22. Glycogen measurement: comparison between 3 different ages-** Analyses of glycogen from different tissues from males of 18-25 weeks old, 1 and 2 years old.

## 3.4 Conclusions

We observed that 10% of Gyg KO mice are able to survive after birth despite increased glycogen content in the heart and muscle. We hypothesize that this can be due to milder heart damage, thus preventing perinatal death.

The most remarkable observation, however, is that glycogen synthesis occurs despite the total absence of the initiator protein. Even more unexpected is the fact that the muscle and heart of Gyg KO animals contain significantly higher glycogen levels compared to control littermates. This accumulation does not

affect longevity, and at first glance, mice do not show major physical phenotypical changes when compared to control animals. In the following chapters, in depth analyses are conducted in order to characterize Gyg KO phenotypes and the consequences of glycogen accumulation.

# 4. Characterization of glycogen synthesized in absence of glycogenin

## 4.1 Introduction

Mutations of genes involved in glycogen metabolism drive the onset of specific pathologies, named glycogen storage diseases (GSDs), which are characterized by glycogen accumulation. These include Lafora, McArdle (GSD V) and Andersen diseases (GSD IV).

Some of these GSDs are characterized by the formation of polyglucosan bodies, abnormally structured accumulations of glycogen and proteins which are not degradable. The first experiments assessed in our Gyg KO model lead us to hypothesize that this is another case of polyglucosan body accumulation. In order to be considered a polyglucosan body, glycogen should present some or all the following characteristics: be amylase resistant, a lower branching degree, lower solubility, and a high phosphate content.

## 4.2 Analysis of Gyg KO glycogen

In muscle and heart preparations, glycogen is localized mainly in the cytoplasm and large accumulations are not present **(Figure 20)**. In order to further analyze glycogen granule distribution and to determine whether glycogen associates with certain cellular organelle and structures, we performed electron microscopy imaging (EM). In EM, glycogen is depicted as small black granules, which represent the glycogen β particles. In order to avoid artifacts that may arise from sample preparation techniques, we performed, in parallel, a specific and delicate polysaccharide staining methodology, known as Thiery staining **(Figure 23).** A comparison of the two techniques reinforced that glycogen staining by the conventional EM method is specific.

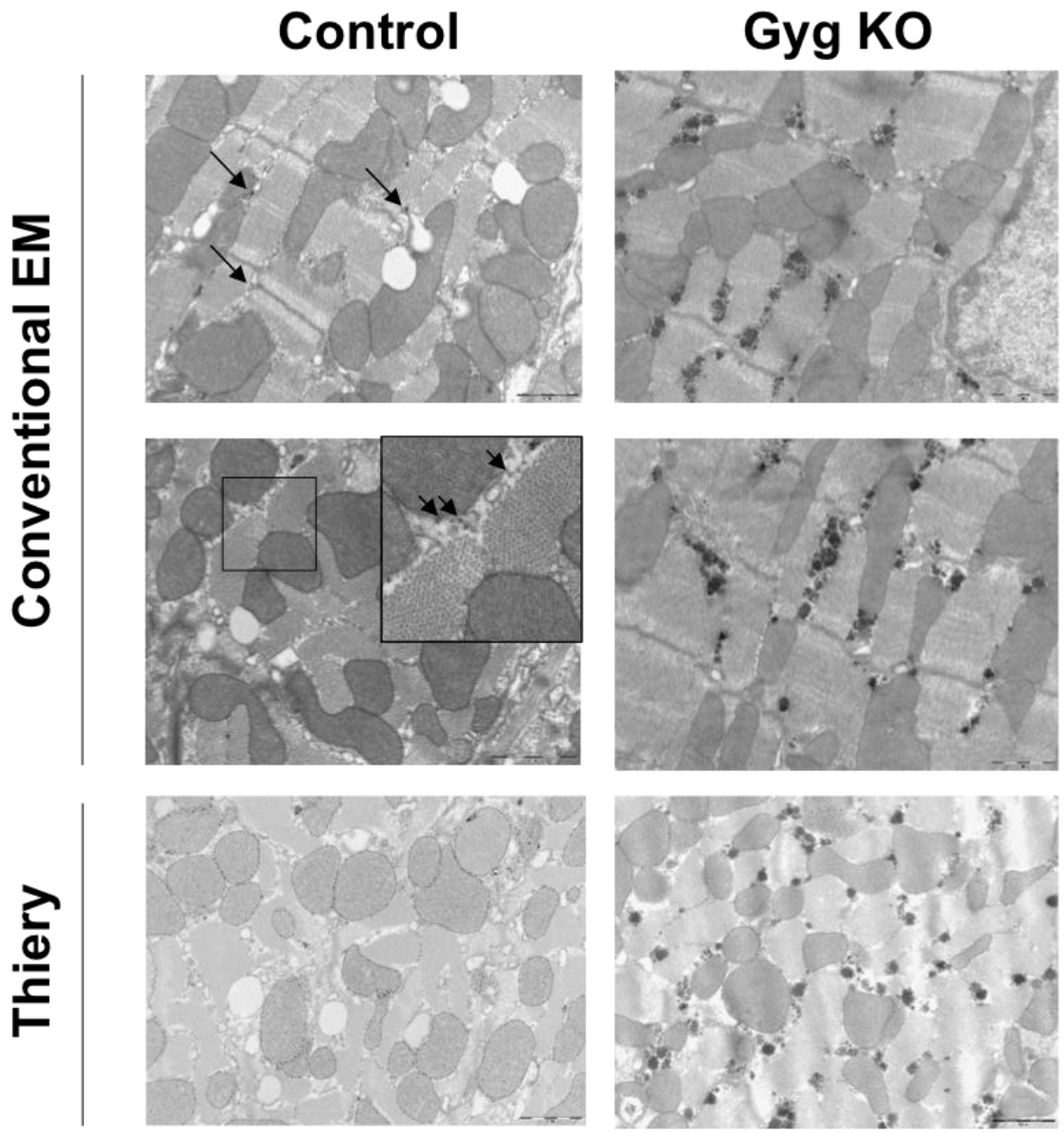


**Figure 23. Comparison of techniques for glycogen detection by EM imaging in heart**- Staining to polysaccharide-specific detection by conventional and Thiery's methods. Arrows indicate localization of glycogen granules. Square represents a magnification of the area. Scale bar = 1um

First, we observed that more glycogen was present in Gyg KO than in WT animals. Secondly, glycogen is localized at myofibril edges, either exactly between them or in the space between fibrils and mitochondria, in both WT and Gyg KO muscle tissue (cardiac and skeletal). More specifically, glycogen localizes near the Z-disk in both WT and Gyg KO heart tissue samples **(Figure 24).**

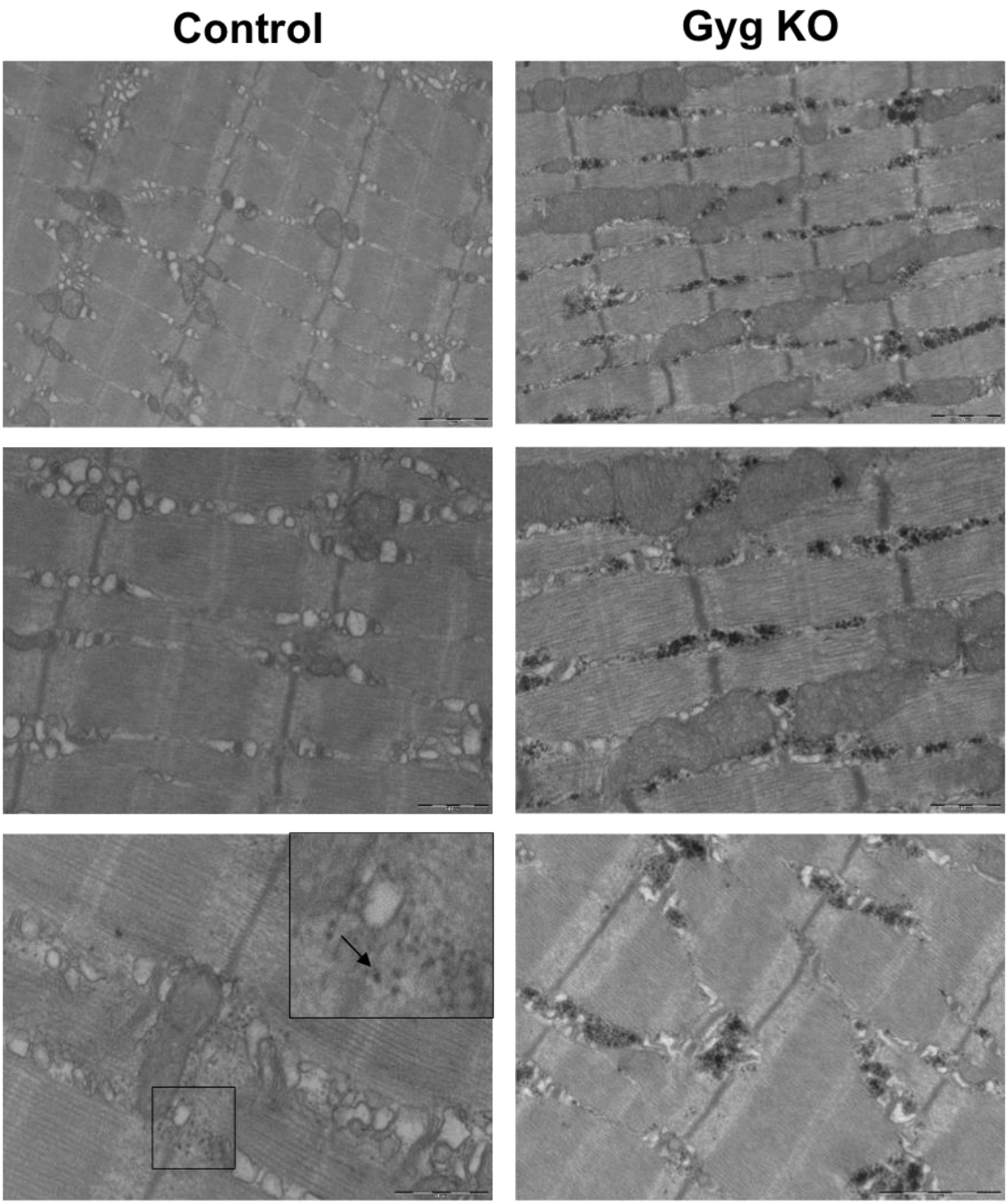


**Figure 24. EM imaging in quadriceps**- Glycogen is located between myofibrils. Sarcomeres, Z-disks and actin microfilaments are also visible

### 4.2.1 Size and shape of glycogen granules

Comparing the glycogen granules from our Gyg KO to a LD mouse model (Malin KO) where polyglucosans are described to accumulate, we observed that the size, shape and distribution were significantly different **(Figure 25).** In fact,

Malin KO muscle and heart accumulate large Lafora bodies, while the glycogen in Gyg KO appears to be quite different as granules are smaller and more widely distributed to cover the whole surface of the cell. LBs, on the other hand, are bigger and exhibit a more uneven distribution in muscle fibers.

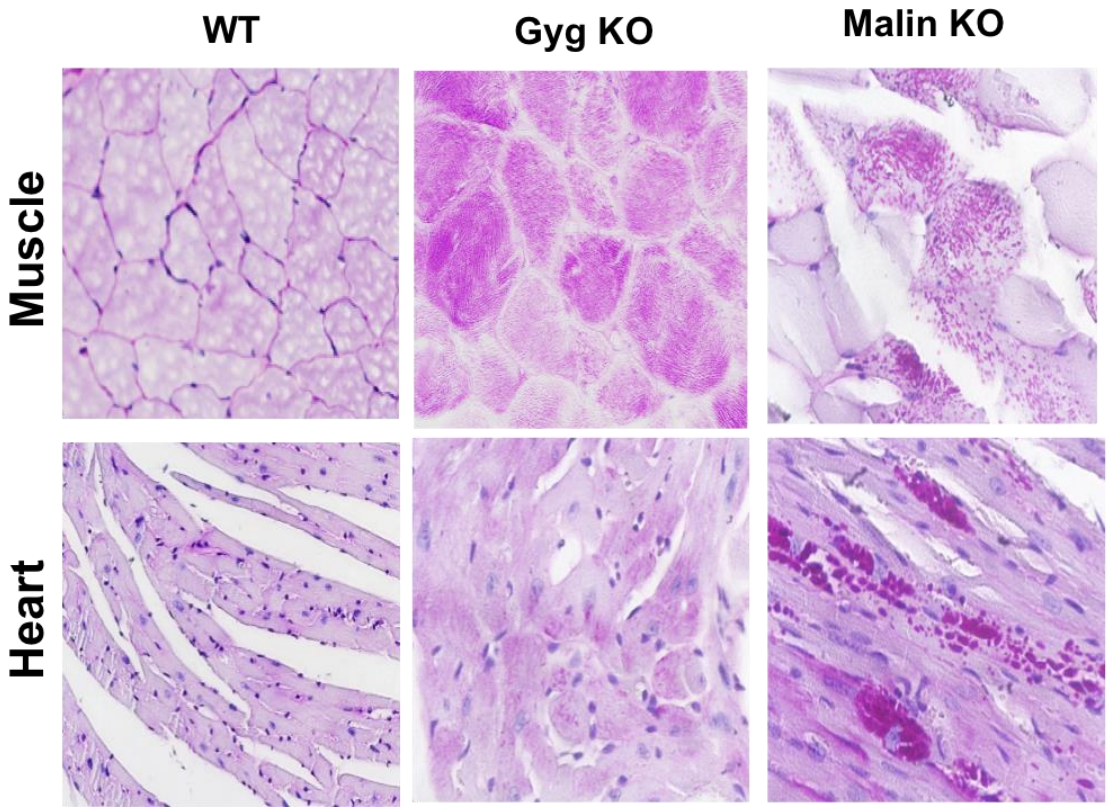


**Figure 25. Comparison of Gyg KO and Malin KO-** PAS staining of muscle and heart specimens from WT, Gyg KO and Malin KO adult animals perfused with 4% PFA. Tissues were embedded in paraffin blocks

### 4.2.2 Resistance to amylase treatment

To analyze the resistance of the granule to amylase degradation, we performed diastase digestion in heart and muscle sections **(Figure 26)**. No PAS positive material was detected after amylase treatment, suggesting a normal degree of degradability of the polysaccharide (as previously observed in embryos).

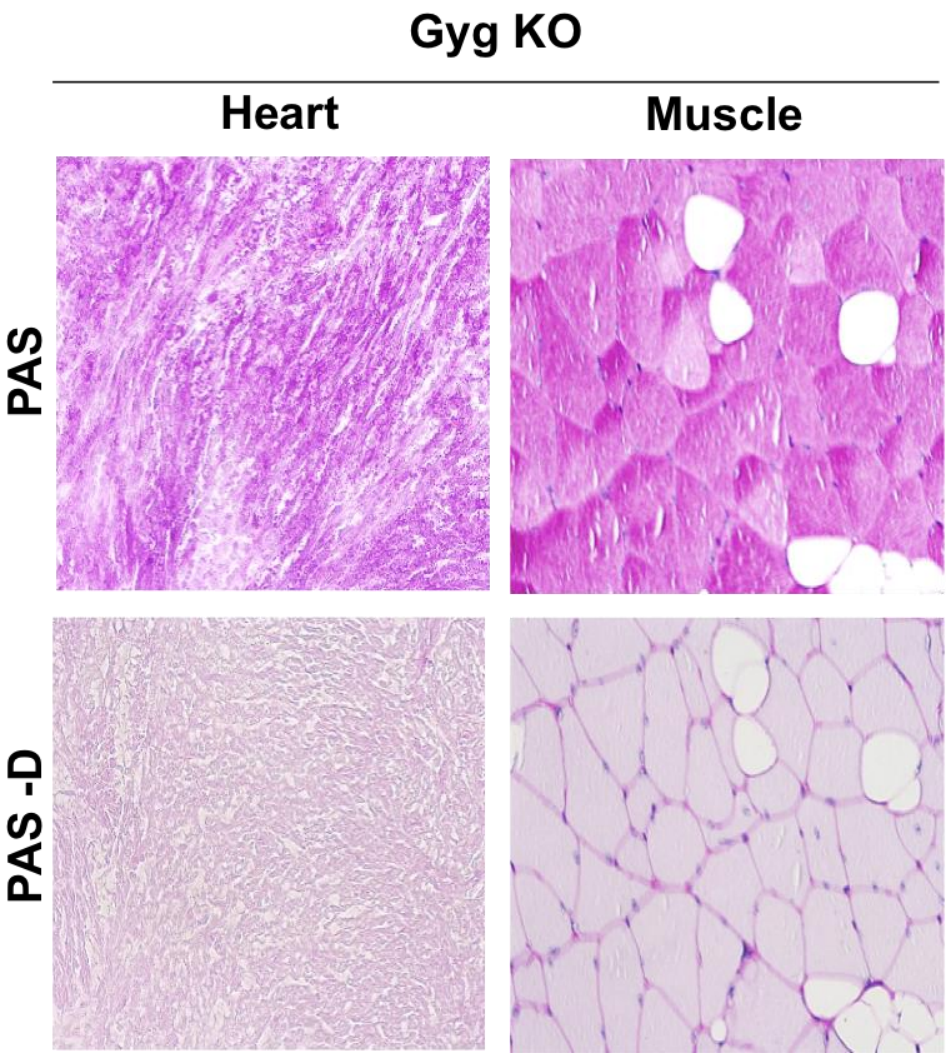


**Figure 26. Diastase treatment and PAS stain in adult tissues**- Sample from adult Gyg KO model. Heart specimen embedded in paraffin blocks. Muscle specimens were frozen in OCT blocks.

### 4.2.3 Degradation of glycogen under energetic request *in vivo*

We also tested *in vivo* glycogen degradability by subjecting mice to an overnight fast, followed by treadmill exercise until exhaustion. In this scenario, both the liver and muscle should be depleted of their glycogen reserves. We then compared glycogen content in these tissues before and after exercise **(Figure 27).**

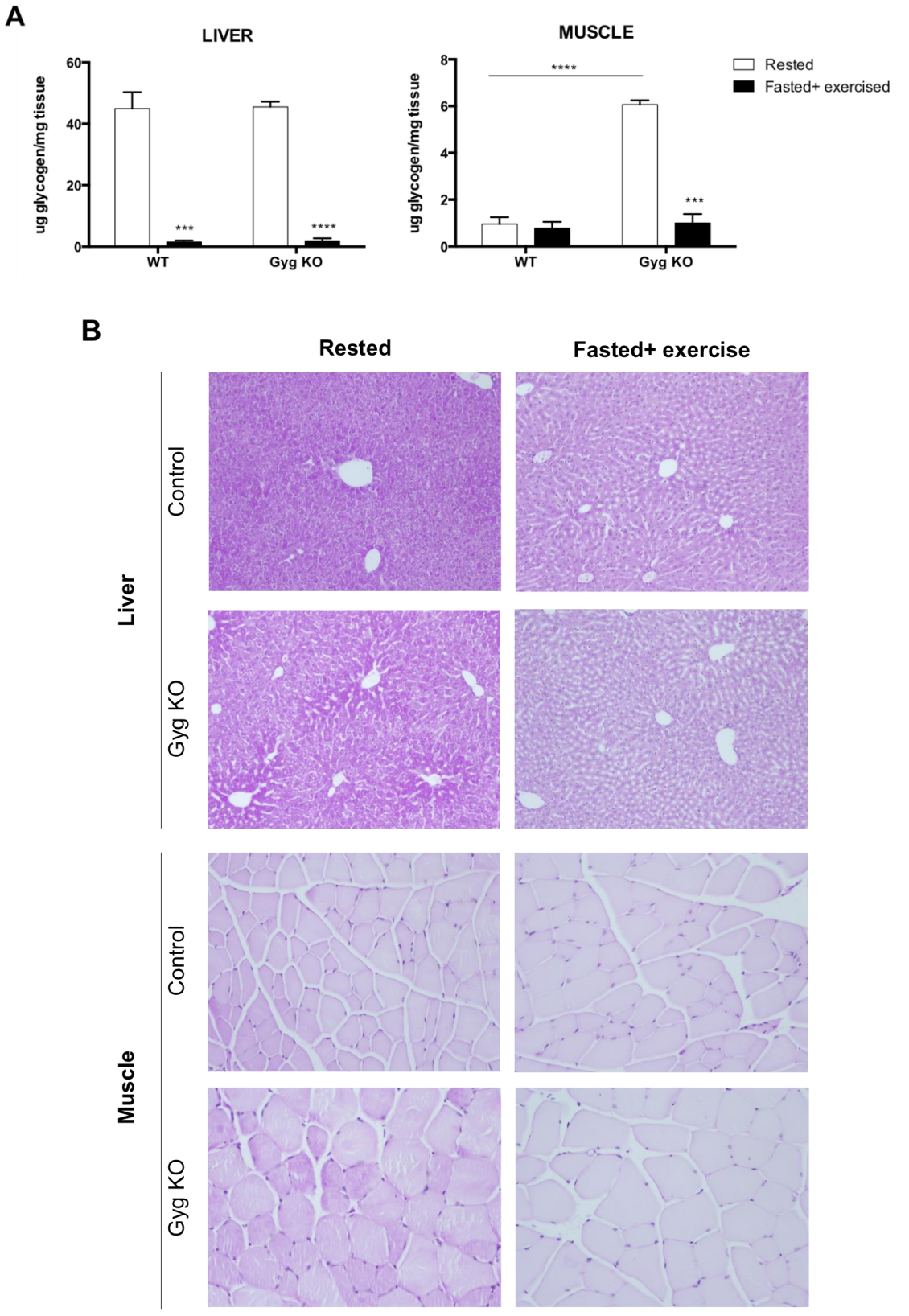


**Figure 27. Glycogen after fasting followed by treadmill exercise-** Adult males (n=5) subjected to fasting and exercise to exhaustion (see material and methods). A) Glycogen level by biochemical measurement from frozen tissue after cervical dislocation. B) PAS stain of different tissues from perfused animals and paraffin embedded tissues.

We observed that under these conditions, Gyg KO mice almost completely degrade their glycogen reserves. This is quite significant considering the fact that glycogen levels in the muscles of Gyg KO mice are much higher than in WT animals. More experiments are shown in chapter 7.

### 4.2.4 Glycogen branching degree

Polyglucosan bodies, such as Lafora bodies, are characterized by poorly branched glycogen. Normal mammalian glycogen has branching points (α-1-6, linkage), on average, every 12 glucose residues. We determined the branching degree of glycogen purified from Gyg KO mice by measuring the visible absorption spectrum using an iodine method developed by Krisman (Krisman CR, 1962). Iodine intercalates into glycogen chains, which allows us to determine characteristic iodine spectra based on glycogen branching level and on the length of uninterrupted segments. This method detects branching level variations between glycogen, amylopectin (branching every ≈ 30 residues) and amylose (linear chain). No difference in the level of branching degree was detected between the glycogen purified from WT and Gyg KO animals **(Figure 28)**.

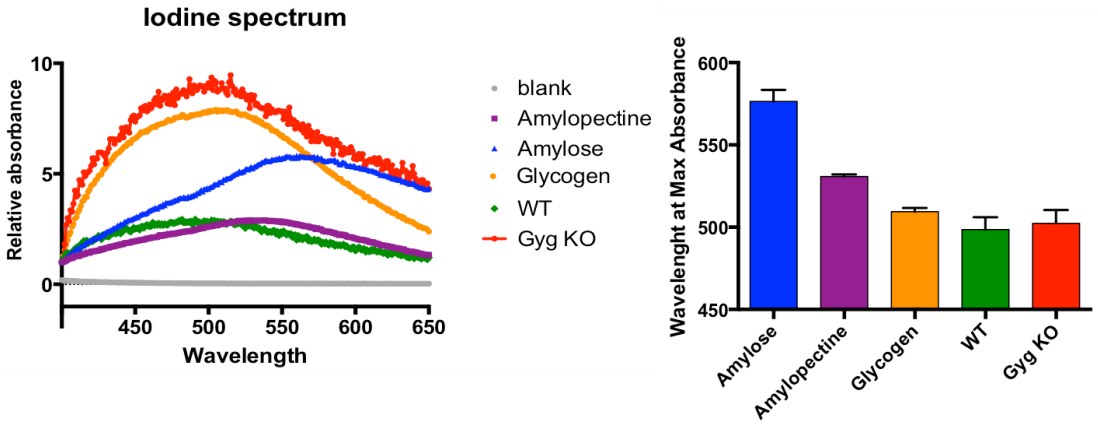


**Figure 28. Glycogen branching degree determination by Krisman assay-** A) Iodine spectrum obtained measuring relative absorbance of samples at different wavelength. Max absorbance is reported in B).

### 4.2.5 Level of glycogen phosphate

Another characteristic of LBs is the level of glycogen phosphorylation. In collaboration with Anna De Paoli-Roach's laboratory, we were able to quantify phosphate levels in Gyg KO glycogen. Despite the fact that total glycogen phosphate is higher in Gyg KO, we have to take into account that there is more glycogen in the Gyg KO skeletal muscle **(Figure 29)**. Again, these data confirm that accumulated glycogen due to glycogenin depletion does not qualify as polyglucosan body-like glycogen. Gyg KO glycogen behaved normally during the purification: it was not water insoluble, which is a common characteristic of glycogen purified from animals with PGBs, such as Laforin and Malin KO mouse models. This is observation is consistent with no changes in glycogen phosphate and branching degree.

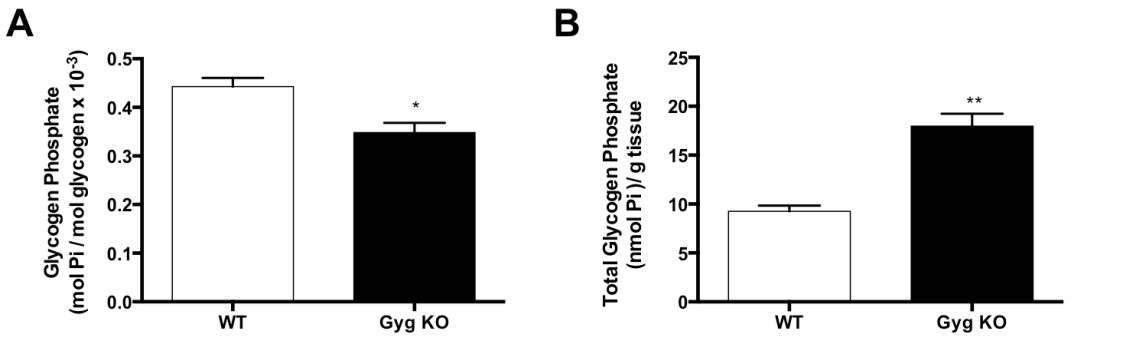


**Figure 29. Skeletal muscle glycogen phosphate level –** Data obtained from frozen skeletal muscle from WT and Gyg KO adult mice. A) Level of phosphate per mol of glycogen; B) Phosphate level per gram of tissue. The absolute value of glycogen phosphate is higher due to the increased glycogen level. (Font. Dr. Anna DePaoli-Roach, University of Indiana)

To further understand the reason behind lower glycogen phosphate levels in Gyg KO animals, we measured Laforin levels, which is the enzyme responsible for glycogen dephosphorylation. Indeed, Laforin protein levels were increased in Gyg skeletal muscle compared with WT animals **(Figure 30).**

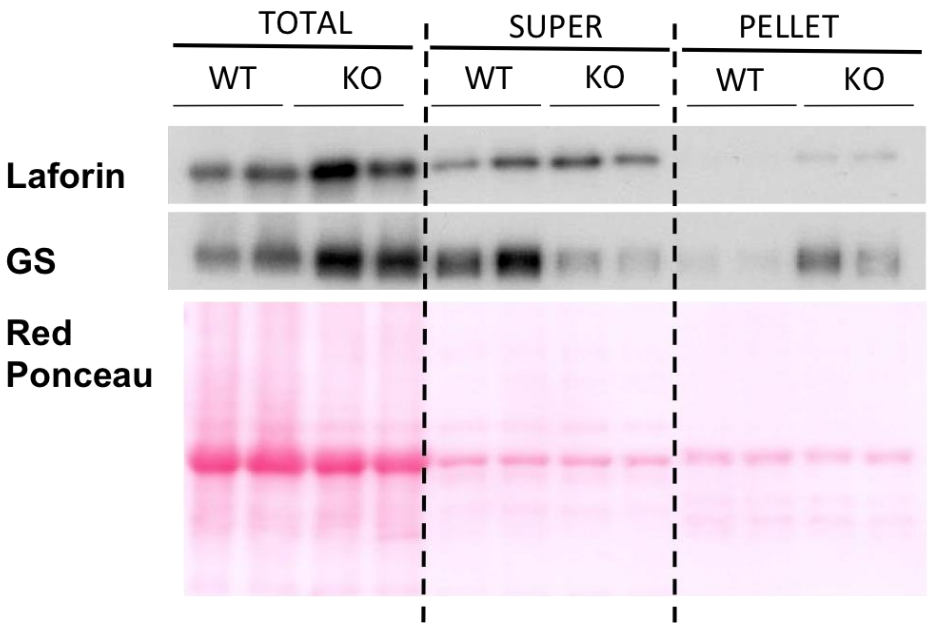


**Figure 30. WB of Laforin in WT and Gyg KO skeletal muscle**- Loading of total homogenate, supernatant and pellet fraction obtained by low speed centrifugation. Comparison of 2 samples from WT and Gyg KO. Loading control: Red ponceau.

## 4.3 Aged Gyg KO animals present lower levels of Corpora Amylacea

To compare Gyg KO glycogen to other situations of glycogen accumulation, we analyzed brains of aged mice. It has been extensively described that glycogen accumulation in the brain occurs with age, ultimately generating Corpora Amylacea (CAs). It is known that in the brain, both neurons and astrocytes have the machinery for glycogen synthesis and degradation. Although glycogen metabolism is very rapid, and the turnover of glucose is very fast, glycogen storage is often low in normal conditions. During aging, glycogen is in complex with many proteins, and neurons are no longer able to degrade glycogen accumulates. CAs have a similar formation process to Malin KO operated by MGS, but in terms of speed and quantity CAs accumulation is much lower.

We do not observe changes in glycogen content along the aging process in Gyg KO mice when compared to WT counterparts. Techniques available for glycogen measurement are not sensible enough to detect glycogen increases in the brain due to CAs. On the other hand, great quantity of polysaccharide is

localized in a single spot, and this localization makes possible to detect it with tissue staining. For this reason we performed a PAS staining in brain of one-year-old mice **(Figure 31).** As expected control mice show presence of CAs in both hippocampus and cortex, although in significant minor degree than the accumulation of Lafora's bodies in Malin KO of 4 months of age (Valles-Ortega et al. 2011). The pattern observed in Gyg KO mice consists in lower glycogen accumulation than control littermates, distributed all over the tissue and not in the typical clusters. Higher magnification images taken from electronic microscopy are included to show closer details **(Figure 32)**.

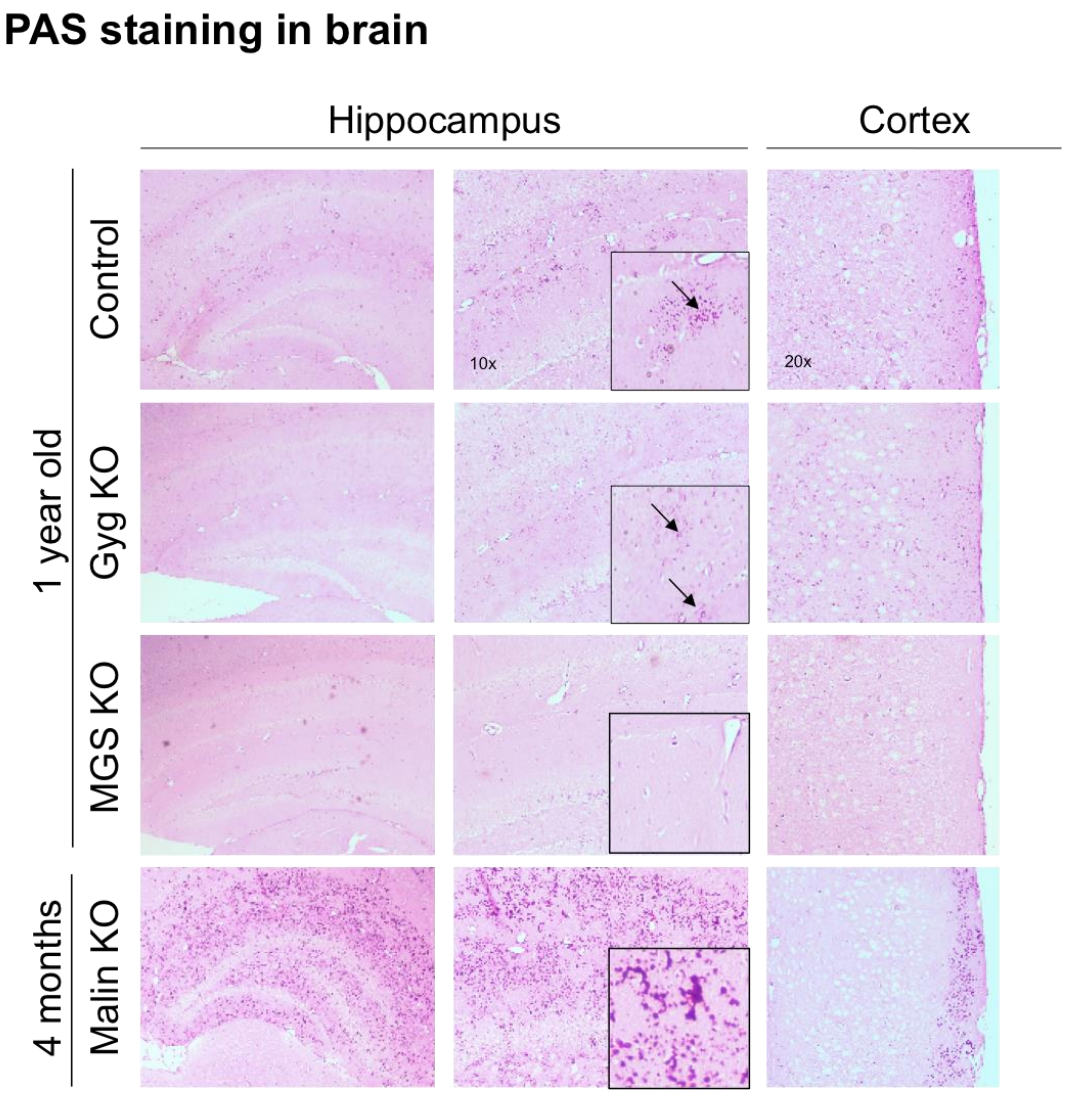


**Figure 31. PAS stain of brain sections** – Comparison of mice brain sections. 4 months-old Malin KO brain is a positive control of LBs (as reported in Ortega-Vallés et al, 2011). 1 year-old MGS KO brain is a negative control for glycogen accumulation. Squares and arrows indicate PAS positive areas.

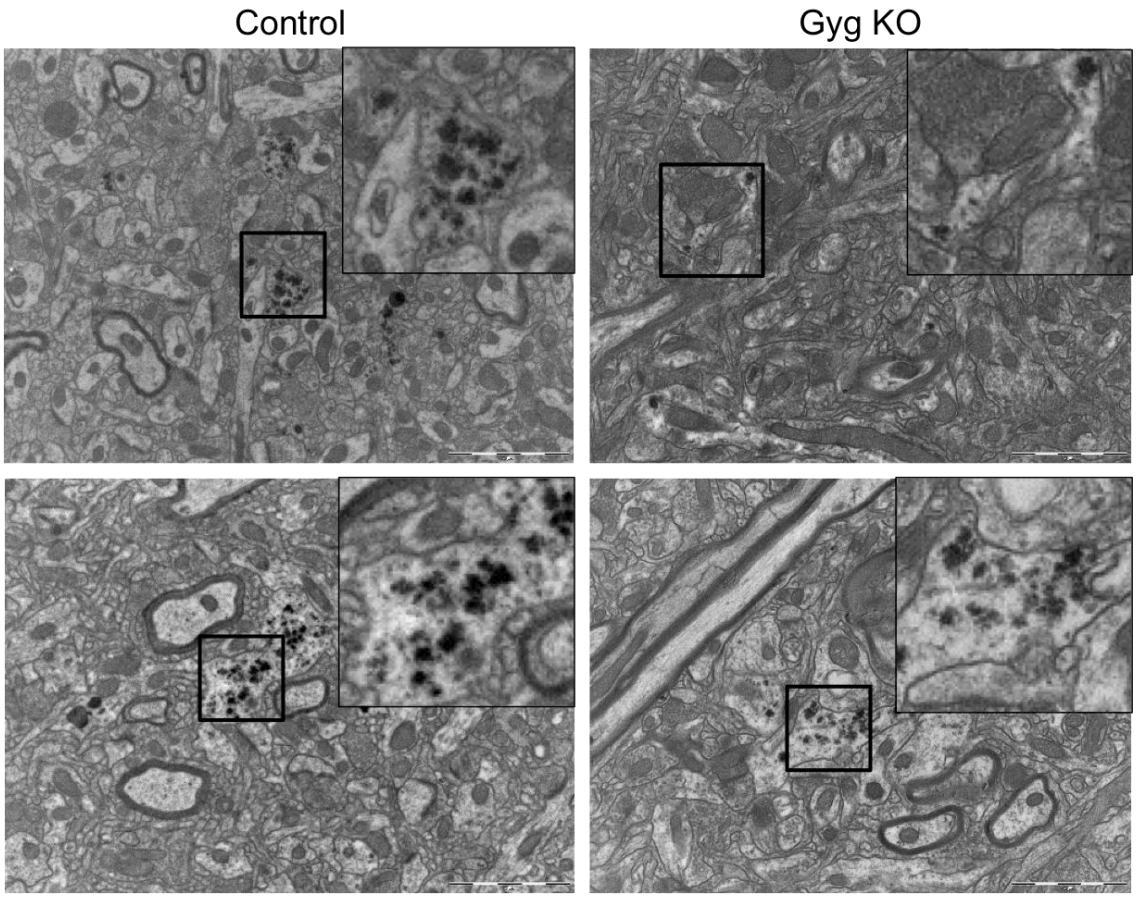


**Figure 32. EM imaging of Gyg KO brain –** Control panels show the structure of a typical CA in 1 year old mice. In the upper right panel reports some isolated glycogen storages. Bottom right panel shows rare accumulations.

By EM imaging of brain, we were able to identify two different situations of glycogen in Gyg KO brain. Glycogen content in aged Gyg KO brains is sparser compared to easy-to-find CAs of control animals. Nonetheless it is possible to identify some rare bigger aggregates similar to CAs **(bottom right panel Figure 32).**

## 4.4 Conclusions

From all the analysis we, we can definitely state that glycogen accumulating by the depletion of glycogenin does not qualify as polyglucosan body-like glycogen. In fact its grade of degradability (*in vitro* and *in vivo*) and its branching level are considered normal.

# 5.

# 5. Search of a putative substitute protein for glycogen priming

## 5.1 Introduction

Facing the new evidence that glycogen synthesis can take place without the presence of glycogenin, one of the main objectives is to identify whether another protein is replacing glycogenin in its role to initiate glycogen synthesis. For the identification of the putative substitute protein for glycogenin we applied mass spectrometry technology to samples previously subjected to deep purification (protocol described in material and methods **Figure 82**).

## 5.2 Determination of glycogenin peptide profile

In order to be able to estimate the profile of peptides covalently bound to glycogen, we first determined the mass spectrometry profile of glycogenin, used as positive control in WT tissue. We expressed the mouse glycogenin protein in CGSC 4997, an E. coli strain lacking UDP-glucose pyrophosphorylase activity, to obtain apo-glycogenin (glycogenin free of glucose residues). Thereby the binding of glucose residues to glycogenin, which could obstruct its detection, is avoided **(annex 1 Supplementary tables)**. In total 104 peptides were identified after trypsin digestion, obtaining 80,10% of coverage of the entire protein. Five of those peptides contained Tyr195, the residue that covalently binds to the first glucose residue of glycogen **(Table 3)**.

**Table 3. List of peptides from purified GN containing Tyr195**

| **Peptide sequence** | |
|---|---|
| HLPFVYNLSSISIYS**Y**LPAFK | YNLSSISIYS**Y**LPAFK |
| SISIYS**Y**LPAFK | YS**Y**LPAFK |
| SSISIYS**Y**LPAFK | SIYS**Y**LPAFK |

## 5.3 Purification of glycogen from liver

The purification of glycogen particles aims at obtaining glycogen granules comprising all the proteins interacting with glycogen (glycogenome). Liver was chosen for the high availability of the tissue, fulfilling the requirement of a high amount of starting material. Along the steps of the purification protocol we checked for the presence of glycogenin **(Figure 33)**. Additionally, other proteins involved in glycogen metabolic pathways, previously described to be part of the glycogenome (Je-Hoon Ryua, 2009), were detected by WB

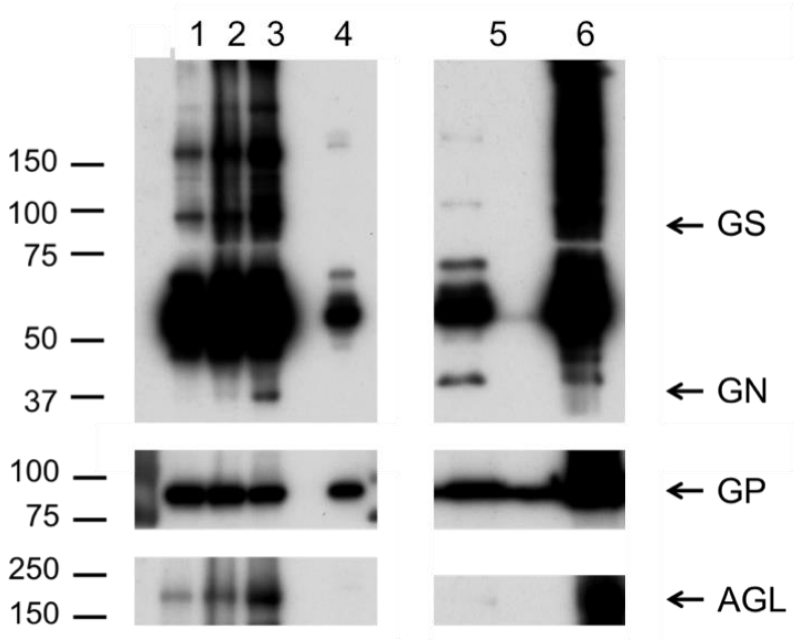


**Figure 33. Glycogen purification: protein detection along protocol steps-** Antibody detection of GS, GN, GP and AGL. Lanes: 1) Total homogenate, 2) Supernatant 6000g, 3) Supernatant 100K g, 4) microsomes, 5) Pellet 300K g with 2 fraction 25-50%, 6) Pellet at 100K g

By trypsin digestion all proteins non-covalently bound to glycogen were removed. In ideal conditions the remaining sample would include the whole glycogen granule together with the peptides directly bound to it. As expected, in WT tissue we identified GN peptides containing the tyrosine 195, the acceptor site for the covalent linkage with the first glucose residue. Hydrolysis of glycogen using either amylase or amyloglucosidase, followed by filtration,

allowed the elimination of all glucose residues. Alpha-amylase is able to degrade α-1,4- glycosidic bonds, thereby degrading all the linear chains of the polysaccharide, and amyloglucosidase (also called glucoamylase) selectively attacks the last bond on the non-reducing terminals, acting on both the α-1,4 and the alpha-1,6 glycosidic linkages. The resulting sample consisted of the peptides of interest that are directly bound to glycogen. This sample was analyzed by mass spectrometry **(Figure 34).**

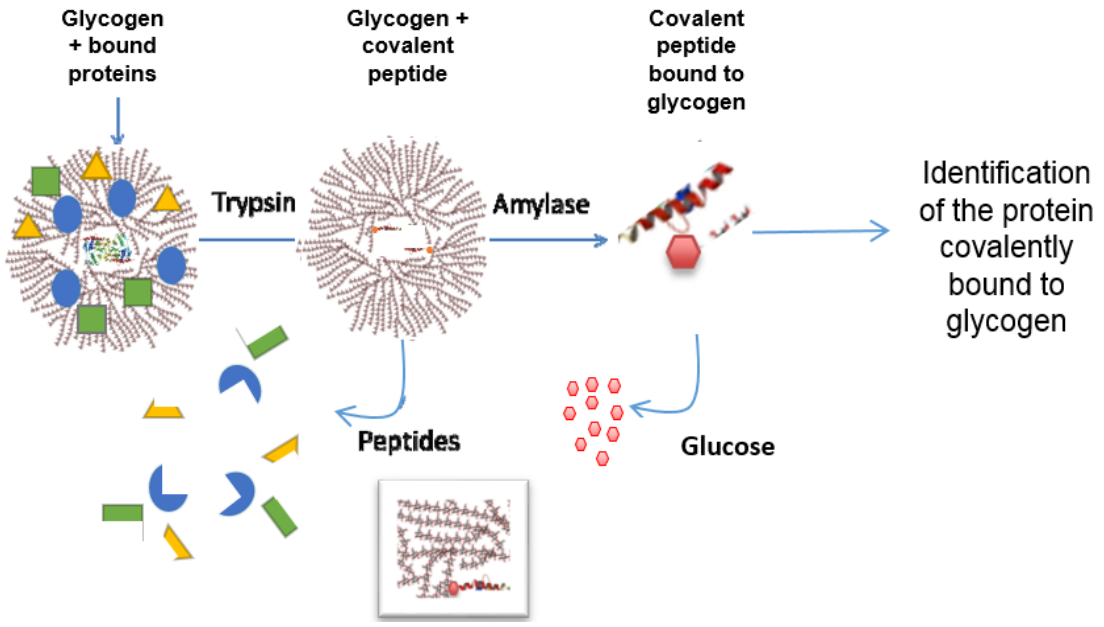


**Figure 34. Schematic steps of peptide covalently bound to glycogen by mass spectrometry**

The experiment was repeated several times in duplicates or triplicates in order to obtain a reliable result. **Table 4 lists** the proteins found with the highest frequency in 5 experiments performed (complete list of proteins in **annex 2**). Glycogenin is the only protein consistently found in WT samples. However, no substitute for glycogenin was consistently identified bound to glycogen in Gyg KO liver.

**Table 4. Summary list of the protein found in liver purified glycogen with higher frequency (nº experiments =5, n of samples per experiment= 2 -3)**

| Description | MW [kDa] | Times of detection (nº of experiments) | |
|---|---|---|---|
| | | Gyg KO | WT |
| Argininosuccinate synthase | 46,6 | 3 | 1 |
| Tubulin β-4B chain | 49,8 | 2 | 2 |
| Carbamoyl-phosphate synthase [ammonia] mitochondrial | 164,5 | 2 | 2 |
| ATP synthase | 23,3 | 2 | 2 |
| UDP-glucuronosyltransferase | 60,8 | 2 | 1 |
| Glycogen phosphorylase, muscle form | 97,2 | 1 | 3 |
| Cytochrome P450 | 58,3 | 1 | 2 |
| **Glycogenin** | **37,4** | 0 | 5 |

## 5.4 Purification of glycogen from muscle

We showed that WT skeletal muscle and heart have a greater amount of glycogenin per weight of tissue than liver. We loaded the same amount of homogenized tissue of liver, muscle and heart on a WB followed by the detection of the level of glycogenin **(Figure 35).**

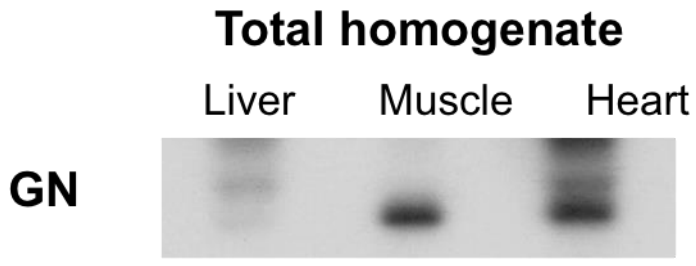


**Figure 35. WB of GN comparing the same tissue weight-** Same amount of tissue (300 ug) was loaded in the gel regardless protein concentration and glycogen content

Skeletal muscle and heart of Gyg KO animals are the most affected tissues in terms of glycogen accumulation. Therefore, we attempted the detection of the putative substitute protein also in muscle.

By applying the same purification protocol as in liver, the final purified glycogen obtained was heavily contaminated with actin and myosin. Therefore, we developed a new protocol based on the digestion of the muscle with 30% KOH. To isolate glycogen we used a treatment with KOH 30% at 100ºC for 15 minutes for the complete hydrolization of skeletal muscle proteins. We hypothesized that glycogenin would be more resistant to KOH hydrolysis than proteins non-covalently bound to glycogen due to its localization in the inner core of the polysaccharide. In the final purification protocol we reduced the time of KOH 30% hydrolysis to three minutes, as described in material and methods. After purification, samples were subjected to glycogen degradation using two different enzymes: α-amylase and amyloglucosidase. We compared the glycogenome obtained with both enzymatic digestions and the results are presented in **Figure 36**.

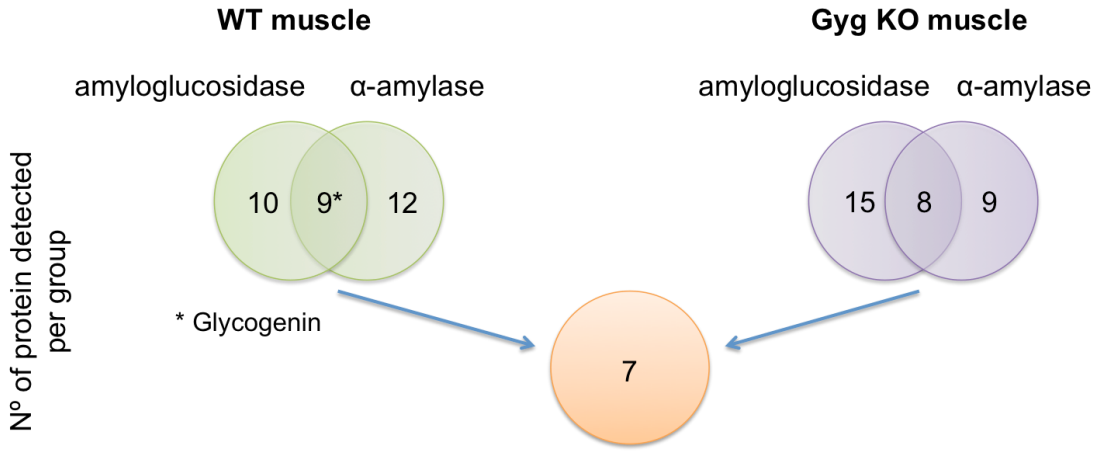


**Figure 36. Schematic representation of the protein identified by mass spectrometry-** The circles indicate the number of proteins identified in each set

Several peptides from different proteins have been identified in all preparations. Only those proteins that are common between the two digestion methods are considered specific. We found 9 specific proteins in WT muscle (among those glycogenin) and 8 in Gyg KO muscle. Between the two groups 7 of the detected proteins are common **(Table 5; complete list in annex 4 of supplementary tables)**.

**Table 5. Protein list of peptides detected in skeletal muscle purified glycogen**

| Samples | Total | Protein |
|---|---|---|
| Gyg KO Amylase, Gyg KO Glucosidase, WT Amylase, WT Glucosidase | 7 | Titin |
| | | Calsequestrin-1 |
| | | Myosin-7 |
| | | Sarcoplasmic/endoplasmic reticulum calcium ATPase 1 |
| | | Myosin-1 |
| | | Myosin-4 |
| | | Creatine kinase M-type |

We also tested which peptides, among all peptides detected in the analysis, retained glucose residues attached. We identified two proteins in the Gyg KO samples: Homeobox protein (ARX) and DNA-directed RNA polymerase III subunit (RPC3) in the fraction treated with amylase. However, they were not found in the amyloglucosidase-treated Gyg KO sample, neither with retained glucose residues attached nor in the absence of bound glucose residues. For this reason, and for their properties (nuclear localization), we excluded them as good candidates for glycogenin substitutes. In WT samples the only protein bound to glucose residues that could be identified was glycogenin. Fourteen glycogenin peptides containing Tyr195 were identified in the sample treated with amyloglucosidase and 4 with α-amylase; in the latter case with one glucose residue attached **(annex 3 Supplementary tables).** No other proteins involved in glycogen metabolism were detected.

## 5.5 Conclusions

By mass spectrometry no good candidate protein that could serve as a substitute for glycogenin was found in Gyg KO liver and muscle. The detection of glycogenin in both WT tissues was reassuring that the experimental setup was functional.

# 6. Changes in glycogen metabolism

## 6.1 Introduction

Cellular glycogen storage is regulated by a delicate mechanism. The localization, the amount and the quality are controlled by many factors and they can vary within species and tissue. It is known that these characteristics are crucial for an efficient system of storage and release of glucose. The accumulation of the polysaccharide is due to the process of synthesis by GS, to the amount of degradation determined by GP, and by lysosomal amyloglucosidase. To understand glycogen accumulation in Gyg KO we analyzed these processes.

## 6.2 Glycogen metabolism in heart and skeletal muscle

We focused mainly on the study of modification in GS and GP, because in Gyg KO animals, glycogen granules are found in the cytoplasm, while the accumulation determined by amyloglucosidase occurs in lysosomes (i.e. Pompe disease).

Glycogen metabolism enzymes in heart and muscle are determined by WB, using specific antibody for the specific muscle isoform expressed in the tissues **(Figure 37).**

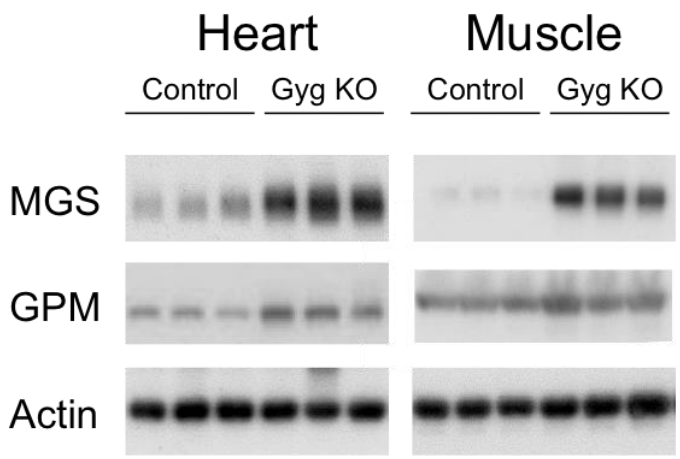


**Figure 37. WB of GS and GP-** WB from total homogenates obtained from different tissues for the detection of specific isoform of GS and GP

The level of GS totally reflects the enhanced amount of glycogen measured in the Gyg KO tissues. Moreover a slight increment of GP is observable as well in both Gyg KO tissues, most likely determined by the higher glycogen amount.
We also tested the relative gene expression of both GS and GP **(Figure 38).** At transcriptional level, no differences in GS and GP expression were observed.

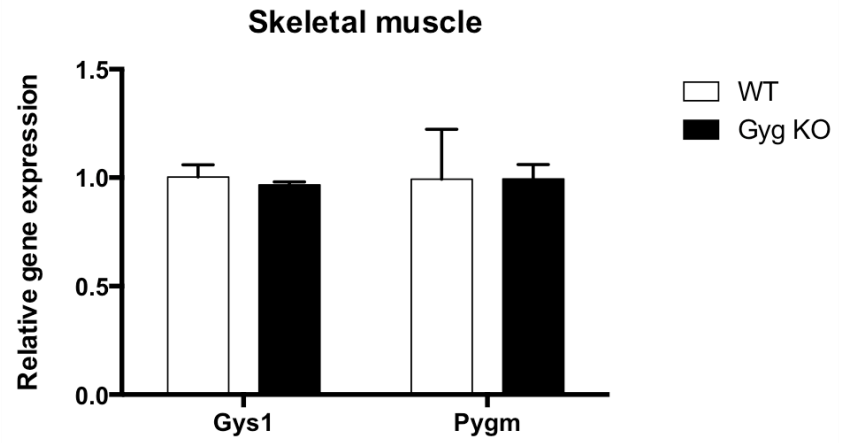


**Figure 38. Relative gene expression –**mRNA level of muscle glycogen synthase and muscle glycogen phosphorylase in skeletal muscle normalized on r18S housekeeping gene

The activities of the enzymes were measured with radioactivity assay (see material and methods) **(Figure 39)**.

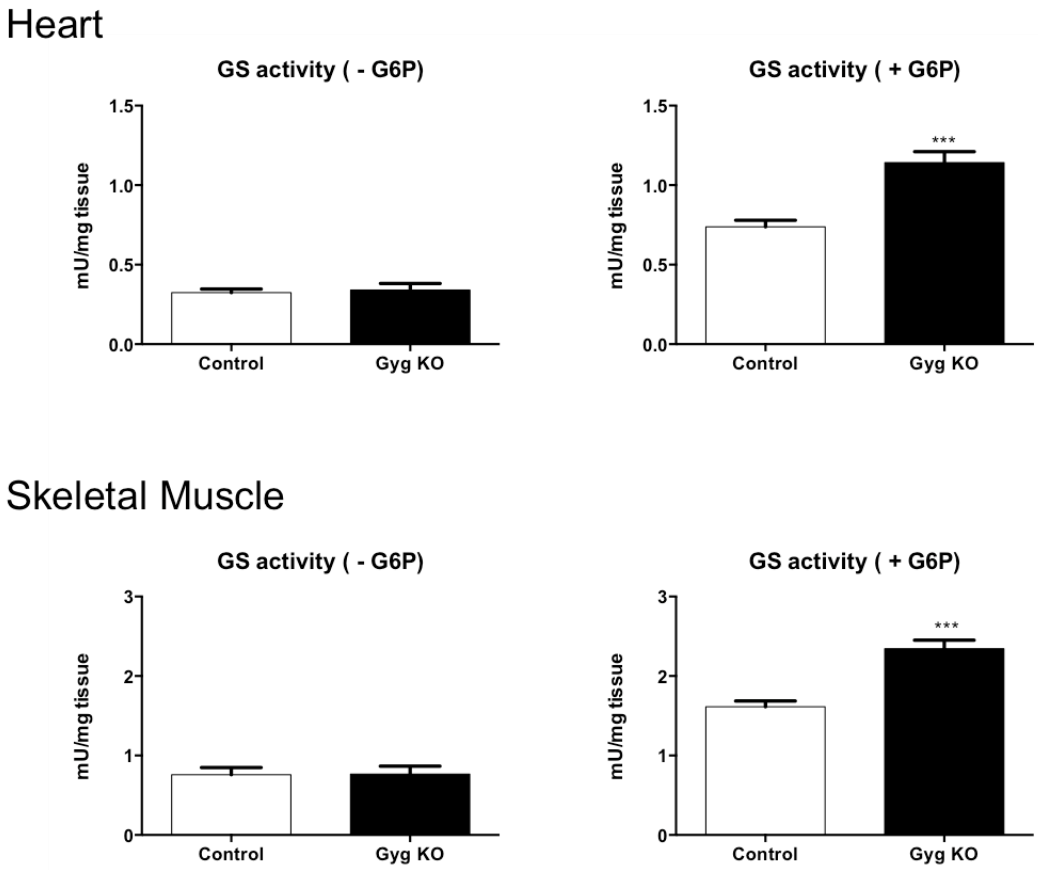


**Figure 39. Glycogen synthase activity assay** Left panels indicate the endogenous active GS (in absence of G-6P). Right panels indicate the total level of GS (activated by G-6P)

No differences are detected in the endogenous active GS does for both tissues. When glucose-6 phosphate (activator of GS) was added, the measurement revealed a higher GS level indicating increased total protein (as in WB results). Both WB and activity assay showed an increase in GS total level, but from the calculation of fold-change increase compared to WT we noticed a discrepancy: 1,45 fold increase is measured by activity and 10,6 times by immunodetection (densitometry of films). Our hypothesis is that not all GS is easily accessible by G-6P, maybe due to the composition of the glycogen granule to which it is bound. The polysaccharide, in fact, interacts with many proteins. Their properties, as solubility, and amount, affect the composition of glycogen granule. We tested if the solubility of glycogen in Gyg KO muscle changed, taking into account the partitioning of the polysaccharide between low speed centrifugation pellet (insoluble) and supernatant (soluble) fractions of the total homogenate. In WT the proportion of glycogen in the two fractions is well

balanced. However, about 80% of Gyg KO glycogen is found in the insoluble fraction **(Figure 40).**

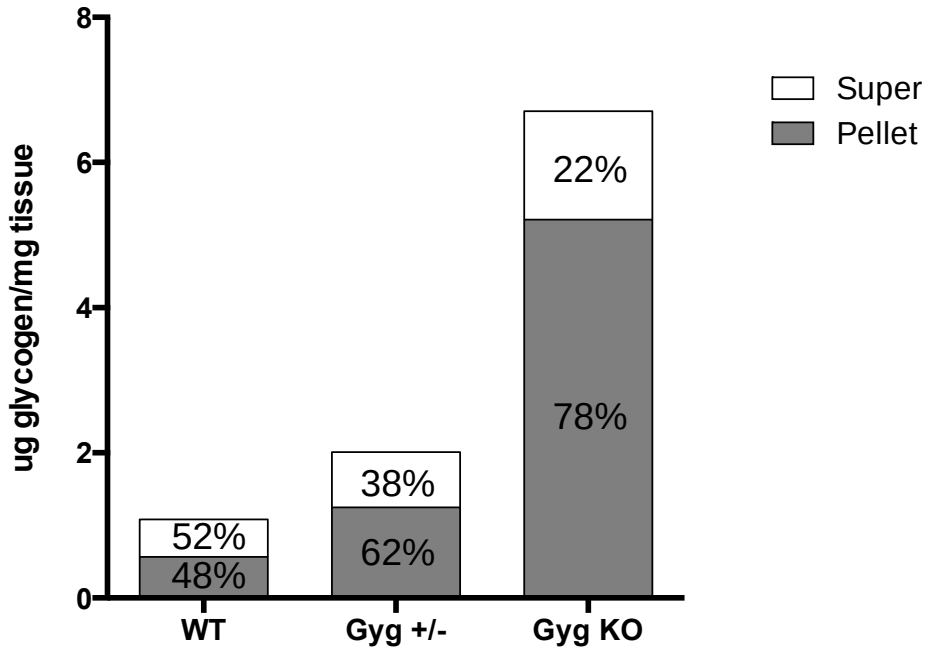


**Figure 40. Glycogen distribution between soluble and insoluble fraction in muscle-** Quantification of glycogen in supernatant and pelletable fraction after centrifugation and calculation of the % to total amount. Before centrifugation, samples were homogenized in WB buffer (see material and methods) followed by KOH 30% treatment. As internal control, also total glycogen was measured by both methods: homogenized directly with KOH or as supernatant and pellet. By both homogenization methods we obtained the same total value of glycogen (Font. Garcia-Rocha M.)

We confirmed that in Gyg KO muscle the solubility of glycogen is greatly diminished compare to WT sample, differently than what it was observed during glycogen phosphate (section 4.2.5) and purification methods in which no changes in solubility were found during the handling of the samples. The differences between the techniques reside in the presence of the proteins, eliminated during the methodology applied in the previous chapters. For this reason, we hypothesize that the protein component of Gyg KO glycogen granules has a relevant role in the determination of its solubility. To test that, we analyzed some of the proteins involved in the glycogen metabolism pathway by WB **(Figure 41)**, comparing total tissue extract to supernatant (super) and pelletable (pellet) fractions.

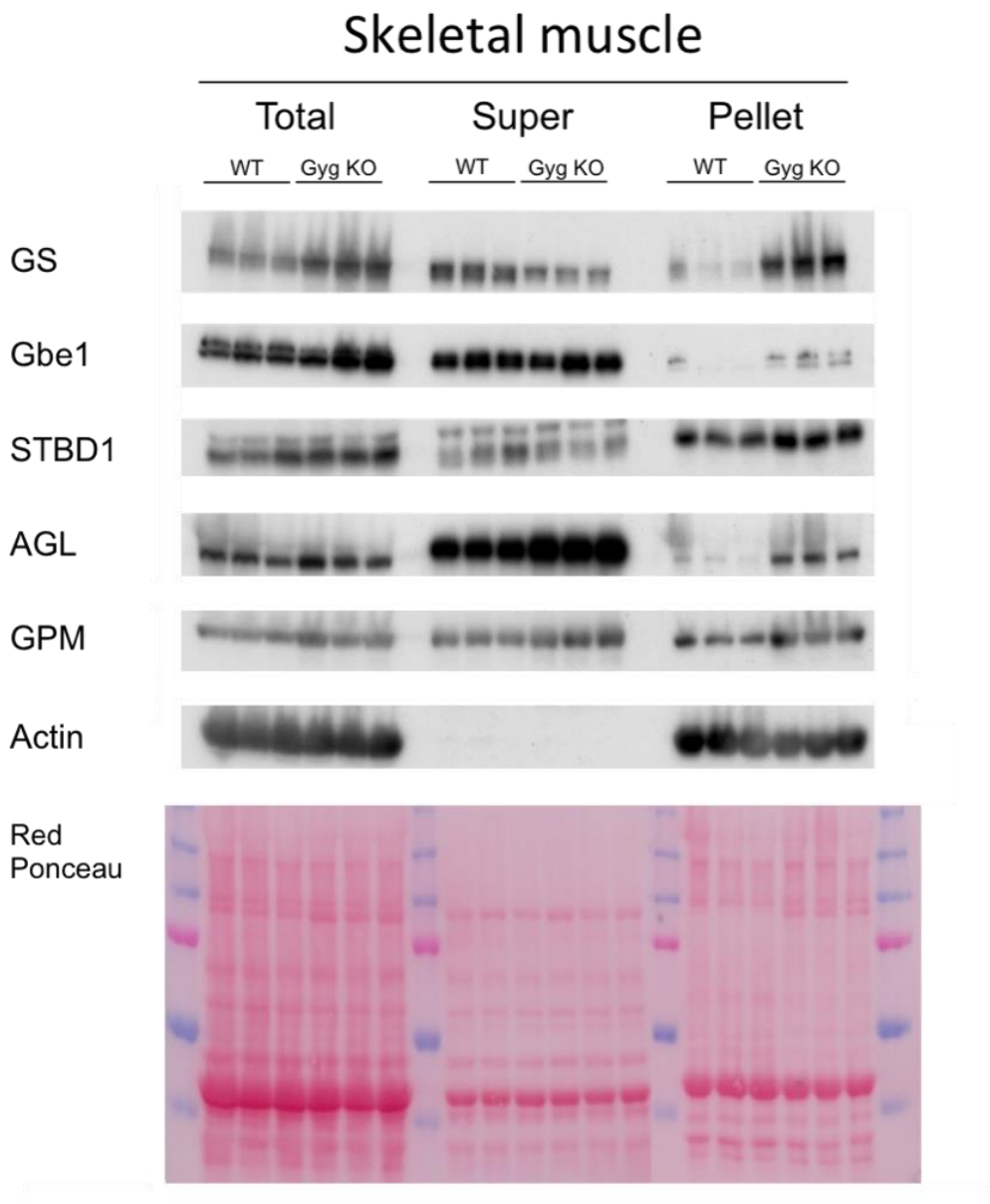


**Figure 41. WB of protein involved in glycogen metabolism-** Comparison of the protein content between WT and Gyg KO skeletal muscle of adult male mice (n=3) in total extract, supernatant and pelletable fractions. Loading of the samples respects the proportions in which tissue extracts were divided in two equal parts: one kept as total and one centrifuged and separated in supernatant and pellet. Pictures of the 3 fractions were taken at the same exposition time, in some cases preventing the optimal signal, but allowing having an overview of the distribution of the protein. The same membranes were tested for all antibodies; in case of stripping of the membrane we performed secondary antibody test to avoid residual signal from previous incubations

As a general conclusion we can state that the changes of glycogen metabolism proteins are reflecting the level of glycogen (higher in Gyg KO) and its solubility (prominent in the insoluble fraction).

Regarding GP, we tested the possibility of alterations in its activity state. A decrease in GP activity would lead to glycogen accumulation, a condition found in other GSDs as McArdle disease **(Figure 42).**

MUSCLE

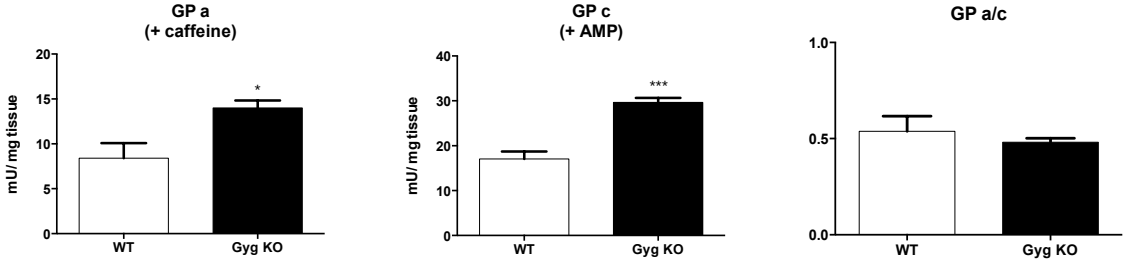


**Figure 42. Glycogen Phosphorylase activity assay-** Quantification of the endogenous activity of MGP (*a* state) and active GP state (*c*) obtained by adult male skeletal muscle (n=5)

Glycogen phosphorylase in skeletal muscle is not the responsible for glycogen accumulation, because we demonstrate that the level of the protein instead of diminishing is slightly increased, most likely due to the high affinity with glycogen and its abundance. We also observed that the state of activation of the enzyme showed in the ratio GP a/c is the same as in the control.

## 6.3 Glycogen metabolism in liver

Liver, not only is the major glycogen storage of the body, but also its metabolism is characterized by different isoforms of the proteins involved in the glycogen pathways. We checked the protein level and measured the activation state of GS and GP proteins **(Figure 43 and 44).**

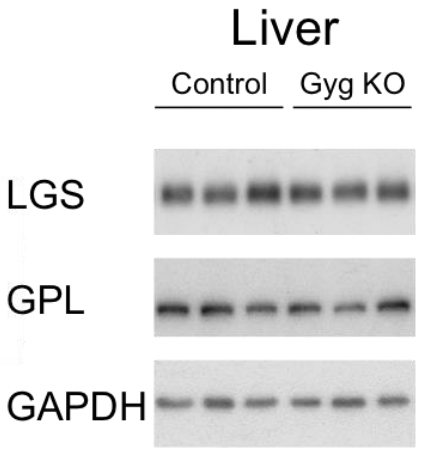


**Figure 43. WB of GS and GP-** WB from total homogenates obtained of hepatic specific isoform of GS and GP

As we observed, no difference at protein level were identified for LGS and GPL**.** We measured the enzymatic activities in condition of overnight fasting followed by morning injection of glucose and sacrifice of the animal after 30 minutes. This practice is applied to avoid variability in the results. After an over night starvation liver glycogen is almost completely degraded to maintain the homeostasis of glucose in the blood**.** This allows starting from the same state of glycogen depletion at time of glucose injection and evaluating objectively the activation state of the enzymes. However, the two animal groups do not show difference.

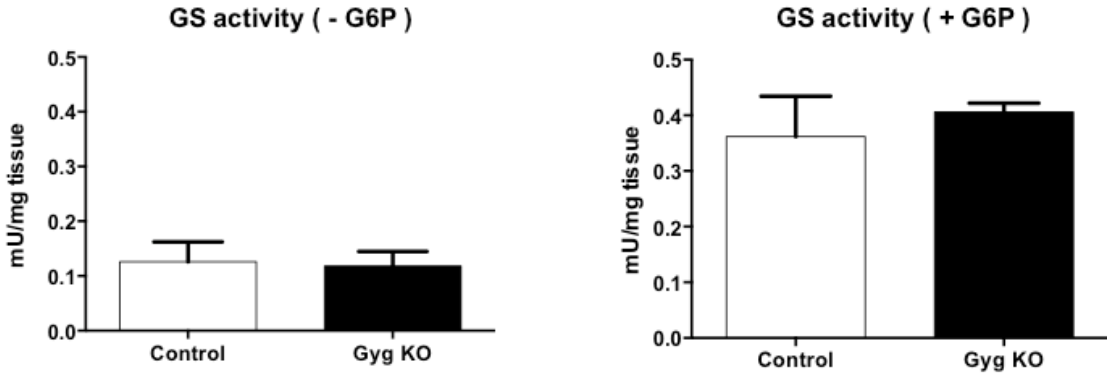


**Figure 44. Glycogen synthase activity assay-** Activation of GS in WT and Gyg KO liver. Left panels indicate the endogenous active GS (in absence of G-6P). Right panels indicate the total level of GS (activated by G-6P)

To detected differences in the activation state of GP, the first approach applied was by the use of a specific antibody that detects the active liver isoform, GPa2 **(Figure 45)**. We also quantified GP activity by enzymatic assay **(Figure 46).** With both methods, WB and activity assay, no significant differences are detected**.**

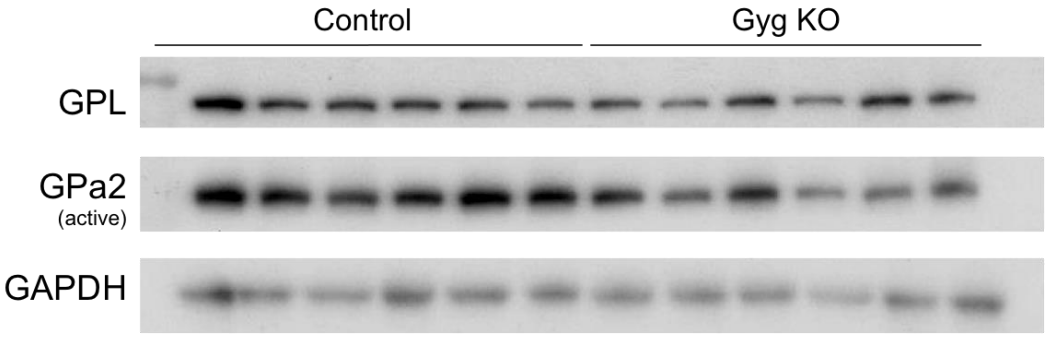


**Figure 45. Immunodetection of GP-** GPL: specific antibody for the total liver isoform; GP2a: specific for the activated liver isoform.

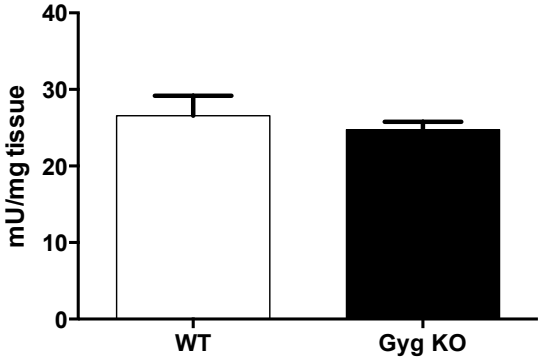


**Figure 46. Liver GP activity assay-** Total GP level

Proteins involved in glycogen metabolism pathway are tested by immunodetection for a deeper characterization of the metabolism in liver **(Figure 47)**.

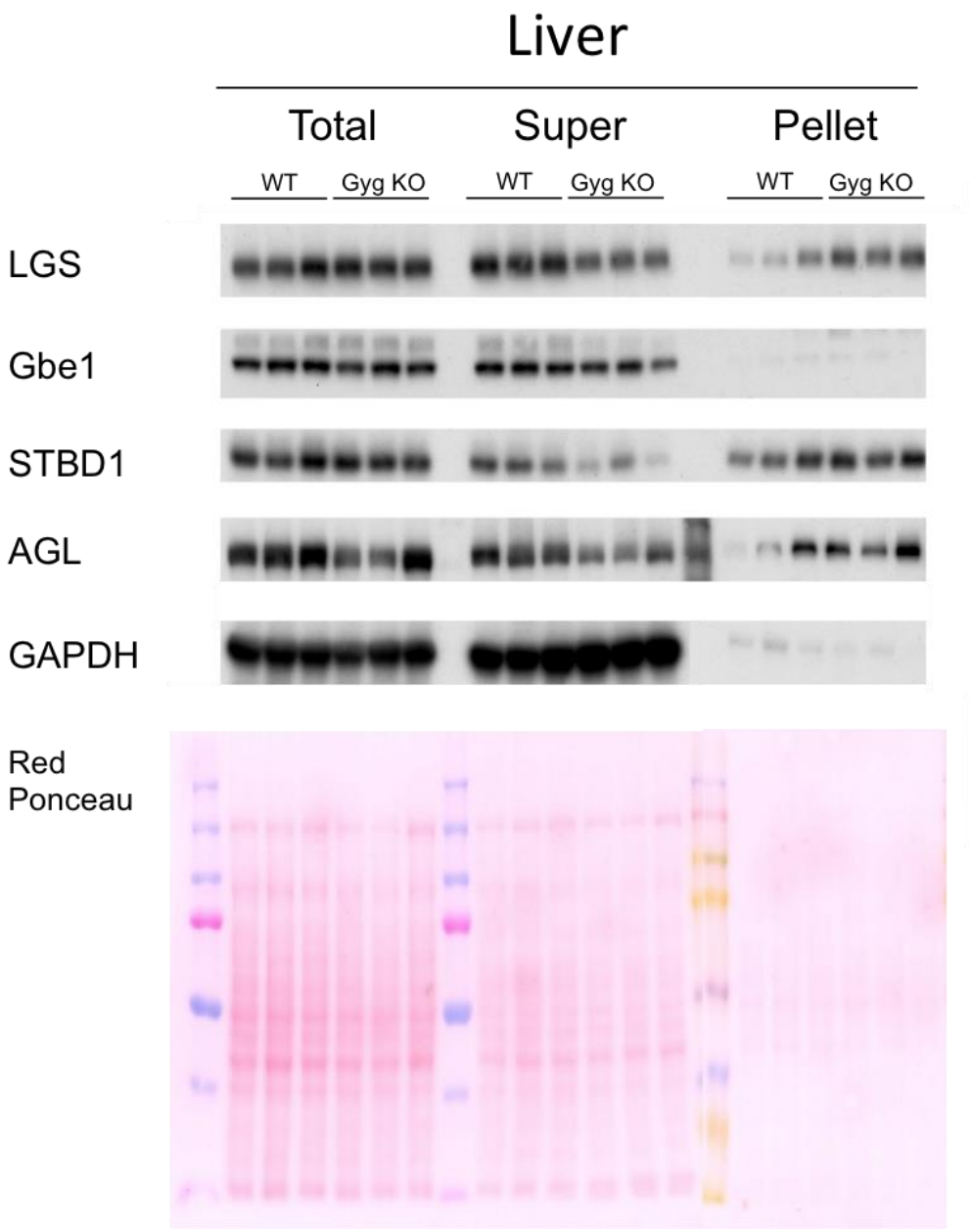


**Figure 47. Immunodetection of protein involved in glycogen metabolism-** Comparison of the protein content between WT and Gyg KO in adult male mice (n=3). Comparison of total, supernatant and pelletable fractions to localize of the proteins analyzed. The same membranes were tested for all antibodies; in case of stripping of the membrane we performed secondary antibody test to avid residual signal from previous incubations.

Despite the total amount of LGS is the same, we clearly observed that it mainly localizes in the insoluble fraction. Also the other proteins analyzed are expressed at the same level in WT and Gyg KO in the total extract, however STBD1 and AGL have a minor localization in the soluble fraction.

## 6.4 Glycogen metabolism in primary hepatocytes

To have a better model to test the degree of degradation and re-synthesis of glycogen we used in vitro cultures of primary hepatocytes of 15-week-old male mice. Cells were subjected to over night fasting (media lacking glucose) in order to completely deplete glycogen and starting at time 0, we replaced the media with the one containing 25mM glucose and we measured glycogen and GS activity at three time points (3, 6, 24 hours) **(Figure 48 and 49).**

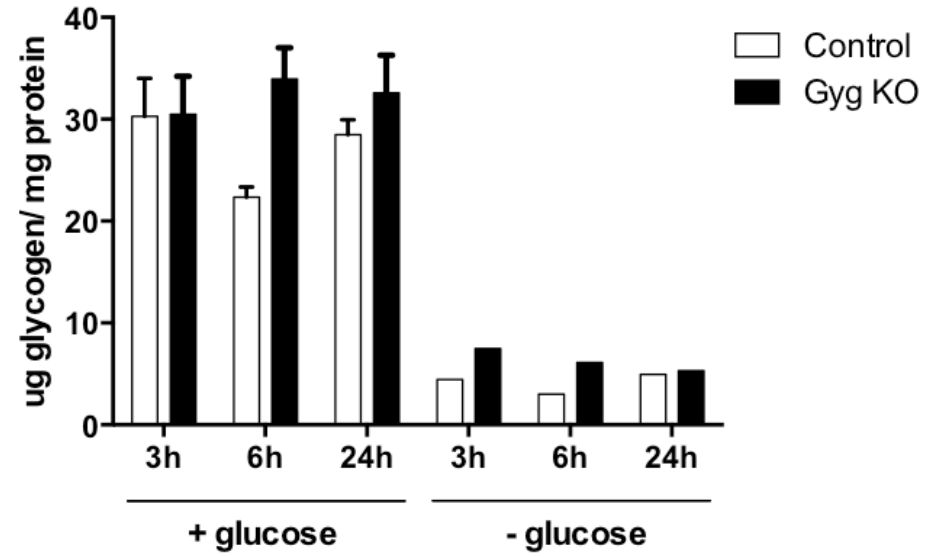


**Figure 48. Glycogen measurement in primary hepatocytes-** On the horizontal axis, time reported indicate the incubation time with the correspondent media, after overnight with glucose-deplete media.

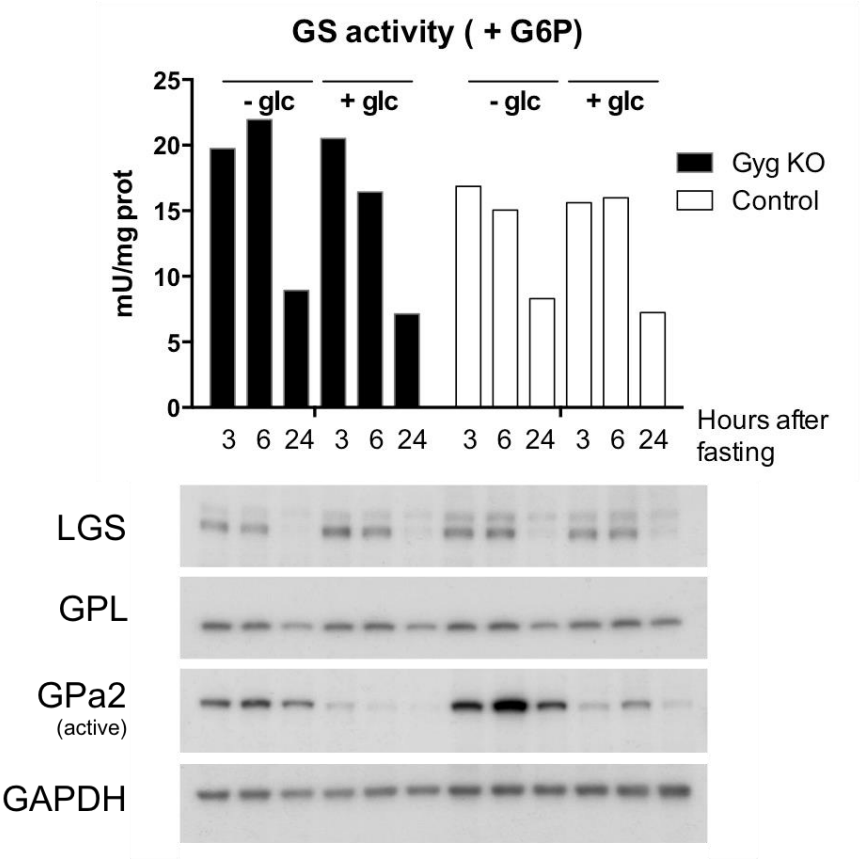


**Figure 49. GS activity and immunodetection in primary hepatocytes-** Top panel report the total GS activity quantified in the time point listed on the *x* axis. Type of media is indicated at the top of the figure. Bottom panel: lanes correspond to the correspondent samples plotted above.

Glycogen synthesized at 3 hours in presence of glucose had already reached the highest level that is then maintained during the following time points. Moreover we do not observe significantly differences between Gyg KO and control. We observed the level of active GP (GP2a) during prolonged fasting: besides having the same total level, Gyg KO GP is less active compared to control **(Figure 49).** For these reasons we further tested a time point activation of the phosphorylase enzyme, inducing the cells a progressive starvation and measuring glycogen level **(Figure 50).**

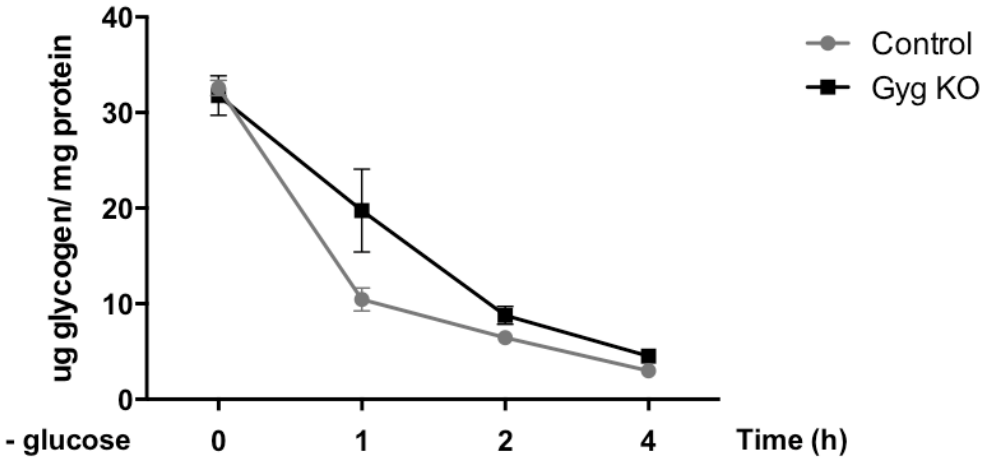


**Figure 50. Glycogen measurement in primary hepatocytes subjected to timed starvation –** Time 0 correspond to cells maintained in complete media for 6 hours. At time 0, media was replaced ( - glucose) for the measurement of the following points.

Following the same procedure as previously described, after overnight fasting we provide complete media to the hepatocytes for 6 hours, allowing reaching the highest glycogen level (this is reported as time=0). Cells were then placed again in a glucose-free media for 1, 2 and 4 hours. This way, starting from the same glycogen level, we observed that Gyg KO has no significant difference with the control in glycogen degradation during fasting, confirming previous results obtained *in vivo*.

## 6.5 Conclusions

From the evidences we obtained n the analysis of glycogen metabolism in muscle and heart we can definitely state that the protein responsible for glycogen accumulation is GS, found increased in total level and activable by G-6P. On the other side, liver GS does not show differences compared to WT animals, and this can explain the equal glycogen level between the two genotypes.

# 7. Physiological characterization of Gyg KO mice

## 7.1 Glycemic response to metabolic stimuli

We aimed to characterize the differences determined by the lack of glycogenin at physiological level. First, we performed time point experiments based on blood glucose level as an indirect measure of glycogen degradation and release from the liver or glucose uptake by other tissues. During fasting, the level of glucose blood is buffered by the constant release of glucose deriving from glycogen in the liver. Lower glycogen degradation would result in a drop of glycemia. Mice were subjected to a long fasting period up to 36 hours, and glycemia were regularly measured **(Figure 51).** No difference are highlighted between WT and Gyg KO mice, in fact both show a drop of blood glucose between 12 and 24h, that is later maintained constant till 36h. This is consistent with the fact that glycogen degradation is not affected in Gyg KO animals.

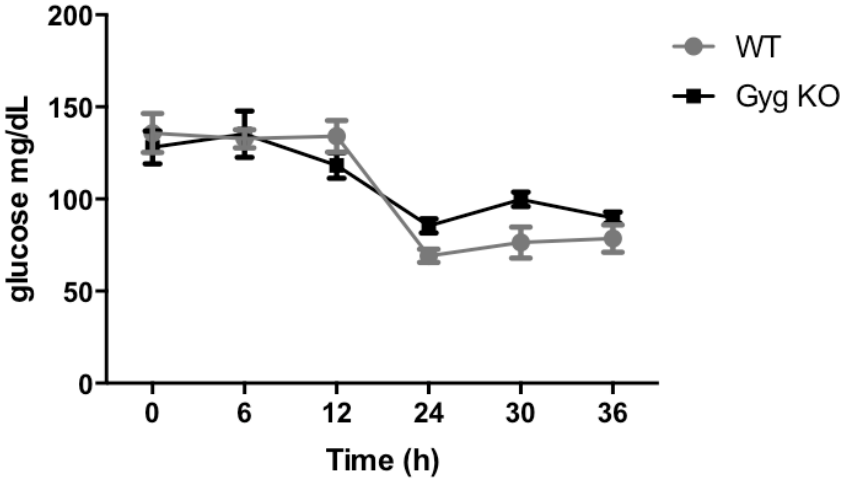


**Figure 51. Glycemia variation during a long-fasting period-** Horizontal axis indicates the hours after food removal.

Another way to test liver responsiveness is to increase the levels of glucagon, a pancreatic hormone released in the blood stream in response to a low glucose level. After 6 hours fasting, glucagon is injected in the mice and glycemia was

recorded at different time points. Also in this case no differences were observed between WT and Gyg KO **(Figure 52).**

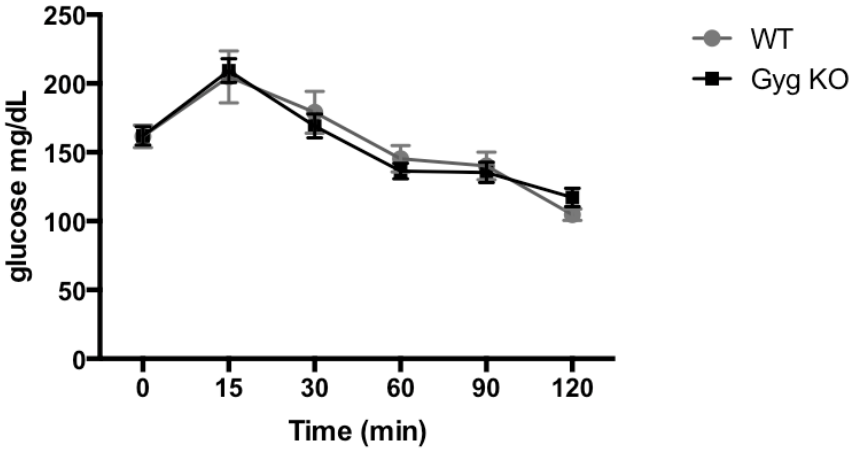


**Figure 52. Glucagon tolerance test-** Horizontal axis reports minutes after glucagon injection.

We performed an ITT (Insulin Tolerance Test), measuring the ability for glucose uptake by tissues **(Figure 53).** After 15 minutes of injection we observed a drop in glycemia that up to 1 hour was higher in Gyg KO than in WT, meaning that Gyg KO have an increased sensitivity to insulin and higher ability to uptake glucose. We also performed a GTT (glucose tolerance test) **(Figure 54).** In this experiment, after an initial increase of glycemia given by the injection, both WT and Gyg KO showed the same tolerance to glucose (no statistical difference of the area under the curve).

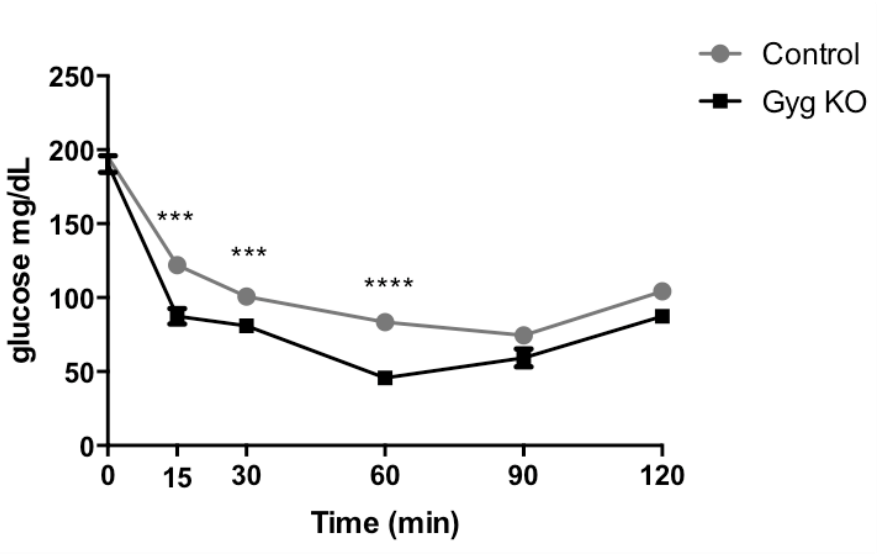


**Figure 53. Insulin tolerance test-** Injection of insulin was performed after 6 hours of fasting applied in the morning

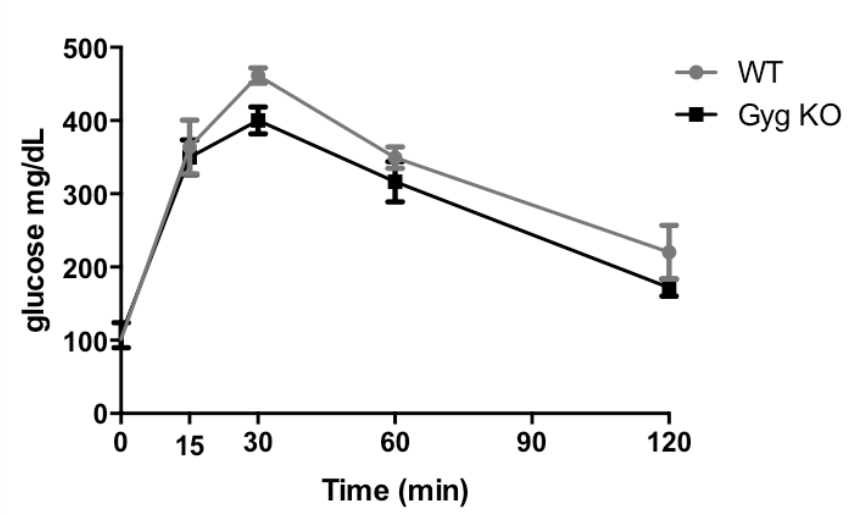


**Figure 54. Glucose tolerance test-** Injection and glycemia measurement were done after overnight fasting

## 7.2 Muscle response to physical exercise

Since skeletal muscle glycogen is enormously increased in Gyg KO compared to WT, we tested the physiology of this tissue by performing a grip test. Basically, we wanted to analyze the ability of muscle glycogen to be mobilized and converted in energy, under a big and fast energy request **(Figure 55).**

However, also this experiment did not elucidate any difference between the two groups.

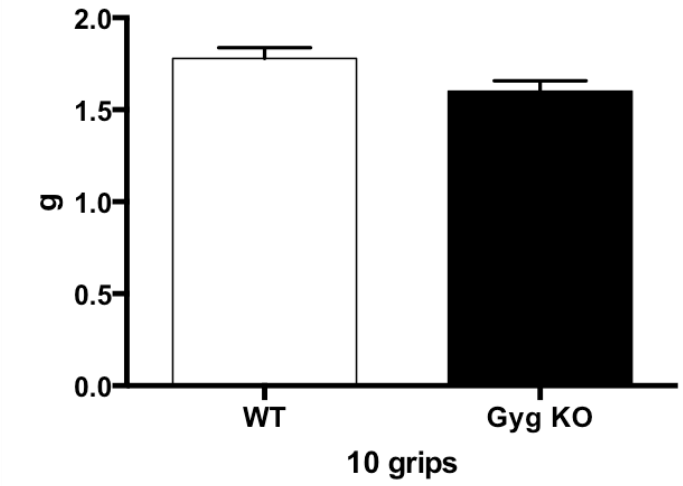


**Figure 55. Grip strength test-** Adult male mice (n=7) were tested on strength performance. Test was performed with upper limbs.

A way to determine motor coordination, as well as balance and physical condition under energy request is rotarod test. Average of duration and speed between WT and Gyg KO are not significantly different, but we observed a trend for Gyg KO to perform worse than WT **(Figure 56A)**. By plotting single value recorded during three experiments in a Kaplan-Meier plot, we observed that WT resisted longer on the rotarod, and so on even run faster **(Figure 56B)**. From the density curve we can also observe that Gyg KO mice reach a sort of breaking point: just before 300 seconds all animals start to fall and by 400 seconds all of them stopped running **(Figure 56C)**. However, WT have a more spread distribution in the timing they fell reaching almost 800 seconds of resistance on the rotarod.

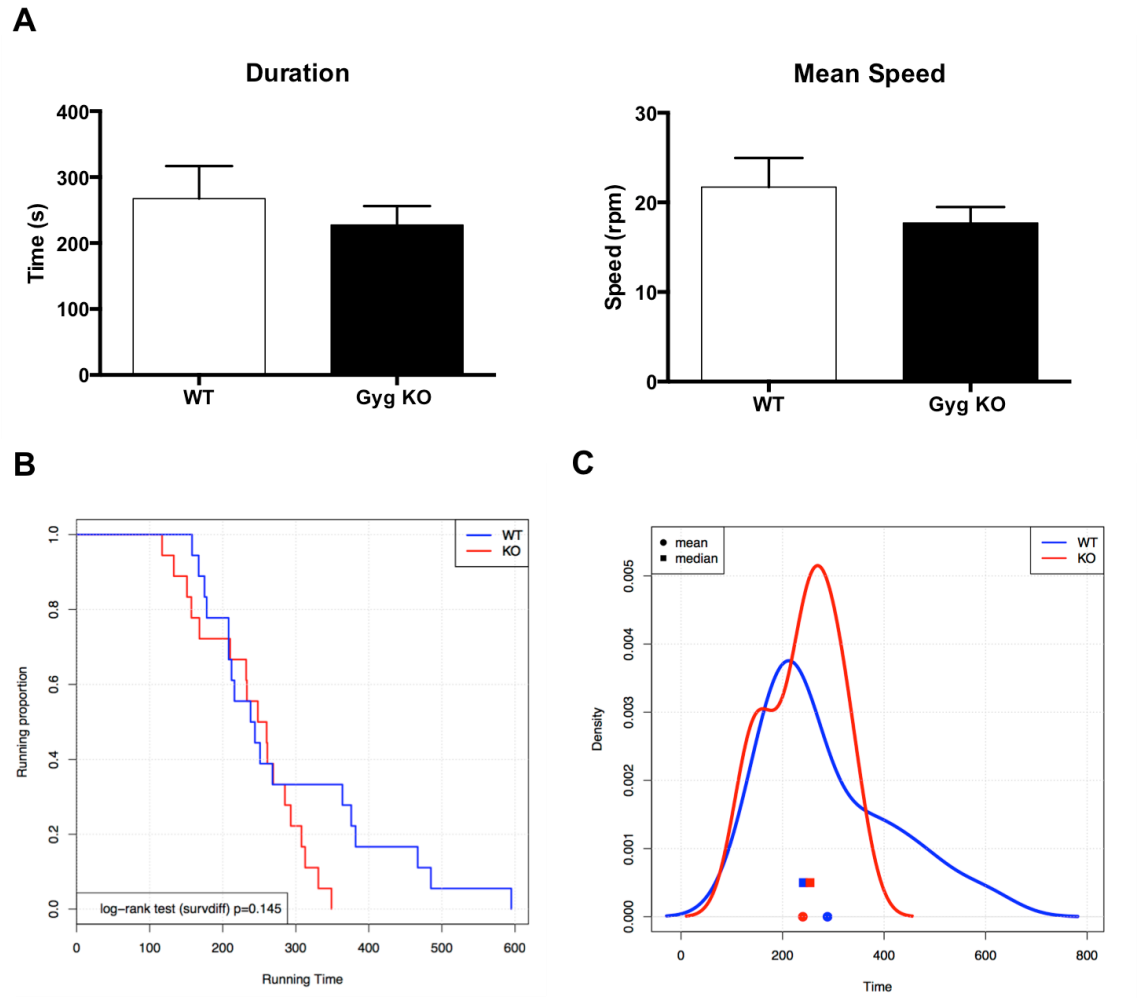


**Figure 56. Rotarod parameters and data analysis –**A) average of duration and mean speed of adult male mice (WT n=5; Gyg KO n=6). B) Kaplan-Meir plot of the running time considering every performances independently (nº experiments= 3). C) Distribution of the running time

We performed a treadmill test, subjecting the mice to a long resistance exercise. WT have the ability to perform better on the treadmill, running almost double distance than Gyg KO **(Figure 57).** Moreover all WT reached the maximum speed of 46 cm/second, while only one Gyg KO did. They run in average at maximum speed of 39 cm/second.

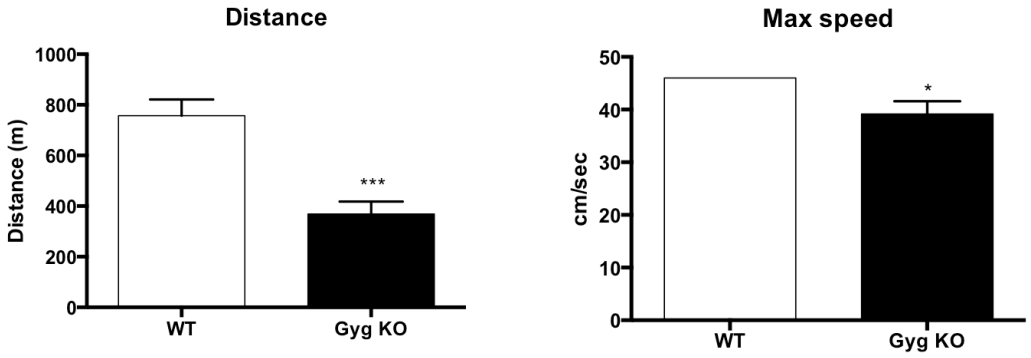


**Figure 57. Treadmill exercise parameters (I)-** Average of the distance run per group (n=6) and average of the maximum speed. All WT animals reached the maximum speed applied for the experiment.

Time of exhaustion **(Figure 58A)** significantly shows a great difference in resistance to exercise between WT and Gyg KO. In addition in the graph of the treadmill shocks are reported the number of times mice were on the shock grid**.** This corresponds to the number of times the mice stopped running. It is clear that Gyg KO mice stopped considerably copious number of times and in a shorter time compared to WT. In **figure 58B**, it is highlighted that indeed Gyg KO mice, plotted by single animal, performed much worse than WT, being unable to last longer than 39 minutes and, starting to get tired earlier on the time scale.

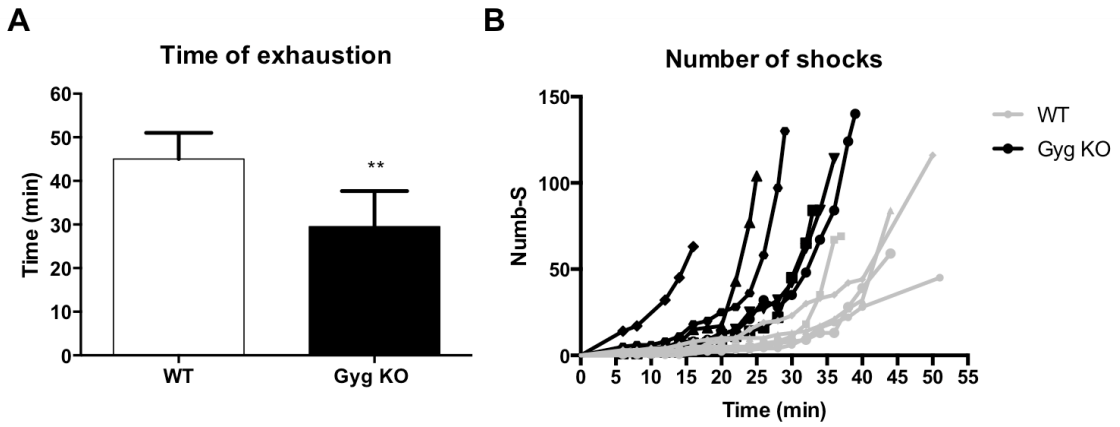


**Figure 58. Treadmill parameters (II)-** A)Average of the exhaustion time per group and representation of the performance of every animal. B) the vertical axis indicate the number of the number of shocks

**Figure 59** shows the average of the time spent on the shock grid by both animal groups, and every time point represents the distribution of the values from all animals (bars). From minute 16 values resulted significantly different between the genotypes. Furthermore we identified a parameter to express the tendency of the Gyg KO to get tired in a shorter period and to get exhausted much faster. This tendency is visual observing single plots slopes: Gyg KO seems to reach a break point from which they cannot last any longer on the treadmill. On the other hand, WT get slower in a more progressive manner (lower slope of the curve): Gyg KO changepoint is at 26 minutes and WT is at 32 minutes.

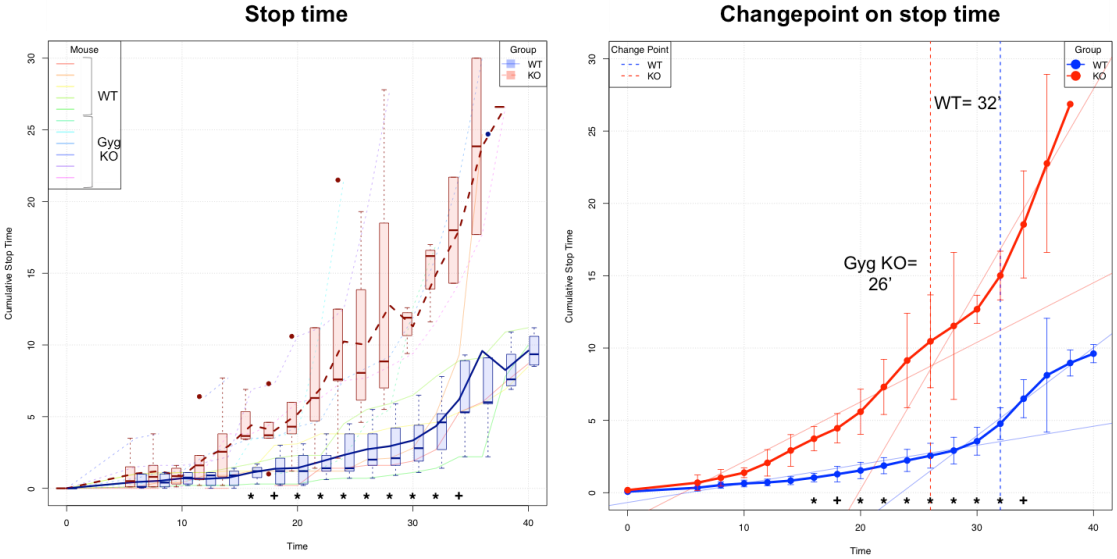


**Figure 59. Time spent on the shock grid during treadmill exercise-** Left panel: Averages of cumulative stop time per group. In light color, single animal values are reported (legend top left corner). Every time point indicates the distribution, average and error of the animals per group. Statistic applied by Wilcoxon - Mann Whitney test. (* = p-value < 0.05; + = p-value < 0.1). Right panel: Dashed vertical lines indicate significant changepoint in mean slope values as detected by the *cpt.mean* function from the changepoint package v1.0.5 (Biostatistics/ Bioinformatics core facility at IRB Barcelona)

With the measurement obtained by the treadmill machine we were able to calculate work performed and power **(Figure 60).** Also in this case, Gyg KO show less efficiency during exercise compared to WT.

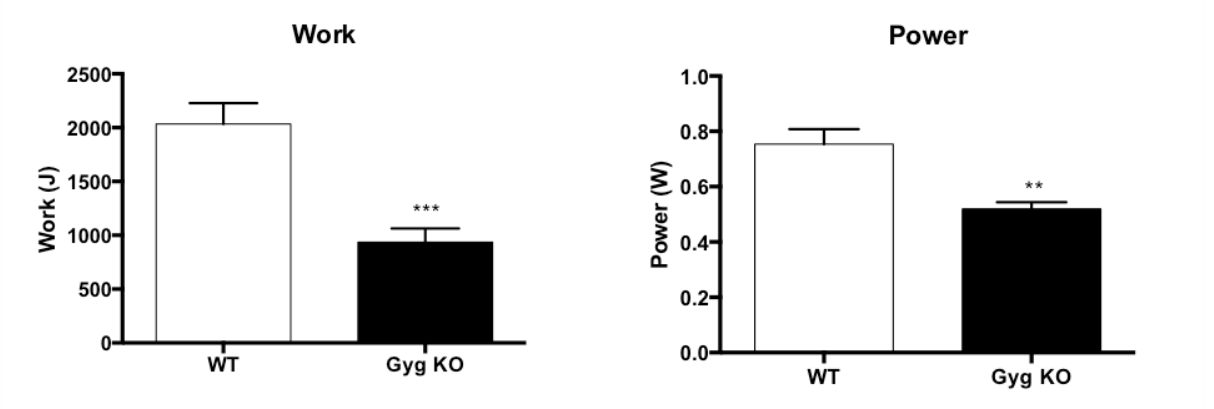


**Figure 60. Treadmill exercise parameters (III)-** Work is obtained by the formula weight * gravity* vertical speed * time and power is equal to weight * gravity * vertical speed

Since Gyg KO animals reached early exhaustion we determined how glycogen content changed after the treadmill test **(Figure 61).** In muscle, even though all animals reached exhaustion, they did no consume all storage of muscular glycogen. Both WT and Gyg KO degraded about 40% of the muscular glycogen **(Figure 61A).** Absolute values of glycogen indicate that Gyg KO is able to degrade 6 times more glycogen in a shorter time (exhaustion): 0.7 ug glycogen /mg tissue in compared to 4ug/mg tissue in the Gyg KO **(Figure 61B).** Although glycogen is degraded faster and in greater amount in Gyg KO animals, they present worst performances in the treadmill test.

In liver (starting from the same glycogen level) WT and Gyg KO animals degraded respectively about 20 ug of glycogen per mg of tissue **(Figure 61C)**.

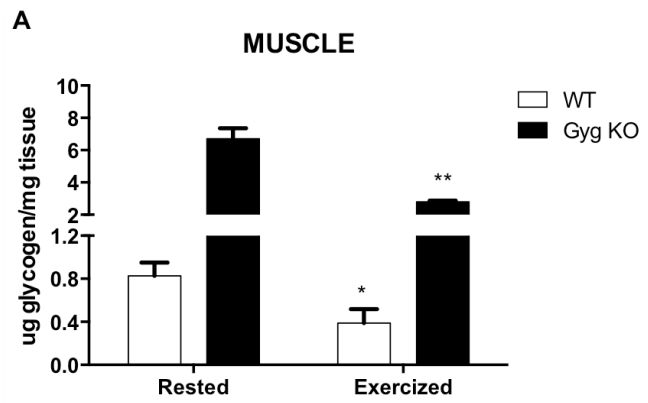


B

| | ug glycogen degraded/ mg tissue | |
|---|---|---|
| | WT | Gyg KO |
| Muscle | 0,69 | 3,91 |
| Liver | 23,11 | 16,08 |

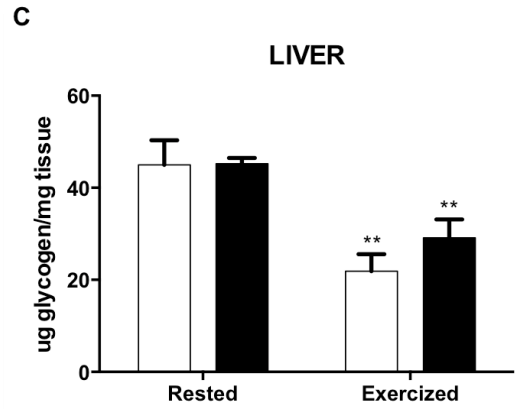


**Figure 61. Glycogen measurement before and after exercise-** A) biochemical quantification of glycogen and comparison between rested state and exercised to exhaustion in muscle; B) Table of glycogen reduction after exercise (ug/mg tissue); C) glycogen measurement after exercise in liver

To have more insight on the physiology of the animals, we analyzed blood metabolites before and after exercise, as glycemia and lactate **(Figure 62)**. As expected in both genotypes metabolites increased after exercise.

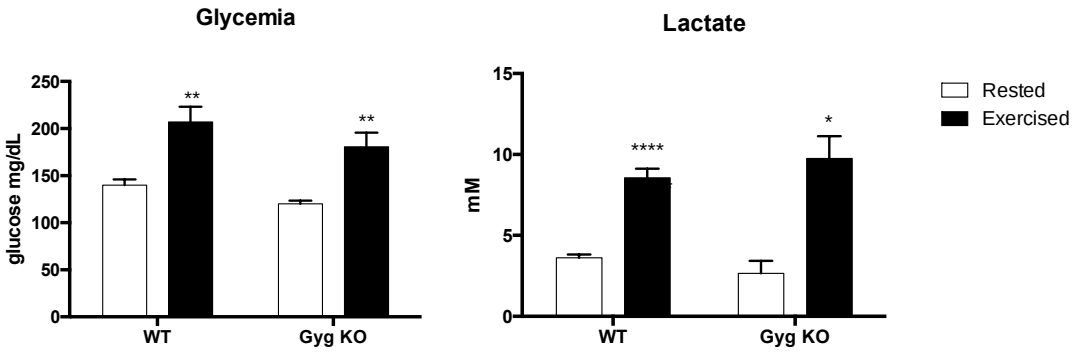


**Figure 62. Blood metabolites after treadmill exercise**

## 7.3 Energy expenditure and calorimetric parameters

In order to examine the reason for the difference in the resistance to exercise, we analyzed the total daily energy expenditure in the two genotypes by measuring volume of oxygen consumption ($VO_2$) and volume of $CO_2$ production ($VCO_2$) by an 8-chamber oxymax apparatus, standardized for body weight. The analysis clearly revealed that Gyg KO have lower $O_2$ consumption and $CO_2$ production **(Figure 63)**. The difference with WT is greater during dark phase, when animals are more active, but also in the light phase the differences are significant. Consequently respiratory exchange ratio (RER) is the same, but total energy expenditure is much lower in the Gyg KO. More information is given by the heat production, also lower in the Gyg KO, and also considering that the total movement is unchanged in the two genotypes. This is a clear explanation for the lower resistance to physical exercise. In order to observe if these animals used more carbohydrates as an energy source we calculated the amount of glucose oxidized, that is less in Gyg KO particularly in the dark phase. Change in lipid oxidation is observed only during light phase, when in fact is usually occurring in the WT **(Figure 64).**

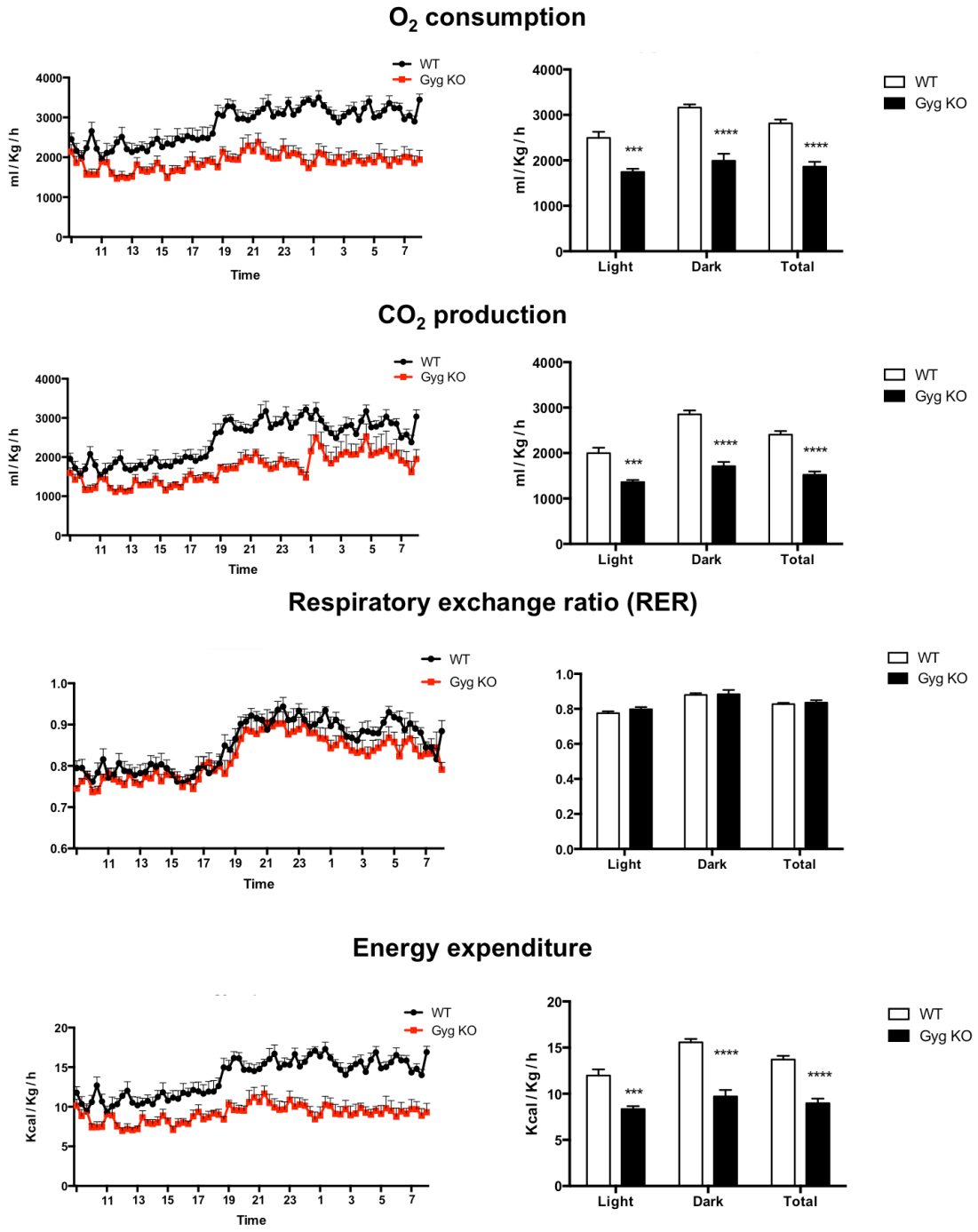


**Figure 63. Oxymax parameters (I)-** Calorimetric data obtained by Oxymax device from 8 animals per group. Each animal was measured for 2 days. All values are normalized by the daily weight of the subject. Graphs represent the average per group and SD. Left panel indicate the variation along the day: on the horizontal axis is reported the time of the day (hours). Right panels show the average of values during light and dark phase, and total.

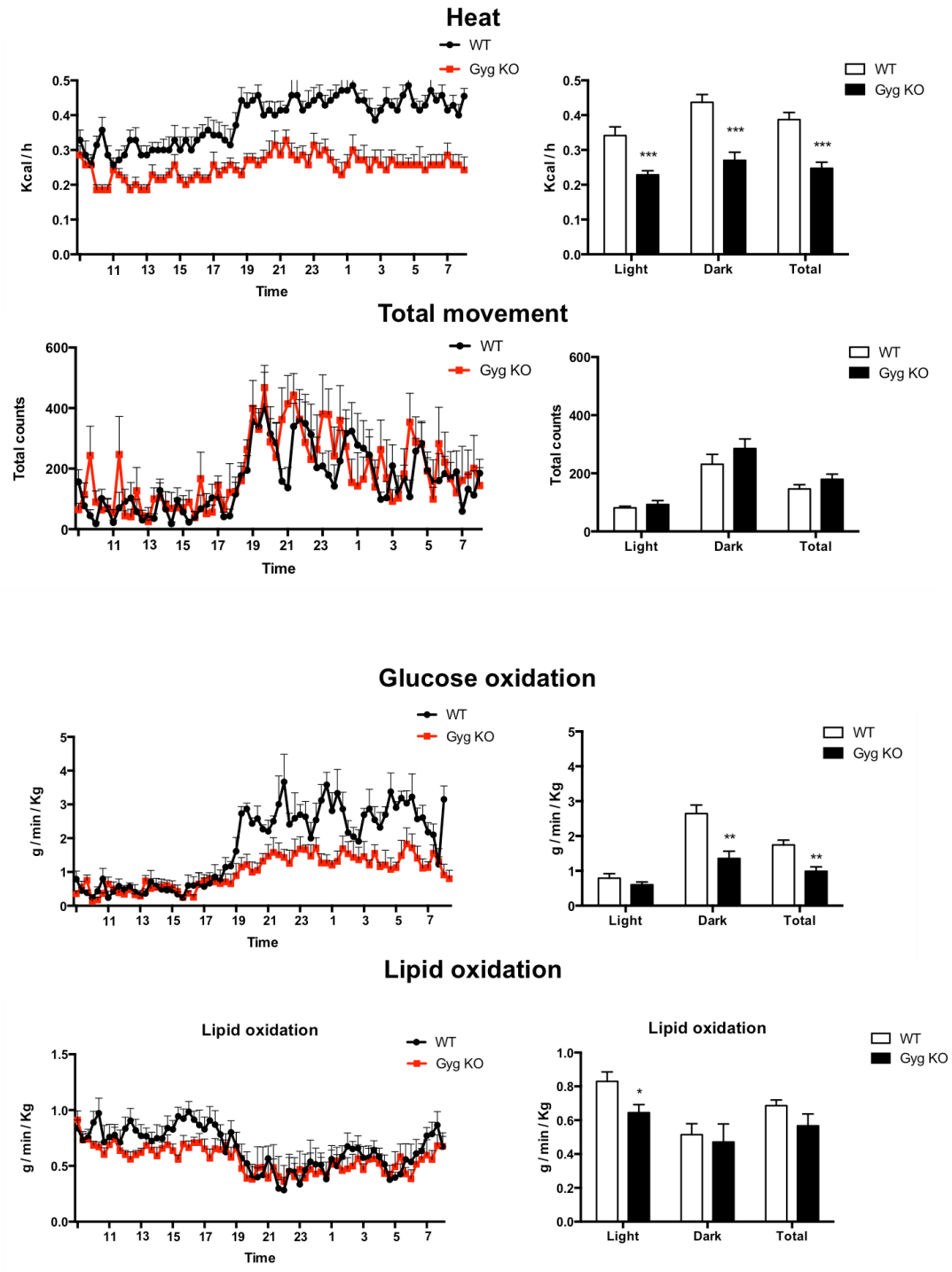


**Figure 64. Oxymax parameters (II)-** Calorimetric data obtained by Oxymax device from 8 animals per group. Each animal was measured for 2 days. All values are normalized by the daily weight of the subject. Graphs represent the average per group and SD. Left panel indicate the variation along the day: on the horizontal axis is reported the time of the day (hours). Right panels show the average of values during light and dark phase, and total

From previous analysis of plasma lactate does not results to be impaired in Gyg KO **(Figure 62),** but obviously a change in metabolism and cellular respiration is occurring. For this reason we measured internal lactate at intramuscular and

hepatic level **(Figure 65)**. Skeletal muscle shows an increase value of retained lactate. To explore this possibility we analyzed mitochondrial parameters and cellular respiration (see chapter 8).

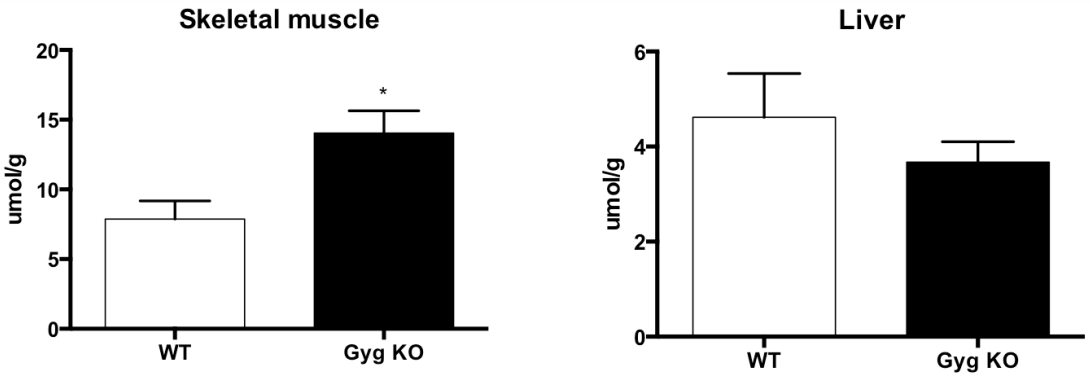


**Figure 65. Lactate measurement in tissue-** Quantification of lactate was performed from frozen tissue of fed and rested adult male animals (n=8)

Since glucose oxidation was lower in Gyg KO, we analyzed muscular and hepatic ATP, together with other nucleotides as AMP, ADP, NAD and NADP by HPLC of tissue homogenates **(Figure 66 and 67).**

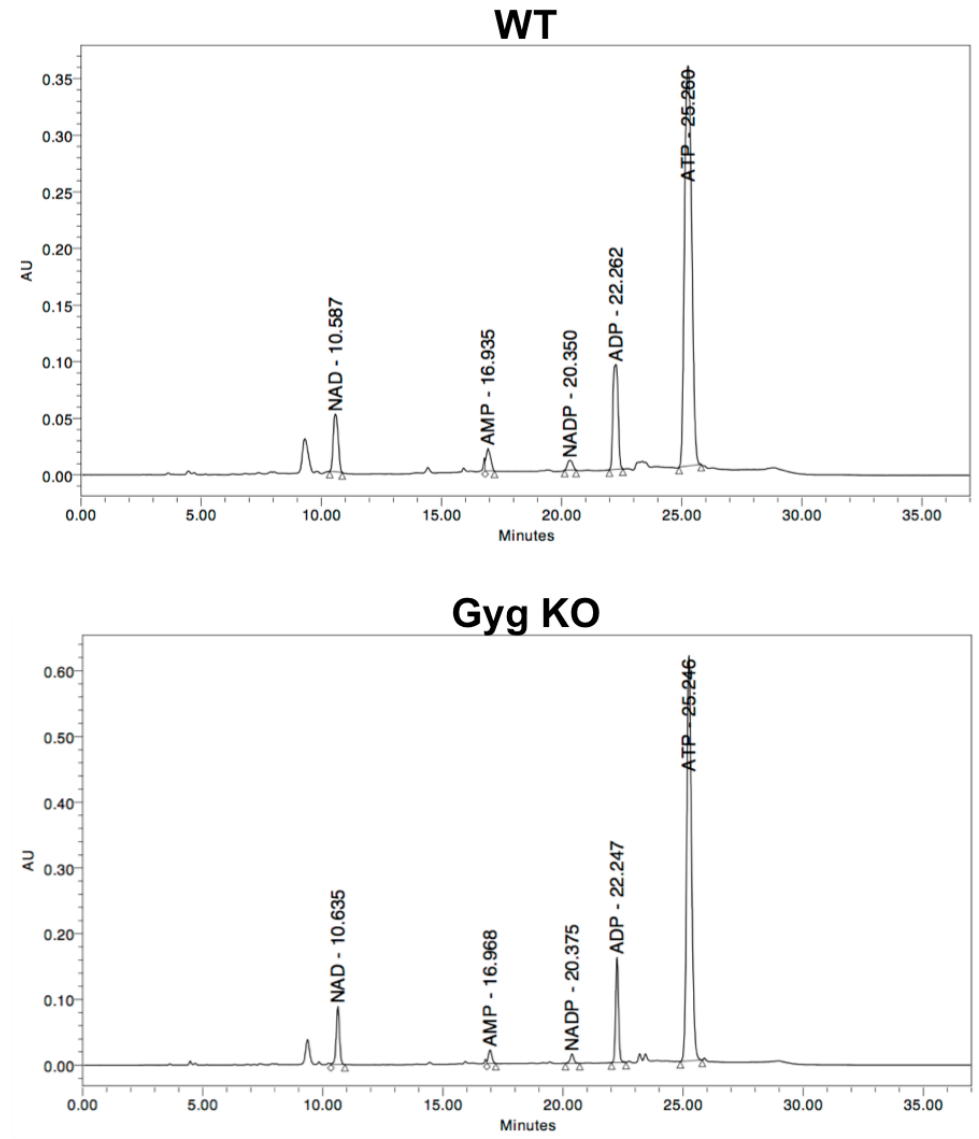


**Figure 66. Nucleotide chromatogram –**Example of skeletal muscle data from frozen tissue from adult male animals (n=8). Values reported in Figure 85 are calculated based on the area of the peak of each nucleotide for each sample

Levels of ATP in liver and muscle were not different. The only change observed is a decrease in AMP level in muscle. In liver no changes are observed **(Figure 67B).**

**A**

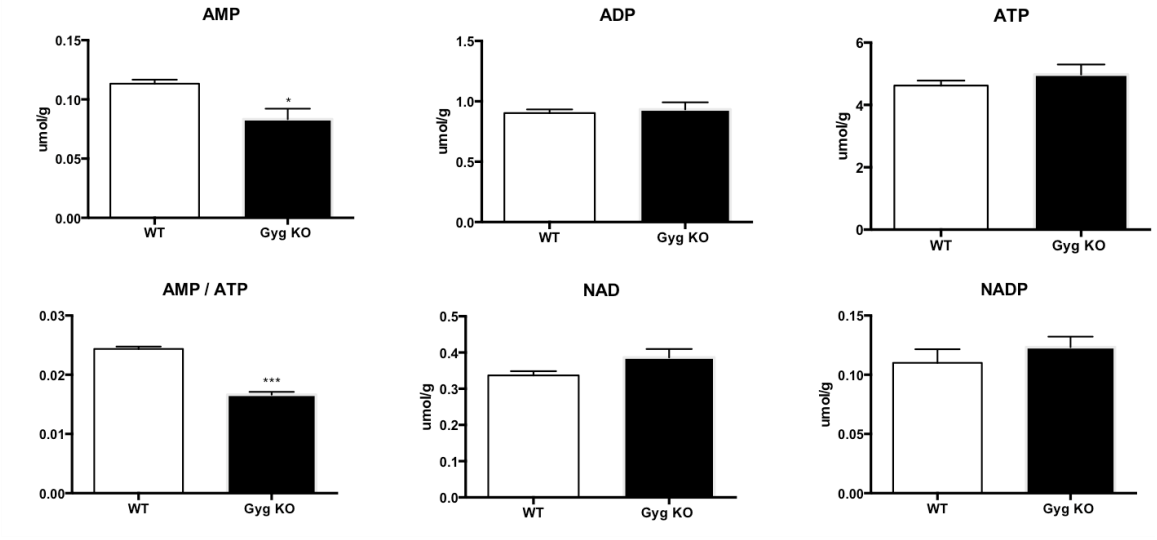


**B**

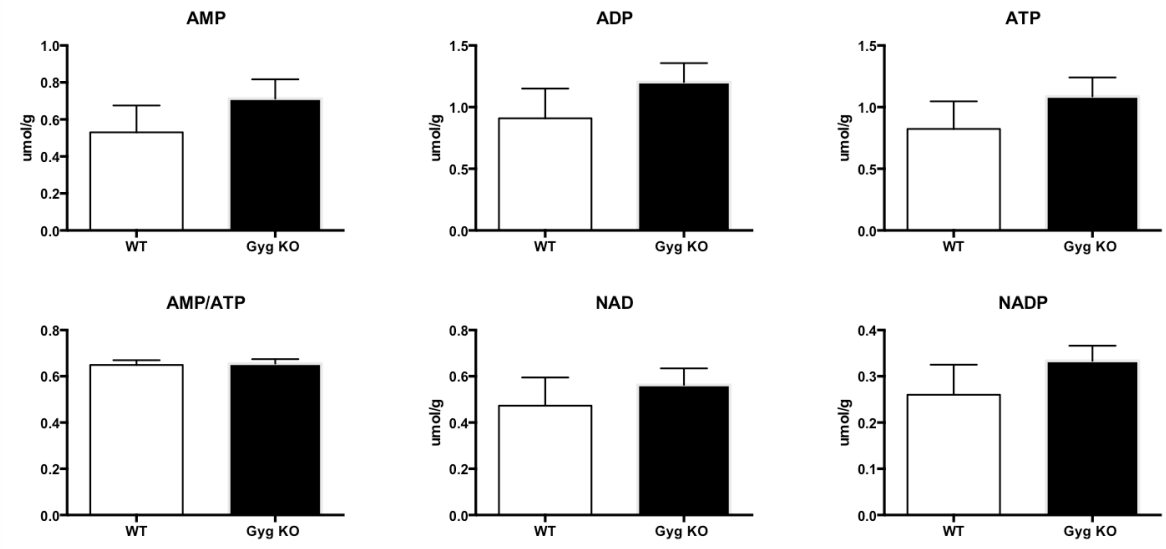


**Figure 67. Nucleotide measurement in skeletal muscle and liver-** A) skeletal muscle; B) liver (n=8)

To keep investigating what the differences in energy expenditure are due to, we analyzed other parameters. We previously described that there are no differences in body weight comparing Gyg KO and WT, but an explanation for the lower metabolism observe could be derived from a lower food intake. However, daily food intake measured for 7 days in 8 animals per groups, show that this is not the cause **(Figure 68).**

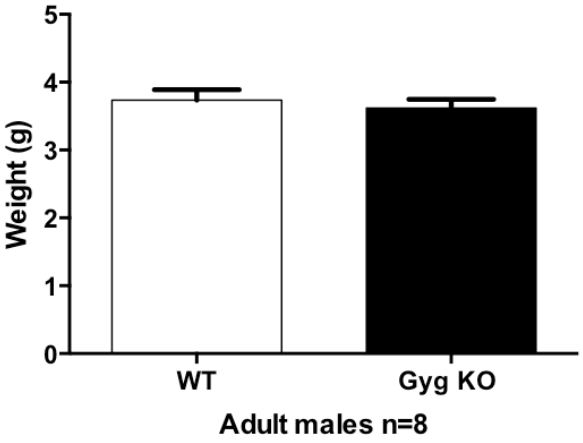


**Figure 68. Average of food consumption-** Quantification of the food consumption was performed every morning at the same time during 7 days in 8 adult males per group.

In addition to heat production, previously measured by oxymax chamber, we also observed body temperature, measured daily with rectal probe. This parameter in fact reveals a lower temperature in the Gyg KO supporting lower energy expenditure **(Figure 69).**

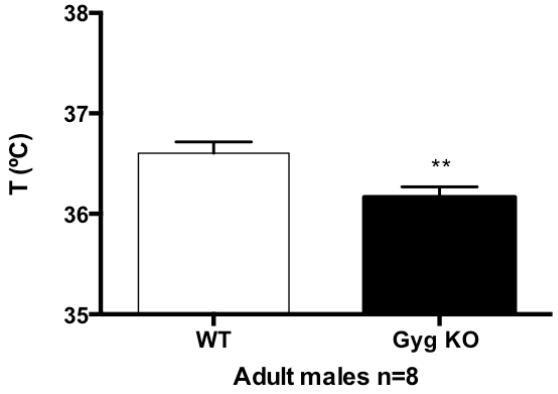


**Figure 69. Average of rectal temperature-** Measurement of the body temperature was performed every morning at the same time during 5 days in 8 adult males per group

A central point for body temperature regulation is adipose tissue, particularly brown adipose tissue. For this reason we explored the possibility that metabolic changes reside in this tissue and as a starting point for this analysis we determined if the different parts have difference in weight **(Figure 70).** However, we did not observe difference in weight either in brown, visceral, epididymal nor subcutaneous adipose tissue.

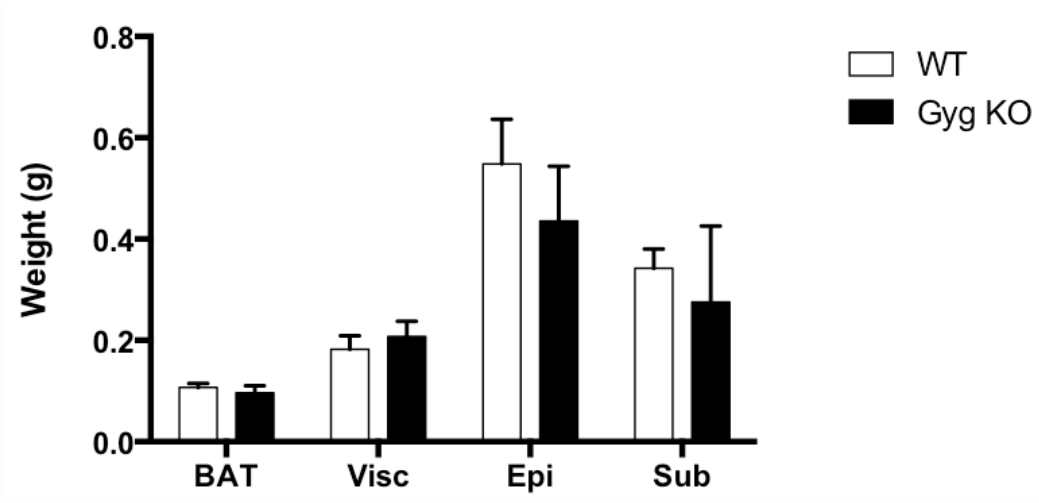


**Figure 70. Adipose tissue weight**

## 7.4 Conclusions

In conclusion, physiology analysis highlights a big difference in the metabolism of Gyg KO animals. Despite no difference was observed under long fasting and glucagon treatment, we saw a different response under high-energy request by the muscle, as treadmill exercise. Exercise resistance resulted to be impaired in Gyg KO that reached exhaustion much faster than WT littermates. Both glucose and lipid oxidation are lower in Gyg KO, even though ATP level is maintained equal. Supported also by the lower body temperature, it seems that Gyg KO animals suffer of a slower metabolism.

# 8. Physiological characterization of Gyg KO mice: skeletal muscle

## 8.1 Introduction

Skeletal muscle is the tissue that shows major physiological differences in Gyg KO. For this reason we performed more specific studies to seek possible metabolic changes that would explain lower energy expenditure in Gyg KO and lower muscular performances. Moreover muscle is the tissue majorly affected by the lack of glycogenin, showing increased glycogen accumulation. Now we explore the possibility of metabolic adaptation of the muscle to the lack of glycogenin or better to the increase of glycogen content.

Glycogen is one crucial energy source in skeletal muscle, particularly in case of rapid and intense activity. For this reason it is also the main energy source for type II fast-twitch fibers, having glycolytic metabolism and a lower number of mitochondria and myoglobin (this is the reason for the lighter color). Examples of muscle that mainly contain type II fast-twitch fibers are extensor digitorum longus (EDL) and tibialis anterior (Tib A/ TA). On the other hand, slow-twitch red fiber, which are used for endurance or resistance have an oxidative metabolism, based on triglycerides as a primary energy source and higher mitochondrial number. Soleus (Sol), Tibialis posterior (Tib P/ TP) and diaphragm (DFG) are examples of muscles containing mainly these fiber types. Muscles as quadriceps (QC) and gastrocnemius are a mixture of both fiber types to supply their extensive functions.

## 8.2 Characterization of glycogen metabolism in different skeletal muscles

We then characterized differences in expression of GS and GN proteins in the different muscles **(Figure 71).** We observed that GN is highly expressed in red

fiber muscle as soleus and tibialis posterior compared to EDL and Tibialis anterior. GS levels reflect the same results. On the other hand GS levels in Gyg KO skeletal muscle are increased compared to WT, as seen previously seen **(Figure 37).** The same results are reflected from the analysis of relative gene expression of Gyg and Gys1 showed in Sol and EDL **(Figure 72).**

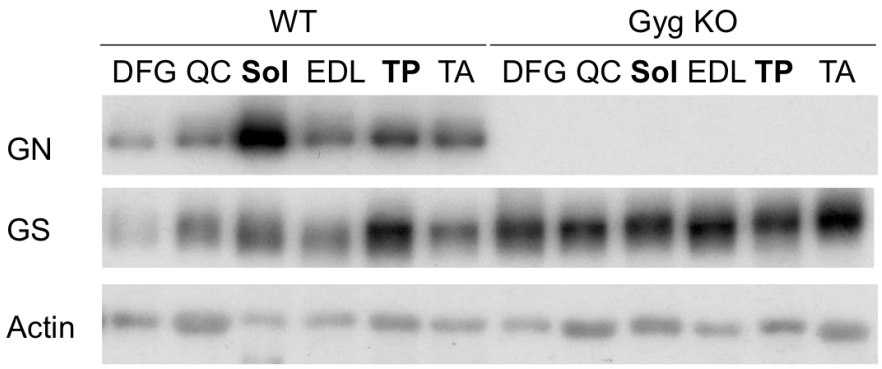


**Figure 71. Immunodetection of GN and GS in different skeletal muscles-** Isolated skeletal muscle were homogenized and same amount of total protein was loaded in the gel. Samples were treated with Amylase in order to detect GN.

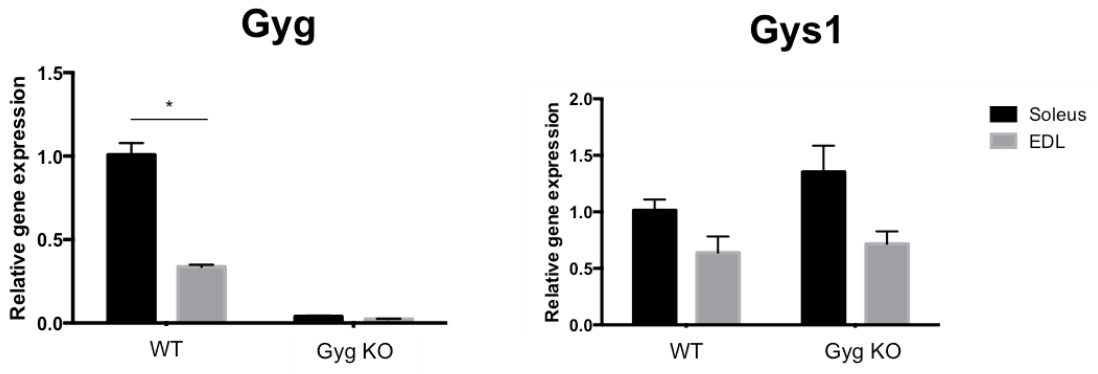


**Figure 72. Relative gene expression of Gyg and Gys1 in soleus and EDL-** Values of gene expression are normalized for WT soleus.

To start the characterization of the physiology of skeletal muscle we measured the glycogen content of different muscle types **(Figure 73).** Accumulation of glycogen in Gyg KO animals occurs in every muscle varying from a fold-change increase of 4 times in DFG to almost 9 times in EDL.

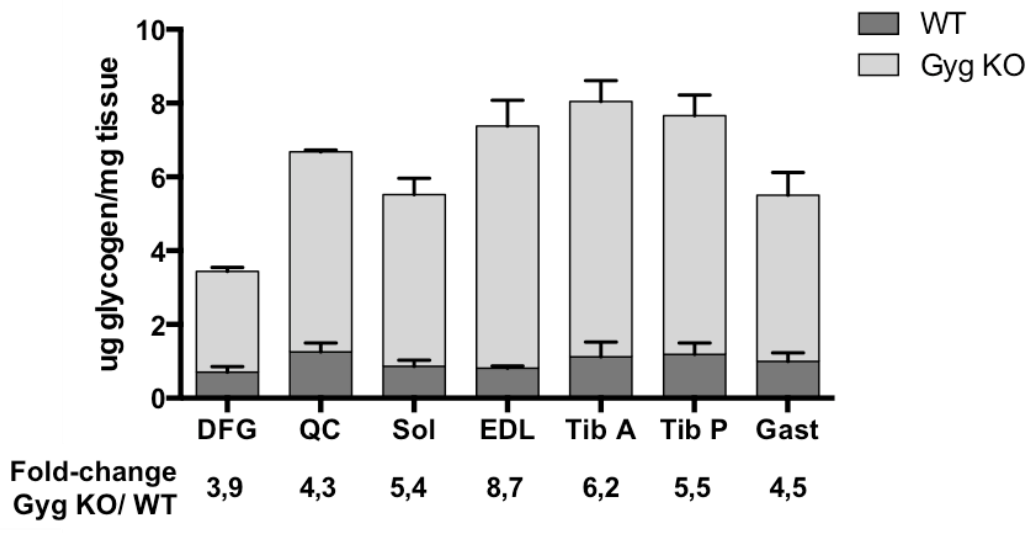


**Figure 73. Glycogen measurement in different skeletal muscles-** Quantification of glycogen from leg skeletal muscles and diaphragm (n=3). Bottom values report the fold-change increase of glycogen in the respective muscle in Gyg KO compared to WT

We analyzed quadriceps mitochondria and glycogen content. From a lower magnification it is visible the inverse proportionality between the marker of glycogen (PAS) and Succinate dehydrogenase (SDH), in blue, as a surrogate for mitochondria detection **(Figure 74).** From higher magnification images it is possible to have a closer look at single-fiber level. In WT the level of glycogen is proportional to the level of SDH, while in Gyg KO quadriceps fibers with very high glycogen correlate with low SDH.

An intermediate situation is represented by the Gyg heterozygous, in which we can classify three categories of fibers:

- Low SDH and low PAS, as in WT
- High SDH and medium PAS
- Medium SDH and high PAS

It seems a sort of adaptation to the intermediate level of glycogen.

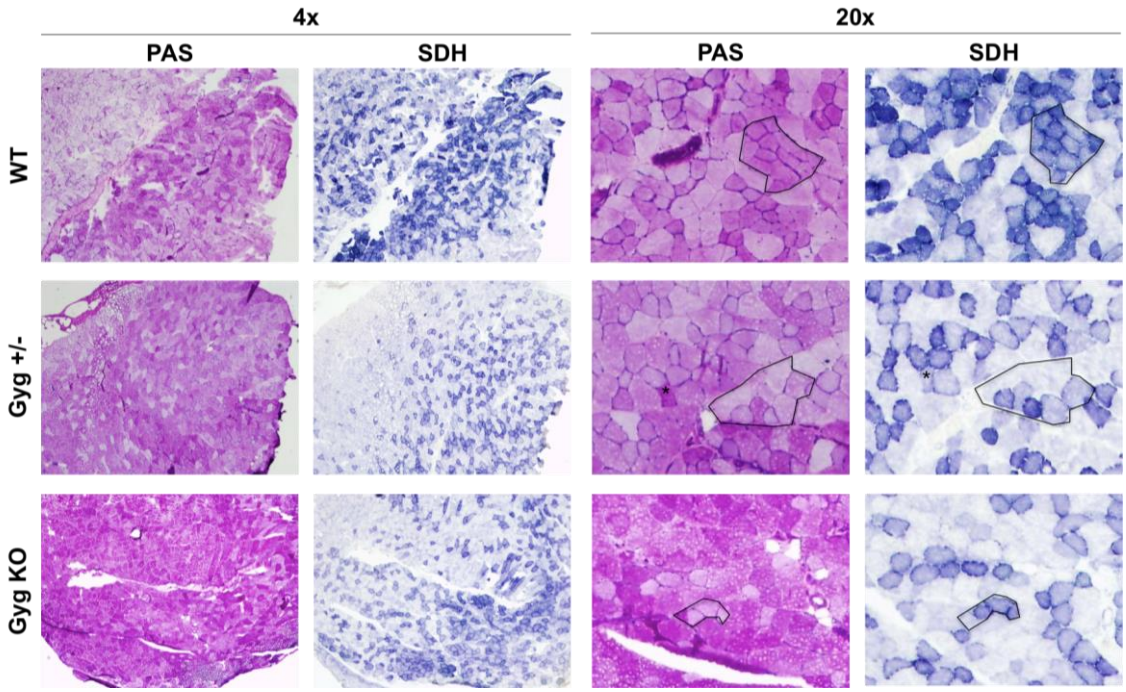


**Figure 74. Comparison of PAS and SDH staining in quadriceps-** Serial slices were used to perform parallel staining with PAS and SDH. Quadriceps from adult mice snap frozen in OCT blocks.

We next focused on the analysis of possible differences between type I and II fiber types, taking advantage of the fact that their metabolic characterization had already been established. Soleus is usually a muscle that does not rely on glycogen as a main energy source, but in Gyg KO this fuel is greatly available, as seen in **figure 75**. We tested whether high glycogen level can be used as a primary fuel in type I fibers analyzing changes of the level of mitochondria as result of a switch from oxidative metabolism to glycolytic. Comparison between WT and Gyg KO was made in three different muscles: soleus, EDL and tibialis (composed by anterior and posterior).

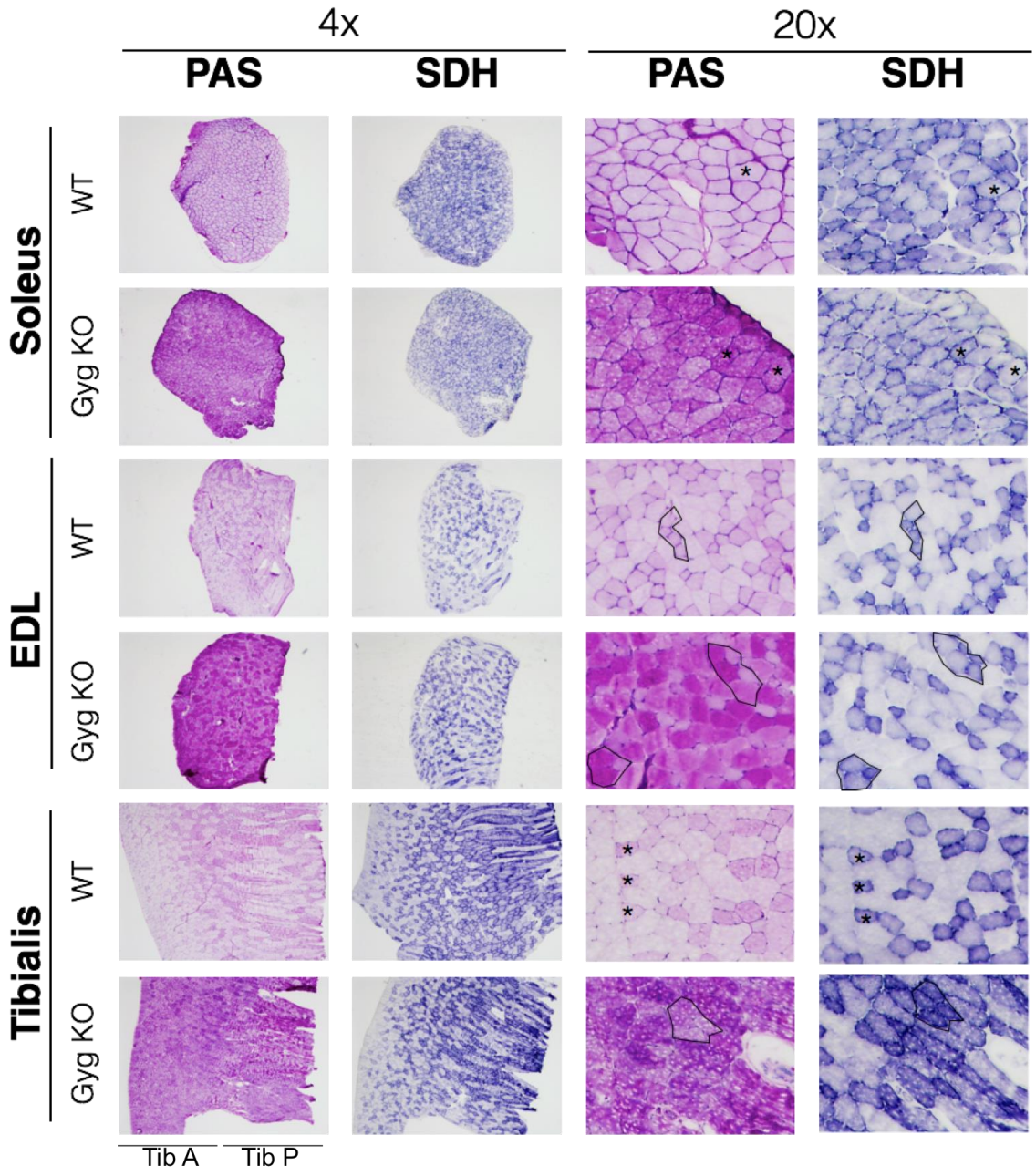


**Figure 75. Histology of adult males skeletal muscle-** PAS and SDH stains were performed on serial slices from OCT block of 4-months-old mice. Comparison of 3 different skeletal muscles: Soleus, EDL, Tibialis. On the right, in higher magnification images: * indicates single fibers or closed line indicates fiber groups, used as guidelines to explain the observations

**In figure 75**, we confirmed the observation we made in quadriceps, regarding glycogen and mitochondria. These observations support our hypothesis of a metabolic adaptation to the high availability of glycogen in the soleus. On the other hand, EDL does not seem to be affected, probably because it has already enough amount of glycogen source to sustain the glycolytic metabolism. To test whether the adaptation belongs from a change at transcriptional level of fiber-

specific genes, we analyzed the mRNA level of MHC I (Myosin heavy chain I) and Myoglobin characteristic of type I fibers and MHC IIb and IIX for type II fibers. In soleus and EDL of Gyg KO animals there were no changes compared to WT **(Figure 76)**, so the adaptation is not due to a change in gene expression.

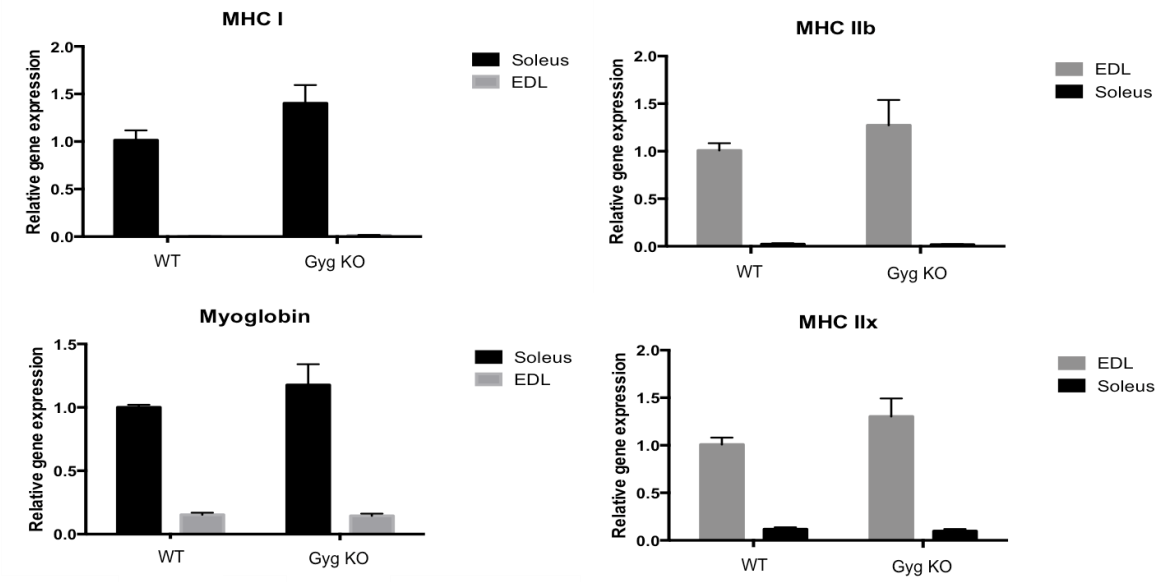


**Figure 76. Relative gene expression of fiber types markers-** Quantification of transcript of Myosin heavy chain I, IIb, IIx and Myoglobin is performed to compare expression in soleus and EDL muscles from adult mice. Data were normalized for WT soleus relative to r18S gene expression.

We proceed testing the functionality of the skeletal muscle. We used the Aurora muscle-strip myograph (collaboration Dr. Pura Muñoz-Canoves, UPF Barcelona), a specific device to measure intensity and speed of the muscle contraction **(Figure 77).**

The first experiment aimed to measure the maximum force a muscle can apply when subjected to increasing frequency stimuli. This is the primary ability supported by Type II fiber muscle, as EDL. We observed that EDL, as expected, responded with high force due to the fast-twitch fiber types and its glycolytic metabolism. As expected WT soleus applied lower maximum force. Gyg KO soleus, on the other hand, responded to the stimuli with higher force, almost double than WT. The values did not reach the same level as EDL, but this experiment is the evidence of faster contractions, correlating to increased

glycogen levels. However, Gyg EDL did not show higher maximal force compared to WT EDL.

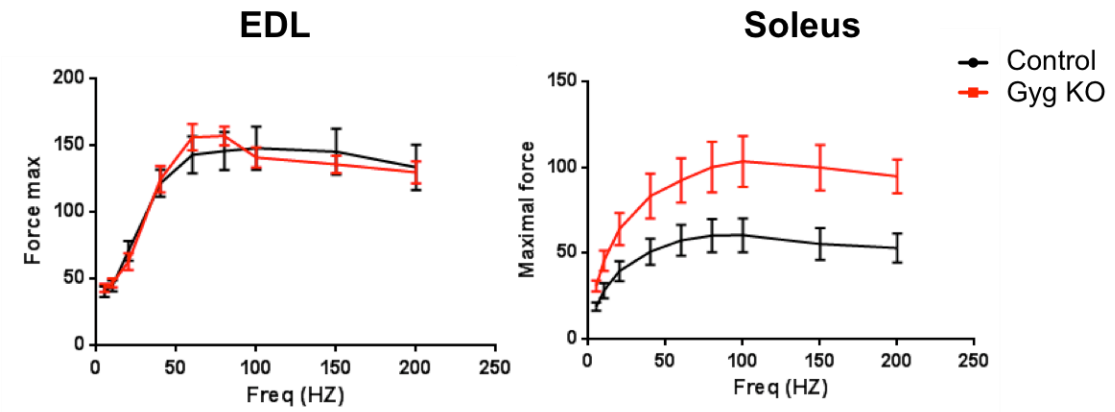


**Figure 77. Force-frequency mean measured by myograph strip-** Increasing frequency stimuli were applied to the isolated muscle, and force was recorded in response to the contraction.

From these results, it is evident that soleus is altered, and the presence of glycogen induces some changes that affect its response to stimuli, histology and muscular performances, as in the treadmill and values in the oxymax. A logical explanation for these alterations could derive from a lower oxidative respiration in muscle fibers of Gyg KO. To test this process, muscle fibers were extracted from adult male mice and permeabilized, in order to measure high-resolution respirometry using the oroboros device **(Figure 78).** Gyg KO soleus show an evident decrease of the oxygen flux in the total cellular respiration compared to WT **(Figure 78A)**. While in Gyg KO EDL the values obtained are comparable to WT EDL **(Figure 78B)**. From the analysis of mitochondria respiration it is clear that Gyg KO $O_2$ production is lower than WT, reaching the same values as EDL. These results support previous observations made by myograph, regarding the alteration of Gyg KO soleus, and explain the data obtained with the oxymax.

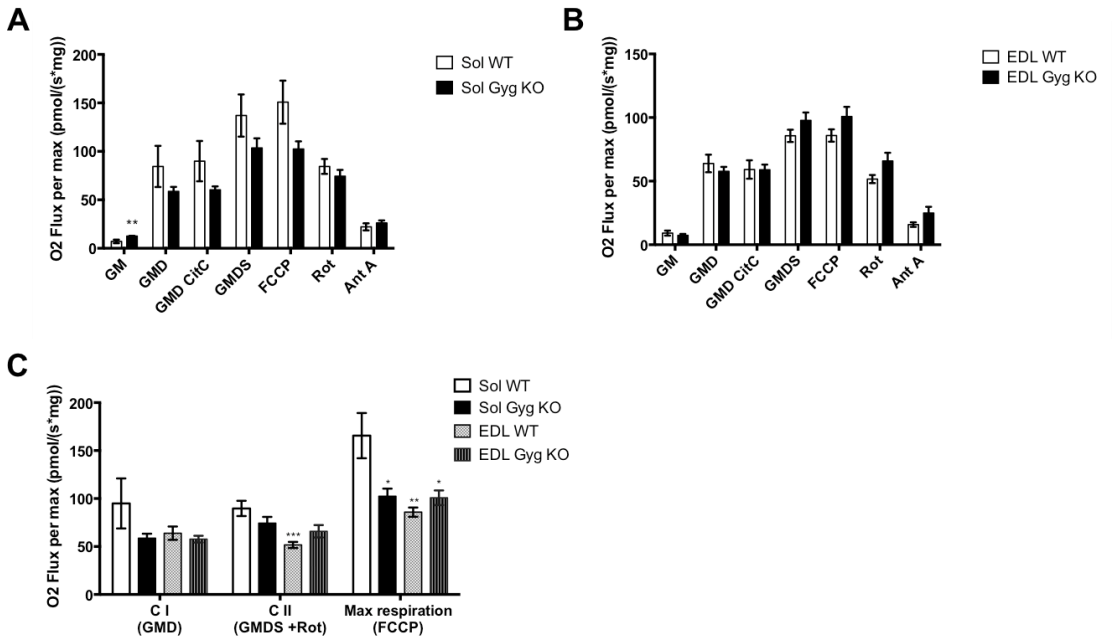


**Figure 78. Effect of Gyg depletion on oxygen consumption in permeabilized muscular fibers.** Measure of total oxygen flux in soleus (A) and EDL (B) permeabilized fibers, in different respiratory states. C) Measure of mitochondria respiration, subtracted the value of oxygen consumption obtained using antimycin A to inhibit complex III, in presence of ADP. Statistical analysis: Student's t test comparing values to Sol WT of each condition (n=3) GM: glutamate + malate; GMD: glutamate+ malate+ ADP; Cit C: cytochrome C; GMDS: glutamate+ malate + ADP + succinate; FCCP: protonophore carbonylcyanide-4-(trifluoromethoxy)-phenylhydrazone; Rot: rotenone; Ant. A: antimycin A

## 8.3 Glycogen accumulation is the responsible for muscle impairment

The question regarding the real cause of these phenotypic changes in Gyg KO remains still open. Gyg KO mice are characterized by the lack of the protein glycogenin, and also by a great accumulation of glycogen in the muscle. To know if the main responsible for the muscular impairment and low energy expenditure is just the lack of protein or its first consequence, as the glycogen accumulation, we generated (Dr. Duran) a muscle-specific MGS Knock-in (Kin) using an MLC1-Cre skeletal muscle-specific Cre recombinase (9A-MGS$^{MLC1}$). This mouse expresses constitutively active glycogen synthase and accumulates 8 times more glycogen in skeletal muscle than WT and moreover retains the presence of glycogenin (higher than WT). From the investigation of specific parameters of interest as exercise performances on a treadmill and oxymax

parameters (data not shown), we obtained similar results as Gyg KO. 9A-MGS$^{MCL1}$ Kin mice showed low energy expenditure and consequently also they reach faster the time of exhaustion on the treadmill **(Figure 79).**

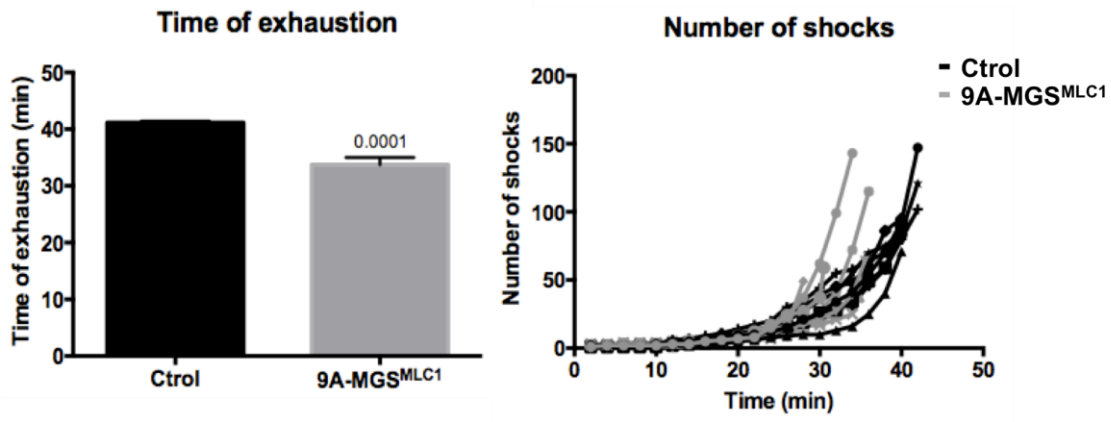


**Figure 79. Treadmill exercise parameter in MGS Kin mice -** Time of exhaustion is the average of animals of the groups. In the panel on the right are plotted cumulative number of shocks for every individual; n=7. (Font. Dr Duran J).

Accordingly to this, the responsible for muscle impairment is the higher glycogen content and not the lack of glycogenin itself.

## 8.4 Conclusions

Glycogenin KO mice have lower energy expenditure, as observed during exercise experiments, by calorimetric analysis and by cellular respiration. We show that excess of glycogen contributes to a change of metabolism in fibers that usually do not rely on glycogen as primary fuel, as we observed in soleus. Slow-twitch fibers are characterized by low force and high cellular respiration, by Gyg KO soleus showed an opposite scenario, reflecting instead characteristics typical of fast-twitch fibers. The changes observed in Gyg KO soleus explain the limited performance of the mice on the treadmill.

# Discussion

In this thesis we show for the first time that glycogenin (GN) is not an absolute requirement for glycogen synthesis. Indeed, GN-depleted mice show the ability to synthesize glycogen in muscle, heart, brain and liver. Moreover, the cardiac and skeletal muscle of this model, not only make glycogen, but also synthesize 6- and 8-fold more than the WT animal, respectively **(Figure 19).**

In the Gyg KO mouse, glycogen accumulation is caused by an increase in its synthesis, since there is more GS protein and activity **(Figures 37 and 39).** In addition, the possibility that glycogen accumulates as a result of an impaired degradation machinery is ruled out since GP is functional and slightly increased **(Figures 41 and 42)**. The accumulated glycogen differs from polyglucosan bodies. In this regard, its degree of branching is normal, its phosphate content is not increased, and it can be degraded **(Figure 28, 29 and 26)**.

In this study, we have demonstrated a new role of GN in glycogen metabolism. GN acts as a negative regulator of GS, thus controlling glycogen levels. GN strongly interacts with GS, and we propose that the ratio of these two proteins plays a crucial role in limiting the maximal amount of glycogen to be synthesized. In this regard, Gyg heterozygous mice, which have only half the amount of GN, show glycogen values falling between those found in WT and Gyg KO animals **(Figure 19)**. Furthermore, as previously demonstrated (Alonso et al. 1995; Ugalde, Parodi, and Ugalde 2003), in WT animals, the level of GN is inversely proportional to the amount of glycogen present. Liver expresses the lowest amount of GN and the highest amount of glycogen **(Figure 35)**.

We tested whether another unknown protein would be able to substitute GN in the priming of the glycogen chain. In order to find such a putative protein, we used mass spectrometry to identify any protein covalently bound to glycogen. The method detected GN in WT samples and identified the GN peptide

containing tyrosine 195, the priming site of glycogen. However, we did not find any other protein covalently bound to glycogen and potentially replacing GN in Gyg KO samples. Therefore, we excluded the involvement of another protein acting as glycogen primer and favor the hypothesis that, in these animals, glycogen is made by GS, without the participation of a protein primer. In fact, in other systems, it has been shown that glucose polysaccharides are synthesized de novo. For example, in *Agrobacterium tumefaciens*, no primer contributes to the action of GS, which catalyzes both the autoglucosylation and elongation of the molecule (Ugalde, Parodi, and Ugalde 2003). In addition, a yeast *Saccharomyces cerevisiae* strain mutated in both genes encoding GN, namely *glg1 and glg2*, conserves the ability to synthesize glycogen (Torija et al. 2005). Another example is found in plants, which do not use a primer for starch synthesis. In this case, this process is performed by the coordinated action of multiple SS (starch synthase) isoforms, which do not self-glycosylate (Szydlowski et al. 2009).

Skeletal muscle was the tissue in which we identified the most significant changes caused by the accumulation of glycogen induced by GN depletion. Glycogen is one the main fuels for muscle contraction, particularly by fast-twitch fibers (type II), which need a rapid supply of ATP to produce force. The metabolism of these fibers is based on glycolysis and they cannot perform for long periods. Here we demonstrate that type II fibers, like those in EDL muscle, are not affected by greater availability of glycogen and that their efficiency is neither decreased or improved. By applying progressive frequency stimuli in Gyg KO EDL ex vivo, we demonstrate that the response is comparable to that of the WT **(Figure 77)**. Moreover, cellular and mitochondria respiration was not altered **(Figure 78)**. An opposite scenario was observed in slow-twitch fibers such as soleus. This muscle relies on oxidative metabolism, which allows a slower but more prolonged contraction, thereby favoring endurance during exercise. Gyg KO soleus was clearly affected by the over-accumulation of glycogen. Force-frequency myograph analysis of the soleus from this mouse model showed an increase in force compared to that of the WT **(Figure 77)**. We hypothesize that while glycogen availability in the soleus allows greater force production, it can compromise other functions. In fact, respirometry parameters

showed decreased oxygen flux compared to the WT animal. This decrease was particularly visible during maximum respiration in the presence of ADP and FCCP. This observation fully correlated with calorimetric values obtained in an oxymax chamber, in which Gyg KO animals showed lower $O_2$ consumption and $CO_2$ production, this indicating low energy consumption **(Figure 63)**. Moreover, glucose and lipid oxidation were also compromised, as were heat and body temperature, which were also significantly lower than WT values **(Figures 64 and 69)**.

Clear differences were observed during endurance exercise on the treadmill test **(Figures 57 and 58)**. Gyg KO animals reached exhaustion faster due to a rapid decrease in energy. Our hypothesis was that type I fibers were subjected to a metabolic switch caused by high glycogen availability. It is known that a fiber type switch occurs in other animal models, such as in PGC1-α muscle-specific knock out mice (a transcriptional regulator of key mitochondria genes), which show a lower number of mitochondria and acquire glycolytic metabolism. In this situation, mice undergo genetic reprogramming, expressing fiber type II isoforms of MHCs (Handschin et al. 2007). However, this is not the case in Gyg KO animals **(Figure 76)**. Therefore, we conclude that, in Gyg KO mice, fiber type switching does not occur but rather a metabolic adaptation caused by increased levels of glycogen.

To determine whether the changes in metabolism are due to the lack of GN or to the level of glycogen, we analyzed a mouse model expressing constitutively active MGS specifically in the skeletal muscle (9A-MGS$^{MLC1}$). These mice retain the expression of GN but have higher glycogen content than the WT and show a phenotype similar to Gyg KO animals: rapid exhaustion during exercise and low energy expenditure **(Figure 79)**, as measured by the oxymax chamber. We thus conclude that the main cause of muscle impairment in Gyg KO animals is glycogen accumulation and not the lack of GN.

The results of the present study may have a great impact on our understanding of the role of GN in glycogen metabolism, but most of all in patients affected by GN depletion. In this regard, no such cases were described prior to 2010; however, since then, various studies report cases of GN depletion (GSD XV),

which is characterized by late onset symptoms affecting mainly muscle function (Malfatti et al. 2014; Colombo et al. 2015; Luo et al. 2015)**.** These individuals show symptomatic muscle weakness and progressive difficulty in walking, and higher glycogen accumulation in muscles, as determined by histological analysis. These observations correlate with the phenotype of our Gyg KO mouse model. These animals provide important insights into the causes of GSD XV and indicate that a strategy to decrease GS activity might offer a potential treatment for this condition. No GS inhibitors are currently available. However, intensive research efforts are being channeled into the discovery of such molecules, which could also find applications in other pathologies involving glycogen accumulation.

# Conclusions

- Depletion of Gyg gene determines high embryonic lethality. 90% of the Gyg KO mice die perinatally due to cardiac malformation. High content of glycogen is observed in the heart of these mice and this could result in a developmental abnormality.
- Surviving adult Gyg KO mice have increased glycogen accumulation in the heart and muscle.
- Glycogen synthesized in absence of glycogenin cannot be classified as a polyglucosan body: it has a normal branching degree, normal degradability, as well as less content of phosphate and a smaller size than polyglucosan. Moreover, this glycogen is degradable with amylase treatment (*in vitro* or *ex vivo*) and by exercise (*in vivo*).
- Glycogen accumulation in heart and muscle are caused by increased GS total activity and protein amount and not by lower GP levels.
- No other protein covalently bound to glycogen has been found in the Gyg KO liver or muscle.
- Gyg KO mice show muscle impairment during physical activity. *In vivo* energy expenditure is decreased and *in vitro* the muscle fiber glycogen level does not correlate to mitochondria level as in WT animals.
- Type I muscle fibers respond to high glycogen availability by increasing their force during contraction. These fibers adapt their metabolism to the energetic fuel available and thus become glycolytic. This affects the resistance of the muscle, as we observed during exercise.
- Low energy expenditure is not primarily caused by glycogenin depletion but by the increased level of glycogen, which is also observed in skeletal muscle-specific MGS knock in mice

# Supplementary tables

## Annex 1

Onestrep-eGFP-3C-GYG (WT) clone encodes for the following protein:

MASWSHPQFEK GGSGGGGGSGGSSWSHPQFEKSSGMVSKGEELFTGVVP
ILVELDGDVNGHKFSVSGEGEGDATYGKLTLKFICTTGKLPVPWPTLVTTLTYG
VQCFSRYPDHMKQHDFFKSAMPEGYVQERTIFFKDDGNYKTRAEVKFEGDTL
VNRIELKGIDFKEDGNILGHKLEYNYNSHNVYIMADKQKNGIKVNFKIRHNIEDG
SVQLADHYQQNTPIGDGPVLLPDNHYLSTQSALSKDPNEKRDHMVLLEFVTA
AGITLGMDELYKSSGLEVLFQGPMTDQAFVTLTTNDAYAKGALVLGSSLKQHR
TTRRMVVLTSPQVSDSMRKVLETVFDDVIMVDVLDSGDSAHLTLMKRPELGIT
LTKLHCWSLTQYSKCVFMDADTLVLSNIDDLFEREELSAAPDPGWPDCFNSG
VFVYQPSIETYNQLLHLASEQGSFDGGDQGLLNTYFSGWATTDITKHLPFVYN
LSSISIYSYLPAFKAFGKNAKVVHFLGRTKPWNYTYNPQTKSVNCDSQDPTVS
HPEFLNLWWDTFTTNVLPLLQHHGLVKDASSYLMMEHVSGALSDLSFGEAPA
APQPSMSSEERKERWEQGQADYMGADSFDNIKRKLDTYLQ
Blue =one-STrEP, green eGFP, red=3cprotease plus linker, black=WT mouse GYG

## Annex 2

Results obtained in different experiments each performed in biological duplicate or triplicate. Peptides listed in the tables are those found after amyloglucosidase digestion. In the lists below **(Table 6)** we cleared out peptides belonging from pig trypsin, from the previous experimental step, and contamination from keratins and ribosomal proteins. In the analysis of the results it is convenient to consider that protein represented by just one peptide have low confidence level.

**Table 6. List of protein correspondent to the peptide detection from Liver mouse purified glycogen. Experiment #1.**

**WT LIVER**

| Accession | Description | Score | Coverage | # Peptides | MW [kDa] |
|---|---|---|---|---|---|
| P69328-2 | Isoform G2 of Glucoamylase OS=Aspergillus niger | 595,7 | 16,5 | 28 | 56,7 |
| **Q9R062** | **Glycogenin-1** | **2,9** | **3,6** | **1** | **37,4** |
| P04919 | Band 3 anion transport protein | 2,1 | 1,9 | 1 | 103,1 |

**Gyg KO LIVER**

| Accession | Description | Score | Coverage | # Peptides | MW [kDa] |
|---|---|---|---|---|---|
| P69328-2 | Isoform G2 of Glucoamylase OS=Aspergillus niger | 621,1 | 16,7 | 30 | 56,7 |
| Q8C7E7 | Starch-binding domain-containing protein 1 | 6,2 | 6,5 | 2 | 36,1 |
| P16460 | Argininosuccinate synthase | 5,7 | 2,7 | 1 | 46,6 |
| P04919 | Band 3 anion transport protein | 4,6 | 1,9 | 1 | 103,1 |
| Q8VCT4 | Carboxylesterase 1D | 3,0 | 2,3 | 1 | 61,7 |

In WT sample, one peptide of glycogenin-1 was identified, although it did not contain Y195.

In the Gyg KO sample, 5 different proteins have been identified, two of which have a good score (≥5). Moreover, two different peptides from the protein STDB1 are found (GDGPGGGGSGGLSPEPSDR, AAPGDGPGGGGSGGLSPEPSDR), and although they do not carry any Tyrosine they share a region containing one Serine, containing hydroxyl side chain, it would be able to create covalent bound for example with oligosaccharides. Furthermore STDB1, would be a good candidate to substitute glycogenin, because it is the last member to be included to be part of the glycogen metabolism pathway and its role has not very well defined. It has been observed that it is able to bind inner cellular membranes and it could be associated to “glycophagy” as a novel cargo binding protein that delivers glycogen to lysosomes in an autophagy-like manner (Jiang et al, 2010 and 2011). In any case, although Glycogenin protein is found in WT sample, no Tyr195-containing peptide has been identified as a positive control. In addition spectrum show very high signal of glucosidase, used for glycogen degradation, that might cover lower signal due to peptides presents in less amount. To test if

STDB1 is the substitute protein, and to be able to identify the positive control peptide, we repeated the experiment in duplicate **(Table 7).**

**Table 7- List of protein correspondent to the peptide detection from Liver mouse purified glycogen. Experiment #2.**

**WT LIVER**

| Accession | Description | Score | Coverage | # Peptides | MW [kDa] |
|---|---|---|---|---|---|
| P69328 | Glucoamylase OS=Aspergillus niger | 334,9 | 50,8 | 136 | 68,3 |
| **Q9R062** | **Glycogenin-1** | **171,1** | **50,8** | **19** | **37,4** |
| Q9ET01 | Glycogen phosphorylase, liver | 80,3 | 21,7 | 17 | 97,4 |
| P00688 | Pancreatic alpha-amylase | 55,5 | 36,2 | 11 | 57,3 |
| Q8C196 | Carbamoyl-phosphate synthase [ammonia], mitochondrial | 44,0 | 11,0 | 12 | 164,5 |
| P00687 | Alpha-amylase 1 | 16,4 | 11,9 | 3 | 57,6 |
| P63268 | Actin, gamma-enteric smooth muscle | 14,8 | 18,1 | 1 | 41,8 |
| P16460 | Argininosuccinate synthase | 14,3 | 11,9 | 3 | 46,6 |
| P20029 | 78 kDa glucose-regulated protein | 13,5 | 7,5 | 3 | 72,4 |
| P04919-2 | Isoform Kidney of Band 3 anion transport protein | 10,6 | 3,9 | 2 | 94,2 |
| P24270 | Catalase | 9,2 | 5,9 | 2 | 59,8 |
| P47738 | Aldehyde dehydrogenase, mitochondrial | 8,9 | 6,0 | 2 | 56,5 |
| P60710 | Actin, cytoplasmic 1 | 8,4 | 16,3 | 1 | 41,7 |
| Q8VCT4 | Carboxylesterase 1D | 8,2 | 5,1 | 2 | 61,7 |
| P02088 | Hemoglobin subunit beta-1 | 8,0 | 21,1 | 2 | 15,8 |
| P56480 | ATP synthase subunit beta, mitochondrial | 7,4 | 6,4 | 2 | 56,3 |
| P0CG49 | Polyubiquitin-B | 6,8 | 21,0 | 2 | 34,3 |
| P01872 | Ig mu chain C region | 6,5 | 3,5 | 2 | 49,9 |
| Q03265 | ATP synthase subunit alpha, mitochondrial | 6,4 | 4,9 | 2 | 59,7 |
| P11714 | Cytochrome P450 2D9 | 5,8 | 4,6 | 2 | 56,9 |
| P29391 | Ferritin light chain 1 | 5,3 | 24,6 | 2 | 20,8 |
| Q91X83 | S-adenosylmethionine synthase isoform type-1 | 4,0 | 3,8 | 1 | 43,5 |
| P26443 | Glutamate dehydrogenase 1, mitochondrial | 3,8 | 3,8 | 1 | 61,3 |
| P68373 | Tubulin alpha-1C chain | 3,7 | 3,3 | 2 | 49,9 |
| Q8BWT1 | 3-ketoacyl-CoA thiolase, mitochondrial | 3,5 | 3,5 | 1 | 41,8 |
| P08113 | Endoplasmin OS=Mus musculus | 3,5 | 1,8 | 1 | 92,4 |
| Q91VS7 | Microsomal glutathione S-transferase 1 | 3,3 | 8,4 | 1 | 17,5 |
| P56395 | Cytochrome b5 | 3,2 | 9,0 | 1 | 15,2 |

| | | | | | |
|---|---|---|---|---|---|
| P54869 | Hydroxymethylglutaryl-CoA synthase, mitochondrial | 3,2 | 2,0 | 1 | 56,8 |
| Q05421 | Cytochrome P450 2E1 | 3,2 | 3,3 | 1 | 56,8 |
| P62806 | Histone H4 | 3,1 | 9,7 | 1 | 11,4 |
| P16858 | Glyceraldehyde-3-phosphate dehydrogenase | 3,0 | 4,5 | 1 | 35,8 |
| P30115 | Glutathione S-transferase A3 | 2,7 | 5,0 | 1 | 25,3 |
| Q8CE72 | Uncharacterized protein C5orf42 homolog | 2,5 | 0,9 | 1 | 358,3 |
| Q8BMS1 | Trifunctional enzyme subunit alpha, mitochondrial | 2,1 | 1,8 | 1 | 82,6 |

**Gyg KO LIVER**

| Accession | Description | Score | Coverage | # Peptides | MW [kDa] |
|---|---|---|---|---|---|
| P69328 | Glucoamylase OS=Aspergillus niger | 488,2 | 48,6 | 139 | 68,3 |
| Q8C196 | Carbamoyl-phosphate synthase [ammonia], mitochondrial | 36,7 | 7,9 | 7 | 164,5 |
| P60710 | Actin, cytoplasmic 1 | 9,8 | 9,9 | 4 | 41,7 |
| P56480 | ATP synthase subunit beta, mitochondrial | 9,8 | 2,8 | 1 | 56,3 |
| P16460 | Argininosuccinate synthase | 7,8 | 3,9 | 1 | 46,6 |
| P68373 | Tubulin alpha-1C chain | 4,0 | 7,8 | 2 | 49,9 |
| P68368 | Tubulin alpha-4A chain | 3,7 | 3,4 | 1 | 49,9 |
| Q63886 | UDP-glucuronosyltransferase | 3,5 | 3,0 | 1 | 60,0 |
| Q9WUB3 | Glycogen phosphorylase, muscle | 2,0 | 1,4 | 1 | 97,2 |

In WT samples 30 different peptides from glycogenin-1 were identified (51% coverage). One of them contained Y195 (SSISIYS**Y**LPAFK) and was identified bound to one hexose.

However, we did not identify STDB1 protein in the Gyg KO in either two of the new samples. On the other hand other protein, as GP (muscle isoform) and Argininosuccinate synthase (previously identified in experiment 1) are found in the Gyg KO samples. We repeated the experiments increasing the biological replicates in order to give consistency to the results and to obtain a clearer view on the complex ensemble of the proteomics results **(Table 8)**.

**Table 8. List of protein correspondent to the peptide detection from Liver mouse purified glycogen. Experiment #3.**

**WT LIVER**

| Accession | Description | Score | Coverage | # Peptides | MW [kDa] |
|---|---|---|---|---|---|
| P69328 | Glucoamylase OS=Aspergillus niger | 165,06 | 26,88 | 51 | 68,3 |
| **Q9R062** | **Glycogenin-1** | **37,87** | **36,34** | **14** | **37,4** |
| Q9ET01 | Glycogen phosphorylase, liver | 9,82 | 6,12 | 4 | 97,4 |
| P00688 | Pancreatic alpha-amylase | 6,61 | 7,48 | 3 | 57,3 |
| Q9WUB3 | Glycogen phosphorylase, muscle | 6,34 | 4,99 | 3 | 97,2 |
| Q8CI94 | Glycogen phosphorylase, brain | 6,34 | 4,98 | 3 | 96,7 |
| P0CG49 | Polyubiquitin-B | 4,71 | 17,05 | 2 | 34,3 |
| P0CG50 | Polyubiquitin-C | 4,71 | 15,94 | 2 | 82,5 |

**Gyg KO LIVER**

| Accession | Description | Score | Coverage | # Peptides | MW [kDa] |
|---|---|---|---|---|---|
| P69328 | Glucoamylase | 127,12 | 26,25 | 36 | 68,3 |

Glycogenin has been identified in the WT sample (16 peptides with 36.34% coverage). Also the three isoforms of GP have been detected in these samples. In Gyg KO no protein but glucosidase are detected.

# Annex 3

**Table 9. Peptide list detected in WT skeletal muscle-** In red peptides found in α-amylase treated samples; In green peptides found in amyloglucosidase treated samples; In green peptides found in both preparation; * indicates peptides found bound to one hexose

| Glycogenin peptides | |
|---|---|
| **Containing Tyr195 (Y)** | **No Tyr195** |
| SSISI**Y**SYLPAFK | YLPAFKAFG |
| ISI**Y**SYLPAFK | TYFSGWATTDITK |
| LSSISI**Y**SYLPAFK | YLPAFKAF |
| LSSISIYSYLPAFKA | SYLPAFKAFG |
| FVYNLSSISI**Y**SY | SYLPAFKAF |
| VYNLSSISI**Y**SYLPAFK | DITKHLPFVY |
| SSISI**Y**SYLPAFKAFG | |
| LSSISI**Y**SYLPAFKAFG* | |
| LSSISI**Y**SYLPAFKAF | |
| I**Y**SYLPAFK* | |
| **Y**SYLPAFKAF | |
| SSISI**Y**SYLPAFKAF* | |
| ISI**Y**SYLPAFKAFG | |
| FVYNLSSISI**Y**SYLPAFK | |
| SISI**Y**SYLPAFKAF* | |

# Annex 4

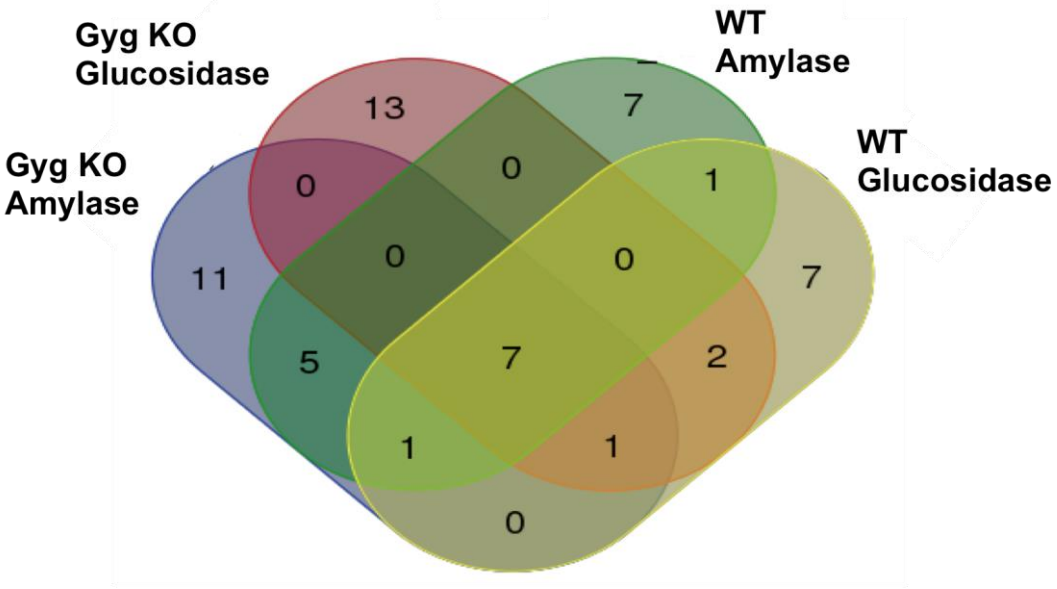


**Figure 80 Venn diagram of shared proteins-** The graph reports the number of protein detected in each subgroup. The sum of every set (colored circle) gives the total of protein detected for that sample. Overlapping circles indicates the number of protein shared for both sets.

**Table 10. List of the shared proteins among the groups**

| Names | Total | Protein |
|---|---|---|
| Gyg KO Amylase, Gyg KO Glucosidase, WT Amylase, WT Glucosidase | 7 | Titin |
| | | Calsequestrin-1 |
| | | Myosin-7 |
| | | Sarcoplasmic/endoplasmic reticulum calcium ATPase 1 |
| | | Myosin-1 |
| | | Myosin-4 |
| | | Creatine kinase M-type |
| Gyg KO Amylase, Gyg KO Glucosidase, WT Glucosidase | 1 | Parvalbumin alpha |
| Gyg KO Amylase, WT Amylase, WT Glucosidase | 1 | Elastin |
| Gyg KO Amylase, | 5 | >sp\|CASB_BOVIN\| |

| | | |
|---|---|---|
| WT Amylase | | ATP synthase subunit alpha, mitochondrial |
| | | Myosin-binding protein C, fast-type |
| | | Tropomyosin alpha-1 chain |
| | | Beta-enolase |
| Gyg KO Glucosidase, WT Glucosidase | 2 | Glucoamylase OS=Aspergillus niger |
| | | ATP-dependent 6-phosphofructokinase, muscle type |
| WT Amylase, WT Glucosidase | 1 | Glycogenin-1 |
| Gyg KO Amylase | 11 | Polymerase I and transcript release factor |
| | | Actin, cytoplasmic 1 |
| | | Isoform 2 of Keratin-associated protein 5-1] |
| | | Isoform B4e17 of Troponin T, fast skeletal muscle |
| | | Formyl peptide receptor-related sequence 1 |
| | | ATP synthase subunit beta, mitochondrial |
| | | DNA-directed RNA polymerase III subunit RPC3 |
| | | >sp\|ALDOA_RABIT\| |
| | | Homeobox protein ARX |
| | | Alpha-amylase |
| | | Neopullulanase |
| Gyg KO Glucosidase | 13 | Putative alpha amylase |
| | | Methyl-CpG-binding domain protein 5 |
| | | Glycogen debranching enzyme GlgX |
| | | Isoform 5 of Interleukin-17 receptor E |
| | | Isoform 3 of Centrosomal protein of 164 kDa |
| | | ATP synthase F(0) complex subunit C1, mitochondrial |
| | | Mitochondrial uncoupling protein 2 |
| | | Cyclin-dependent kinase 11B |
| | | RNA polymerase sigma factor SigA 1 |
| | | Aspartate aminotransferase |
| | | Putative secreted bifunctional |
| | | Alpha-amylase and endo-alpha-glucosidase: starch degradation and integral membrane protein |
| | | Uridine phosphorylase 2 |
| WT Amylase | 7 | Splicing factor, proline- and glutamine-rich |
| | | Low-molecular-weight glutenin subunit (Fragment) |
| | | Alpha-1,3-glucan synthase |
| | | Oxidoreductase HTATIP2 |
| | | Glyceraldehyde-3-phosphate dehydrogenase |
| | | Trehalose synthase |
| | | RING finger protein 207 |
| WT Glucosidase | 7 | High mobility group protein B1 |
| | | NADH-ubiquinone oxidoreductase chain 5 |
| | | Seminal vesicle secretory protein 4 |
| | | Isoform 2 of Zinc finger protein GLIS3 |
| | | Transmembrane transport protein |
| | | Pyruvate kinase PKM |
| | | Polysugar degrading alpha-amylase |

In Gyg KO treated with α-amylase we found two peptides with glucose residues attached:

- ERAFQKTH**Y(2Hex)**PDVFTREELAMRLDLTEARVQVW (Homeobox protein (ARX);
- **T(Hex)**VNVLSAARMLLHRCY (DNA-directed RNA polymerase III subunit (RPC3).

# Material and Methods

## Generation of the animal model and mice handling

### Generation of Gyg KO mice

Mice heterozygous for the glycogenin gene ($Gyg^{tm1a(KOMP)Wtsi}$) were obtained from the Knockout Mouse Project Repository (KOMP), University of California, Davis, CA. In these mice, the Gyg coding region for exon 3 and 4 is replaced with a cassette containing the following elements:

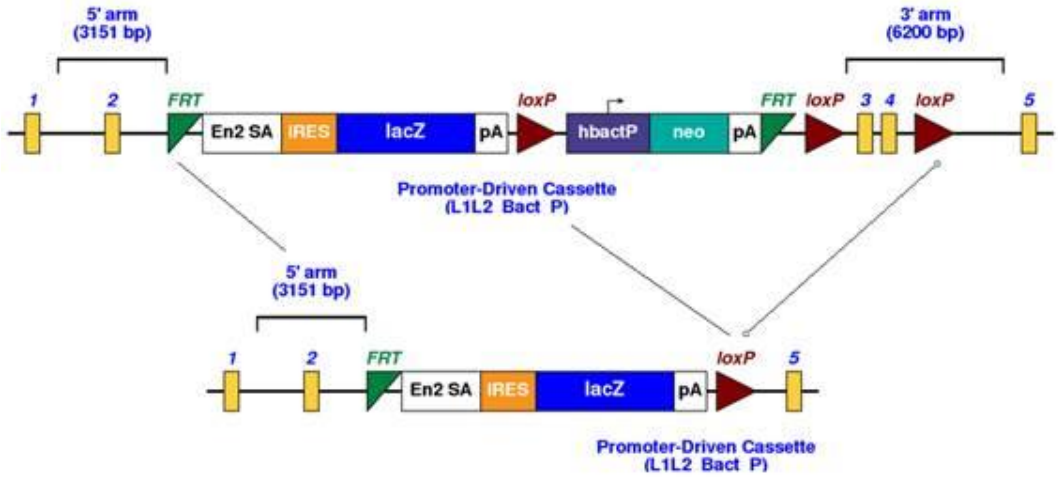


**Figure 81. Disruption of the Gyg gene**

FRT, Flippase recognition target for site-directed recombination; En2 SA: splice acceptor site; IRES: internal ribosome entry site; lacZ: gene for β-galactosidase; pA: polyA stop coding sequence; loxP: sequence recognized by Cre recombinase; hbactP: autonomous promoter; neo: neomycin resistance gene.
These Gyg +/- heterozygotes C57BL/6J mice were crossed with each other to generate the wild type, heterozygous, and homozygous knockout mice used in the studies presented here. Genotype was identified by PCR using initially oligonucleotide primer pairs for both the 5'-end and the 3'-end of the Gyg-disrupted region:

- GYGKOf1: TGTTGGGGACACATGCTGCGA;
- GYGKOr1: GAACTTCGGTTCCGGCGCCAG;

- GYGKOf4: TCACATTGAGATGGCGCAACGC;
- GYGKOr4: CCACTCGTCAGCTGTGAAGATGGC.

Transnetyx, Inc performed the following genotyping. Further confirmation of the disruption was obtained by RT-PCR of Gyg mRNA. For the generation of the Gyg Del mouse model, we mated Gyg heterozygous with an heterozygous mouse for Ub-Cre: B6_Cg-Tg(UBC-cre-ESR1)1Ejb-J (Jackson laboratory ref. 008085). This mouse expresses the Cre recombinase under the promoter of ubiquitin, in order to be constitutively expressed in all tissues. After obtaining the first double heterozygous mice we mated them to obtain Gyg Del. For the generation of the colony 9A-MGS$^{MLC1}$, mice expressing the recombinant cassette 9A-MGS, for the constitutive expression of active MGS, were crossed with mice expressing MLC1-Cre recombinase expressed under the control of the promoter of Myosin Light Chain 1. Tissue-specific expression of MGS occurs only in skeletal muscle. These mice are named MGS Kin.

All comparisons were among littermates. Mice were maintained in temperature- and humidity-con- trolled conditions with a 12h light–12h dark cycle and were allowed food and water ad libitum. All procedures were approved by Barcelona Science Park's Animal Experimentation Committee and were carried out in accordance with the European Community Council Directive and the National Institute of Health guidelines for the care and use of laboratory animals.

For timed mating, breeding pairs or trios were established by introducing female mice into cages with male mice in the late afternoon. On the following morning, females were checked for vaginal plugs indicative of mating. The date when a plug was found was designated embryonic day 0.5. Neonates for survival test were obtained by Caesarean section and placed in a tempered room at 30ºC. The lung float test is method used to identify whether the dead individual had undergone respiration before dying. The procedure consists in immerging lungs in water and observing if they precipitate.

# Microscopy analysis

## Sample preparation

Pregnant mice were sacrificed at various stages of gestation by cervical dislocation. Embryos were harvested, and fixed in 10% neutral buffered formalin by standard methods. Whole body embryos embedded in paraffin blocks were sectioned completely and serial slices of interest were selected for staining. Adult tissues used for histological analyses were removed after perfusion with 4% PFA of anesthetized animals with tiobarbital. Fixed samples were embedded in paraffin, sectioned (3 um), and stained with hematoxylin-eosin to examine organ morphology. Adult skeletal muscles, used for PAS and SDH staining, were removed after cervical dislocation and snap frozen in OCT blocks in 2-methylbutane maintained in liquid nitrogen. Embryonic and adult tissues used for biochemical assays were isolated from mice sacrificed by cervical dislocation and frozen directly in liquid nitrogen.

### Histological staining

PAS staining: selected brain sections were oxidized with 5% periodic acid for 10 min, stained with Schiff reagent for 30 min, dehydrated and mounted. To confirm the specificity of the staining sections were also treated with diastase, enzyme that degrade glycogen (PAS-D). This technique allows identifying specific glycogen signal, replacing the typical magenta color of Pas with light pink. PAS and PAS-D stain was performed by Artisanlink Pro machine using the kit DAKO AR165.

SDH staining: Succinate dehydrogenase (also known as complex II in the mitochondrial respiratory chain) is responsible for the oxidation of succinate to fumarate. A simple enzymatic reaction can be used to determine the relative SDH activity of individual muscle fibers in a skeletal muscle (in cryosections maintained at -20ºC. Selected slices are placed in incubation buffer prepared fresh from sodium succinate + NBT in 0,2M phosphate buffer ph. 7,6 (T=37ºC).

Masson’s trichrome: protocol suited for distinguish cells from surrounding connective tissue. Preparations were treated with Bouin’s solution, Weigert’s

reactives, Bierbrich scarlet acid fuchsin, phosphotungstic phosphomolybdic acid, aniline blue an acetic acid. Stain was performed by Artisanlink Pro machine using the kit DAKO AR17392-2.
Slides were observed by optical microscopy at the Nikon Olympus E600 of the Advanced Digital Microscopy Core Facility at IRB Barcelona.

### Electron microscopy

Animals were perfused with 2.5 % glutaraldehyde-2% paraformaldehyde in 0.1M phosphate buffer. Tissues of interest were extracted and cut in $1mm^3$ of volume and placed in the same fixation solution. After post-fixation in the same solution overnight, tissue slices were transferred to 1% osmium tetroxide, stained with 0.8% potassium ferrocyanide, dehydrated and infiltration in EPON resin. Blocks were embedded in silicon molds and polymerized at 60ºC fro 48 hours. Ultrathin sections from heart, liver, quadriceps, and hippocampus samples were processed at the Electron Microscopy Unit of the Core Scientific Services at the University of Barcelona (CCiT), and sections were then collected on copper grids. Sections were then stained with 2% uranyl acetate in water and lead citrate solution. Electron micrographs were taken using a Tecnai Spirit transmission electron microscope. Theiry staining was performed with periodic acid 1%, thiocarbohydrazyde (TCH) 0.2% in acetic acid 20% and silver proteinate (PATAg reaction) 1%.

## RNA isolation, cDNA synthesis and qPCR

Total RNA was isolated from mouse liver tissue by homogenizing (Polytron) 100 mg of the sample in 1 ml of TRIzol (Invitrogen). RNA of brain, muscle and heart was prepared with the RNeasy Mini kit (Qiagen). DNase digestion was performed with the RNase-free DNase Set of Qiagen. 5 µg of total RNA from each sample was reverse-transcribed for 50 min at 42 °C in a 15-ml reaction volume using 200 units of SuperScript III reverse transcriptase (SuperScript First-strand Synthesis System for RT-PCR (Invitrogen) in the presence of 50 ng

of random hexamers. Real-time qPCR using the Light Cycler 480 (Roche Diagnostics) was performed with a five-fold dilution of the cDNA. Each 10 µL-assay contained 5 µl of Fast SYBR Green Master Mix (Applied Biosystems), 2 µL primer mix for each gene (0.5 µM each final concentration), and 3 µL of diluted cDNA. The primers were selected from the Primerbank of Harvard. Each reaction was performed in triplicate. PCR cycling consisted of denaturation at 95°C for 5 min, 50 cycles of 95°C for 10 s and 60°C for 30 s, and detection for 1 s at 72°C. The temperature profile consisted of 40 cycles of 15 s at 95 °C and 1 min at 60 °C. Data were analyzed with the $2^{\Delta\Delta Ct}$ method using 18S rRNA as endogenous control. Primers sequences used were as follows:

**Table 11. RT-PCR primers**

| Gene | Name | Sequence |
|---|---|---|
| **Gyg** | mGlycogenin FW | 5'-TGGAGTCTTTGTCTATCAACCCT-3' |
| | mGlycogenin REV | 5'-TTGCCCAGCCACTAAAATATGT-3' |
| **Gys1** | mMGS FW | 5'-GAACGCAGTGCTTTTCGAGG-3' |
| | mMGS REV | 5'-CCAGATAGTAGTTGTCACCCCAT-3' |
| **Pygm** | mMGP FW | 5'-CTTAGCCGGAGTGGAAAATGT-3' |
| | mMGP REV | 5'-GTAATCTCTCGGAGTAGCCACA-3' |
| **Gys2** | mGys2 FW | ACCAAGGCCAAAACGACAG |
| | mGys2 RV | GGGCTCACATTGTTCTACTTGA |
| **Pygl** | mLGP FW | GAGAAGCGACGGCAGATCAG |
| | mLGP RV | CTTGACCAGAGTGAAGTGCAG |

# Protein detection

### Sample preparation, homogenization and fractionation for biochemical analysis

Tissues were stored at -80ºC until use. Tissue samples were added to 10 volumes of ice-cold homogenization buffer containing 10 mM Tris- HCl (pH 7), 150 mM KF, 15 mM EDTA, 15 mM 2-mercaptoethanol, 0.6 M sucrose, 25 nM okadaic acid, 1 mM sodium orthovanadate, 10 mg/ml leupeptin, 10 mg/ml aprotinin, 10 mg/ml pepstatin, 1 mM benzamidine and 1 mM phenylmethanesulfonyl fluoride. They were then homogenized (Polytron) at 4ºC. For sample fractionation, homogenates were centrifuged at 13000 g for 15

min at 4ºC. Sediments were resuspended in the same volume as the corresponding supernatant with homogenization buffer. Total homogenates, supernatants and sediments (pellet) were recovered for glycogen measurement and Western blotting. Samples were treated with amylase 110 U/ml for 1 h at 37ºC to analyze glycogenin by WB, in order to liberate the protein from the polysaccharide and entering the gel **(Figure 82)**. Protein quantification was performed using Bradford methodology (Bradford, 1976) based on the colorimetric change due to different protein concentration. In an acidic solution, Coomassie brilliant blue binds to proteins and changes the maximum absorbance peak from 495 to 595 nm.

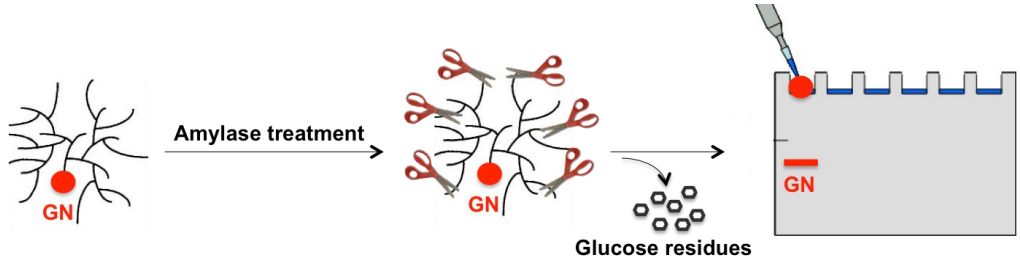


**Figure 82. Protocol for glycogenin detection by WB**

## Electrophoresis and immunoblotting

Immunoreactivity was determined by separating homogenates by 10% SDS-PAGE. Samples were transferred onto an immobilon membrane (Millipore). As a loading control, membranes were stained for Red Ponceau, and destained with PBS, Tween-20 0,1% at pH 7,4. Membranes were probed with the following antibodies: a rabbit antibody against mouse total GS (Cell Signaling 3886), a mouse antibody against GN (Novus Biological 3B5), a mouse antibody against glyceraldehyde-3-phosphate dehydrogenase (GAPDH; Sigma), a mouse antibody against actin (Sigma), a guinea pig antibody anti p62 (Progen GP62-C), a rabbit antibody against GBE1 (Proteintech 20313-1-AP), and homemade antibodies against LGS, GP2 (LGP), GPa2, GPM, GPB, AGL and STBD1 (gently donated by Dr. Stapleton D.). Secondary antibodies conjugated to horseradish peroxidase against rabbit (GE Healthcare) were used. Immunoreactive bands were visualized using an ECL Plus kit (GE Healthcare), following the manufacturer's instructions. For in-gel protein staining in polyacrylamide we used silver

# Enzymatic activity assays

## Glycogen synthesis activity

The enzyme activity was determined by measuring the incorporation of UDP-[$^{14}$C] -glucose to glycogen (Schlender et al. 1968). GS activity can be measured in the absence and presence of G-6P. To determine the activity of glycogen synthase in the absence G-6P we used a test solution composed of UDP- [$^{14}$C] -glucose, 6.7 mM UDP-glucose, 10 mg / ml glycogen, 25 mM KF, 20 mM EDTA, 50 mM Tris and adjusted to pH 7.8 with HCl. If it is determined in the presence of G-6P the same solution was prepared adding 10.8 mM G-6P. To perform the test, were placed 40 ul of the solution in a test tube. Then 20 ul of sample were added and the mixture incubated 10 minutes. Once past those minutes, 50 ul of the reaction mixture were deposited on a piece of paper 31 ET (Whatman). The glycogen is precipitated in 66% ethanol at a temperature of -20°C for 10 minutes. This change of temperature determines the precipitation and fixation of glycogen present in the mixture. After two more washes in ethanol at room temperature, papers were soaked in acetone to displace the ethanol and to dry them completely. Dried papers were introduced into vials containing scintillation liquid Ecolite (MP). Radioactivity was counted with a scintillation counter Rack BETA 1217 (LKB). GS activity measured in the presence of saturating G-6P (+ G-6P) corresponds to the total amount of enzyme, whereas measurement in its absence (- G-6P) is an indication of the active GS form. The -G-6P / +G-6P activity ratio (GS activity ratio) is an estimation of the activation state of the enzyme

## Glycogen Phosphorylase activity

Determination of GP activity was measured from tissues pulverized maintained at -80ºC, which was prepared in the same buffer and in the same condition indicated for the activity of GS. This activity was measured using a radiometric assay consists of measuring the incorporation of [$^{14}$C]-glucose-1P to glycogen, following the technique described by Gilboe (1972), in absence or presence of different effectors. The assay is based on the incubation of GP in conditions in which glycogen is synthesized. The activity assay mixture consisting of 75mm

[$^{14}$C] -glucose-1P, 125mM KF and 0.6% glycogen at ph 6.3 was used to determine GP. GP activity was measured in the presence of the allosteric activator, AMP, at a concentration of 5 mM and in muscle isoform (sensitive to activation by AMP), it could be taken as a measure of the total amount of the enzyme. The radiometric activity assay was conducted in the same manner as for the GS at 30ºC for 30 minutes using the same procedure and the same test conditions. The outcome is the amount of glycogen produced by the GP. The GP can be found in phosphorylated and active state (GPa) and dephosphorylated and inactive state (GPb).

## Glycogen measurement

Tissue and hepatocytes glycogen content was determined by an amyloglucosidase-based assay, as described elsewhere (Garcia-Rocha, 2001). Briefly frozen tissue was homogenized with Polytron in a relation 1:4 (w/v) with 30% (w/v) KOH, and 35mm petri dish with hepatocytes were scraped with 60ul of KOH; the extract was then boiled for 15 min and the resulting solution was spotted on chromatography paper 31ET (Whatman, Maidstone). Glycogen was precipitated by placing the papers in ice-cold 66% (v/v) ethanol. After two washes in ethanol, the papers were air-dried and incubated with amyloglucosidase 25U/l (Sigma) prepared in sodium acetate buffer100mM at pH 4.8, using the original method of Chan (Chan and Exton 1976). Glucose units were measured by reaction with hexokinase-G-6P dehydrogenase (*Glucose HK CP, ABX Pentra*) and adapted to the Cobas Bio autoanalyzer (*ABX Diagnostics*) (Bergmeyer, 1974). Results are expressed in ug of glycogen per mg of tissue or mg of protein.

## Glycogen branching determination

Glycogen branching degree was determined using Krisman protocol (Krisman CM, 1962). Samples from skeletal muscle were homogenized in KOH 30% and boiled at 100ºC for 15 minutes. Purified glycogen was obtained by three

precipitation in 66% (v/v) ethanol and it was resuspended in a solution of $NH_4Cl$ (sat): $H_2O$ (1:2). The solution was added to the iodine-iodide solution containing 1.5 M KI and 100 mM $I_2$ ($I_2/I^-$). Absorbance spectrum was recorded from 400 to 700 nm.

## Glycogen phosphate

Tissues were boiled in 30% KOH for an hour, followed by 3 ethanol precipitations. A solution of MeOH:$CHCl_3$ (4:1) was added to dried pellet from speed vac and samples were placed at 80ºC for 5 minutes, cooled in ice and centrifuged to remove supernatant with fat. This step was repeated for the high amount of fat in the tissue. After another EtOH precipitation the samples were treated with 50% (w/v) Trichloroacetic acid (TCA) followed by centrifugation. The supernatant was collected and precipitated with EtOH and centrifuged again to obtain the pelletable fraction. Purified glycogen obtained at this step was subjected to dialysis and to another precipitation. Pellet was resuspended in MQ water and hydrolyzed in 3:1 60% $HClO_4$:10N $H_2SO_4$ before adding the Malachite Gold + the reaction accelerator PiColorLock Gold (Innova Bioscience). Assay was done in a 96 well plate and absorbance was read at 650nm after 30minutes. The assay was performed by Dr. Anna DePaoli-Roach at the University of Indiana.

## Mass spectrometry analysis

### Liver glycogen purification

The protocol was adapted from Je-Hoon Ryu (Ryu et al. 2009). Tissue was homogenized into 5 volumes of glycogen isolation buffer at 4ºC with bigger polytron: 50 mM Tris pH 8, 150 mM NaCl, 2 mM EDTA, 50 mM sodium fluoride, mini-complete protease inhibitors (Roche Applied Science). To remove cell

debris and nuclei we performed a low g-force spin at 6000 × g for 10 min at 4 °C. The resultant supernatant was placed to a ultracentrifuge 100,000 × g for 30 min Optimax TX – rotor TLA 55). The pellet obtained contains glycogen and microsomal membranes to be removed. Pellet was resuspended into 1.5ml of glycogen isolation buffer and loaded on sucrose gradient 25, 50% (w/v) in the same buffer. Centrifugation at 300,000 × g for 1h allowed to separate the microsomal/membrane layer from the glycogen that precipitated at the bottom **(Figure 83)**.

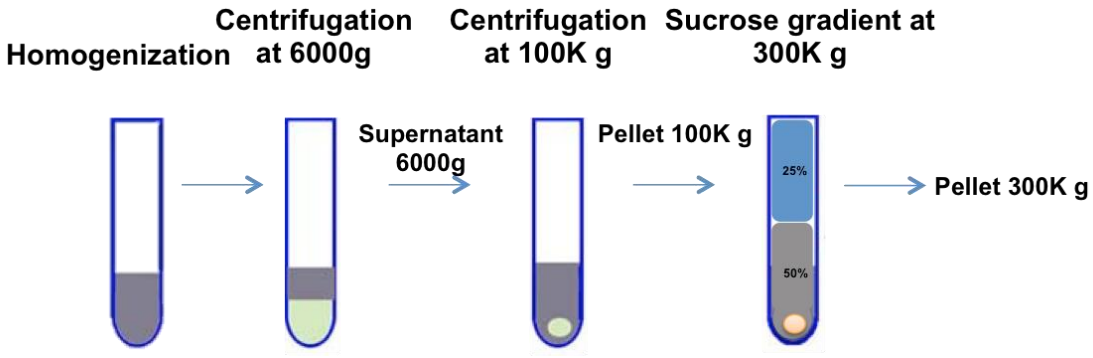


**Figure 83. Steps of liver glycogen purification-** Schematic representation of the protocol and percentage of glycogen measurement from each step of the protocol.

## Muscle glycogen purification with KOH

Frozen skeletal muscle was rapidly homogenized in KOH 30% at 4ºC for 18 seconds at increasing speed of the polytron. Samples were boiled for 3 minutes at 100ºC and quickly cooled down in ice. Temperature and time can greatly affect the integrity of the sample. Glycogen was precipitated with EtOH for 5 times, centrifuged and resuspended in water. Sample were extracted with acetonitrile: 1% formic acid (1:1) and sonicated for 5 minutes, centrifuged and the supernatant was removed. These steps were repeated 3 times. Sample resuspended in water was used for glycogen measurement and mass spectrometry applications.

## Mass spectrometry

Starting from glycogen pellet obtained directly from the sucrose gradient in liver and from KOH treatment in muscle, we resuspended it in RNAse free $H_2O$, and treated it with trypsin (2% w/w) to digest protein peptides and we loaded it onto FASP filters to have a protein-enriched sample. The eluted fraction from FASP filters corresponds to those protein peptides not covalently bound to glycogen. The filter retained glycogen and the region of glycogenin or any other unknown protein that may covalently bound to the polysaccharide **(Figure 84)**. Then glycogen was digested in the filter: by amyloglucosidase for 96 hours at 37ºC (In liver and muscle) or by amylase for 72 hours at 37ºC (in muscle) **(Figure 85)**. Amylase and amyloglucosidase were retained in the filter, together with non-hydrolyzed glycogen (if some was left). In the eluted fraction we found low molecular weight elements, as digested peptides of glycogenin and other peptides from other proteins that were analyzed by LC-MS/MS (performed by Mass Spectrometry core facility at IRB Barcelona), as follows:

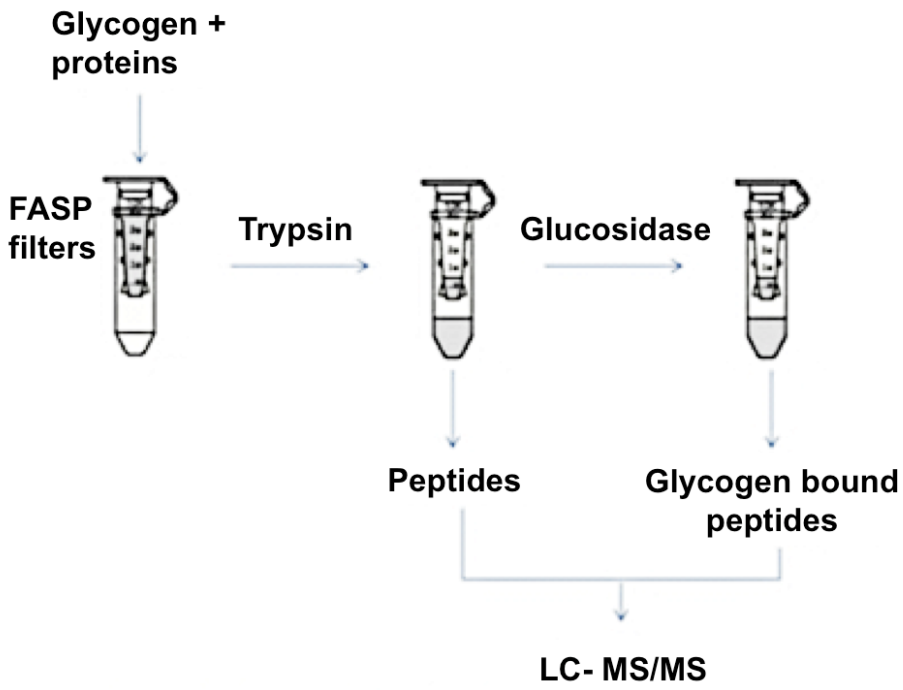


**Figure 84 Experimental workflow scheme-** Protocol steps of mass spectrometry sample preparation. (Font. Mass Spectrometry core facility IRB Barcelona)

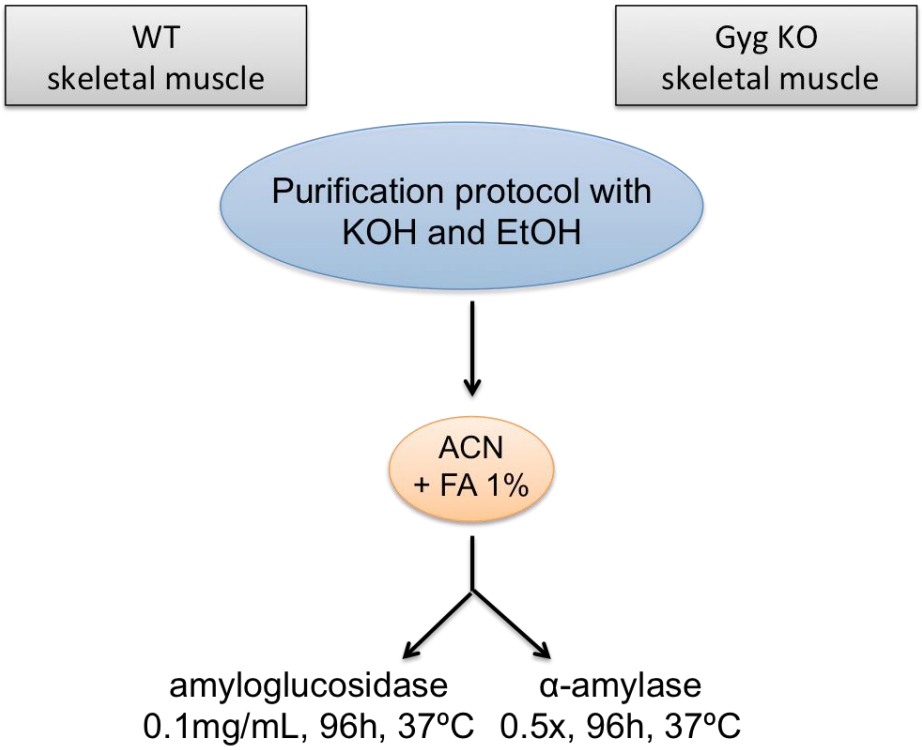


**Figure 85. Protocol illustration of the purification of glycogen after KOH 30% treatment**

Comparisons performed:

- WT vs. Gyg KO for the identification of substitute protein
- Purified sample treated either with amyloglucosidase (Aspergillus Niger) or α-amylase (Homo Sapiens), for reproducibility of the results.

In all sample we looked for dynamic modifications:

- Methionine oxidation
- 1 to 3 hexoses in tyrosine (WT samples)
- 1 to 3 hexoses in serine, threonine and tyrosine (KO samples).

The volumes of the samples were reduced to approximately 15 µL in a vacuum centrifuge and were cleaned with PolyLC C18 pipette tips (see attached protocol MS23a). The nano-LC-MS/MS was set up as follows. Digested peptides were diluted in 1% FA. Samples were loaded to a 180 µm × 2 cm C18 Symmetry trap column (Waters) at a flow rate of 15 µL/min using a nanoAcquity Ultra Performance LCTM chromatographic system (Waters Corp., Milford, MA). Peptides were separated using a C18 analytical column (BEH130TM C18 75

μm × 25 cm, 1.7 μm, Waters Corp.) with a 130 min run, comprising three consecutive steps with linear gradients from 1 to 35% B in 90 min, from 35 to 50% B in 15 min, and from 50 % to 85 % B in 2 min, followed by isocratic elution at 85 % B in 10 min and stabilization to initial conditions (A= 0.1% FA in water, B= 0.1% FA in CH3CN). The column outlet was directly connected to an Advion TriVersa NanoMate (Advion) fitted on an LTQ-FT Ultra mass spectrometer (Thermo). The mass spectrometer was operated in a data-dependent acquisition (DDA) mode using an inclusion list with tryptic peptides containing tyrosine 195 and the same peptides modified with 1 to 3 hexoses. When the inclusion list ions were not found the most intense ions were fragmented. Survey MS scans were acquired in the FT with the resolution (defined at 400 m/z) set to 100,000. Up to six of the most intense ions per scan were fragmented and detected in the linear ion trap. The ion count target value was 1,000,000 for the survey scan and 50,000 for the MS/MS scan. Target ions already selected for MS/MS were dynamically excluded for 30 s. Spray voltage in the NanoMate source was set to 1.70 kV. Capillary voltage and tube lens on the LTQ-FT were tuned to 40 V and 120 V. Minimal signal required to trigger MS to MS/MS switch was set to 1000 and activation Q was 0.250. The spectrometer was working in positive polarity mode and singly charge state precursors were rejected for fragmentation. A database search was performed with Proteome Discoverer software v1.4 (Thermo Scientific) using Sequest HT search engine and SwissProt database [Mus musculus, amyloglucosidase from Aspergillus niger and amylase, release 2014_07 the common Repository of Adventitious Proteins (cRAP database)]. Searches were run against targeted and decoy databases. Search parameters included no-enzyme specificity and methionine oxidation, 1 to 3 hexoses in tyrosine in WT samples or 1 to 3 hexoses in serine, threonine and tyrosine in KO samples as dynamic modifications. Peptide mass tolerance was 10 ppm and the MS/MS tolerance was 0.6 Da. Peptides with a FDR < 1% were considered as positive identifications with a high confidence level. Peptides from glycogenin and peptides, which contain glucose residues, were manually validated.

### Hepatocytes isolation and cell culture

Collagenase perfusion was used to isolate hepatocytes from male mice, as described previously (Massague, 1977). Cells were suspended in Dulbecco's modified Eagle's medium (DMEM), supplemented with 10 mM glucose, 10% (v/v) fetal bovine serum (FBS), and then seeded onto plastic plates of 60-mm diameter treated with 0.001% (w/v) collagen solution (Sigma) at a final density of $8*10^4$ cells/$cm^2$. Media were replaced with fresh DMEM containing 25 mM glucose and 1% (v/v) FBS. Media were then replaced by DMEM without glucose or FBS, and another incubation of 12–14 h was carried out. Cells were then incubated in DMEM in the absence or presence of 25 mM glucose, At the end of each manipulation, cell monolayers were flash-frozen in liquid $N_2$ and stored at -80 °C until analysis.

### Metabolites determination

Blood glucose levels were measured using a glucometer (Ascensia Breeze 2, Bayer Healthcare).

Hepatic triglycerides samples were prepared in 3 mol/l KOH, 65% ethanol extracts, based on the method described by Salmon and Flatt for liver saponification (Salmon and Flatt 1985), were quantified using a TAG kit (Sigma). In intramuscular and plasma lactate (HORIBA ABX), was measured spectrophotometrically by standard techniques adapted to a COBAS Mira analyzer.

The intracellular concentrations of ATP and other nucleotides were measured from perchloric acid extracts of skeletal muscle tissue. They were quantified after HPLC in column Brisa LC2 C18 (Teknokroma) by the CCiT (Centros Científicos y Tecnológicos at the University of Barcelona).

### Glucose, insulin and glucagon tolerance tests

For glucose tolerance tests, overnight fasted (16 h) mice were injected intraperitoneally with glucose (2 g/kg). Whole blood was drawn from tail tip for

glucose measurements. For insulin and glucagon tolerance tests, mice fasted for 6 h were injected intraperitoneally respectively with glucagon (100 ug/kg) and insulin (0.75 U/kg), and glycemia was measured from tail blood taken at the indicated times after injection.

## Functional performance in mice

### Grip strength test

Grip Bioseb is used to measure the neuromuscular function as maximal muscle strength of forelimbs. Mice hold by the tail grab with the upper limbs on a grid that is connected to a sensor. Ten trials are carried out in succession measuring forelimb-strength.

### Rotarod

Rotarod test was performed in mice to test motor coordination (Deacon 2013). Animals are placed on a horizontal rod that rotates about its long axis. To perform the exercise, mice need strength, in particular in the forelimbs in order to grab the bar. A training period of 5 days was provided to the animals, consisting in walking on the rotarod at 4rpm and accelerating progressively to 40 rpm, twice a day. The day of the experiment, the rotarod was set at 4rmp for 5 minutes and then with acceleration rate of 20rpm/min. The experiment was repeated four times the same day and only the three best performances were considered for the calculations of duration and speed.

### Treadmill exercise

The protocol is adapted from Handschin (Handschin, Chin et al. 2007) Briefly, for 10 days, animals were acclimatized to treadmill running (Columbus Instruments) for 5 min at a speed of 10 m/min and on a 0% grade. On the day of the experiment, animals ran on a treadmill tilted 10% uphill starting at a speed of 10 m/min for 5 min. Every subsequent 2 min, the speed was increased by 2 m/min until mice were exhausted or a maximal speed of 46 m/min was

reached. On the experimental day animals run on the treadmill with a shock grid at the posterior extremity to avoid mice spontaneous stopping. Exhaustion was defined as the inability of the animal to remain on the treadmill. Time of exhaustion was recorded and mice were removed from the treadmill after the following observations:

- Greater than 5 consecutive seconds on the shock grid without attempting to reengage the treadmill
- Spending greater than 50% of the time on the shock grid
- The third time a mouse is willing to sustain two seconds or more of shocking rather than return to the treadmill

Running time was measured and running distance, work, and power calculated. Distance is a function of time and speed of the treadmill. Work is calculated as the product of bodyweight (kg), gravity (9.81 $m/s^2$), vertical speed (m/s * angle), and time (s). Power is the product of bodyweight (kg), gravity (9.81 $m/s^2$), and vertical speed (m/s * angle). On the day of the experiment blood from tail tip was taken for glucose and lactate measurements before and after the exercise. Treadmill exercise was also performed after O/N fasting.

**Indirect calorimetry, food intake, and body temperature**

Indirect calorimetry was performed using an 8-chamber Oxymax system (Columbus Instruments) to measure heat production, calculated from oxygen consumption and $CO_2$ production. Mice were allowed to acclimate to the cages for two days before one or two cycles of 24h measurements. Energy expenditure was calculated as $EE = (3.185 + 1.232 \times RER) \times V_{O2}$ and respiratory exchange ratio (RER) as $RER = VCO_2/VO_2$. Glucose oxidation (in $g/min/kg^{0.75} = [(4.545 \times VCO_2) - (3.205 \times VO_2)]/1000$), and lipid oxidation (in $g/min/kg^{0.75} = [1.672 \times (VO_2 - VCO_2)]/1000$) were calculated (Chen and Heiman 2001). Ambulatory and total locomotor activity was monitored by an infrared photocell beam interruption method. Body temperature was determined using an animal rectal probe thermometer (Cibertec). In order to monitor food intake mice were housed individually and acclimatized for one week prior to study. Food intake was measured daily for five consecutive days.

**Myo-mechanical analysis of isolated skeletal muscle**

To assess the in vivo force generation and fatigability in treated muscle we evaluated myo-mechanical properties in freshly explanted hindlimb muscle from the mouse, based on protocol from Oishi (Oishi, Cholsiripunlert et al. 2011). Briefly, muscles were removed and transferred to. After removal and during the duration of the experiment, muscles were maintained in Krebs Henseleit solution at 25ºC with $O_2/CO_2$ (95%/5%). Muscles were mounted in a muscle strip myograph (Aurora myograph strip model 1200A), and the measurement of maximal twitch (force-frequency) normalized to muscle weight. We performed the experiments using both soleus and EDL from each individual. Allow muscle to rest for 3 minutes. Force-frequency: apply trains of supramaximal stimuli at 5,10, 20, 40, 60, 80, 100, 150, and 200 Hz with 1 minute rest between each stimulus. We plotted force-frequency relationship (% maximal force vs. stimulation frequency) (protocol by Dr. Muñoz-Canoves laboratory, UPF Barcelona).

**High-resolution respirometry**

The respiration of permeabilized muscle fibers were measured at 37 °C by high-resolution respirometry with the Oxygraph-2k (Oroboros Instruments) as described (Verhoeven, Claeys et al. 2006). Soleus and EDL muscles was removed and placed on a plastic Petri dish containing 1 mL of ice-cold isolation solution [10 mM Ca-EGTA buffer (2.77 mM $CaK_2EGTA$ + 7.23 mM K2EGTA), 20 mM imidazole, 20 mM taurine, 50 mM K-Mes, 3 mM $K_2HPO_4$, 6.5 mM $MgCl_2$, 5.7 mM ATP, 15 mM phosphocreatine, and 0.5 mM DTT (pH 7.1)]. Individual fiber bundles were separated with two pairs of sharp forceps and then permeabilized for 30 min in 2 mL of ice-cold isolation solution containing 50 µg/ mL saponin. After rinsing muscle bundles in respiration medium [0.5 mM EGTA, 3 mM $MgCl_2 \cdot 6H_2O$, 20 mM taurine, 10 mM $KH_2PO_4$, 20 mM Hepes, 1 g/L BSA, 60 mM K-lactobionate, and 110 mM sucrose (pH 7.1)], we weighed and transferred them (typically 2–4 mg wet weight) into the Oxygraph chamber containing 2 mL of air-saturated respiration medium. For permeabilized muscle fibers and liver isolated mitochondria, all respiration measurements were made

in triplicate and followed this protocol: resting respiration (state 2, absence of adenylates) was assessed by the addition of 10 mM glutamate and 2 mM malate as the complex I substrate supply and then state 3 respiration was assessed by the addition of 2.5 mM ADP. The integrity of the outer mitochondrial membrane was established by the addition of 10 µM cytochrome c. The addition of 10 mM succinate provided state 3 respirations with parallel electron input to complexes I and II. We examined ADP control of coupled respiration and uncoupling control through the addition of the protonophore carbonylcyanide-4-(trifluoromethoxy)-phenylhydrazone (FCCP) (optimum concentration for maximal flux). The addition of 0.5 µM rotenone resulted in inhibition of complex I, thereby allowing examination of O2 flux with complex II substrate alone, whereas 2.5 µM antimycin A was added to inhibit complex III to observe non-mitochondrial respiration (protocol by Dr. Zorzano laboratory, IRB Barcelona).

## Statistical analysis

Results are presented as mean ± s.e.m. of independent experiments. Unless otherwise stated, significance between two variables was analyzed by the Student's t test using the GraphPad Prism software (La Jolla, CA, USA). p-value <0.05 was considered to be statistically significant. * p-values <0.05, ** p-values 0.01, and *** p-value <0.001.

### General analysis and bloxplot / changepoint plots (treadmill data)

All analysis were performed in R (base/stats packages) using the Wilcoxon/ Mann Whitney U-test (non-paralog analog for two-sample t-test), to compare variables of interest between WT and Gyg KO; except otherwise indicated. For statistical significance symbols, * indicates $p < 0.05$; + indicates $p < 0.10$. In boxplots, top and bottom of the box indicate the 25th and 75th percentiles of the data, respectively, with the centerline indicating the median. Whisker coefficient is set to top/bottom quartiles +/- 1.5 IQR. Observations outside this

range (if any) are indicated as individual dots. In changepoint plots, smoothed splines for means by group were computed in R and shown by interval. Vertical whiskers indicate standard error of the mean. Dashed vertical lines indicate significant changepoint in mean slope values as detected by the *cpt.mean* function from the changepoint package v1.0.5, using the default parameters.

## General analysis and survival/density plots, rotarod data

For the rotarod analysis, survival and kernel density plots were produced in R with the survival v2.37.2 and base/stats packages. The log-rank test was used to assess statistical significance of the differences between both genotypes ($p>0.10$). In kernel density plots, round and square dots along the x-axis indicate respectively group mean and medians.

Statistical analyses of treadmill and rotarod experiments were performed by the Biostatistics and bioinformatics core facility at IRB Barcelona.

# References

Acin-Perez, R., P. Fernandez-Silva, M. L. Peleato, A. Perez-Martos, and J. A. Enriquez. 2008. 'Respiratory active mitochondrial supercomplexes', *Mol Cell*, 32: 529-39.

Alonso, M. D., J. Lomako, W. M. Lomako, and W. J. Whelan. 1995. 'A new look at the biogenesis of glycogen', *FASEB J*, 9: 1126-37.

Alonso, M. D., J. Lomako, W. M. Lomako, W. J. Whelan, and J. Preiss. 1994. 'Properties of carbohydrate-free recombinant glycogenin expressed in an Escherichia coli mutant lacking UDP-glucose pyrophosphorylase activity', *FEBS Lett*, 352: 222-6.

Arany, Z., N. Lebrasseur, C. Morris, E. Smith, W. Yang, Y. Ma, S. Chin, and B. M. Spiegelman. 2007. 'The transcriptional coactivator PGC-1beta drives the formation of oxidative type IIX fibers in skeletal muscle', *Cell Metab*, 5: 35-46.

Arbuckle, M. I., A. M. Brant, I. W. Campbell, T. J. Jess, S. Kane, C. Livingstone, S. Martin, N. W. Merrall, L. Porter, R. Reid, and et al. 1994. 'Mammalian glucose transporters: intracellular signalling and transporter translocation', *Biochem Soc Trans*, 22: 664-7.

Baqué, Susanna, Joan J. Guinovart, and Juan C. Ferrer. 1997. 'Glycogenin, the primer of glycogen synthesis, binds to actin', *FEBS Letters*, 417: 355-59.

Bell, G. I., C. F. Burant, J. Takeda, and G. W. Gould. 1993. 'Structure and function of mammalian facilitative sugar transporters', *J Biol Chem*, 268: 19161-4.

Bengtsson, A., K. G. Henriksson, and J. Larsson. 1986. 'Reduced high-energy phosphate levels in the painful muscles of patients with primary fibromyalgia', *Arthritis Rheum*, 29: 817-21.

Bergstrom, J., L. Hermansen, E. Hultman, and B. Saltin. 1967. 'Diet, muscle glycogen and physical performance', *Acta Physiol Scand*, 71: 140-50.

Bradford, M. M. 1976. 'A rapid and sensitive method for the quantitation of microgram quantities of protein utilizing the principle of protein-dye binding', *Anal Biochem*, 72: 248-54.

Cameron, J. M., V. Levandovskiy, N. MacKay, R. Utgikar, C. Ackerley, D. Chiasson, W. Halliday, J. Raiman, and B. H. Robinson. 2009. 'Identification of a novel mutation in GYS1 (muscle-specific glycogen synthase) resulting in sudden cardiac death, that is diagnosable from skin fibroblasts', *Mol Genet Metab*, 98: 378-82.

Carling, D., and D. G. Hardie. 1989. 'The substrate and sequence specificity of the AMP-activated protein kinase. Phosphorylation of glycogen synthase and phosphorylase kinase', *Biochim Biophys Acta*, 1012: 81-6.

Chan, T. M., and J. H. Exton. 1976. 'A rapid method for the determination of glycogen content and radioactivity in small quantities of tissue or isolated hepatocytes', *Anal Biochem*, 71: 96-105.

Chen, Y., and M. L. Heiman. 2001. 'Increased weight gain after ovariectomy is not a consequence of leptin resistance', *Am J Physiol Endocrinol Metab*, 280: E315-22.

Chin, E. R., and D. G. Allen. 1997. 'Effects of reduced muscle glycogen concentration on force, Ca2+ release and contractile protein function in intact mouse skeletal muscle', *J Physiol*, 498 ( Pt 1): 17-29.

Chomyn, A., and G. Attardi. 2003. 'MtDNA mutations in aging and apoptosis', *Biochem Biophys Res Commun*, 304: 519-29.

Colombo, I., S. Pagliarani, S. Testolin, C. M. Cinnante, G. Fagiolari, P. Ciscato, A. Bordoni, F. Fortunato, F. Magri, S. C. Previtali, D. Velardo, M. Sciacco, G. P.

Comi, and M. Moggio. 2015. 'Longitudinal follow-up and muscle MRI pattern of two siblings with polyglucosan body myopathy due to glycogenin-1 mutation', *J Neurol Neurosurg Psychiatry*.

Cori, C. F., G. Schmidt, and G. T. Cori. 1939. 'The Synthesis of a Polysaccharide from Glucose-1-Phosphate in Muscle Extract', *Science*, 89: 464-5.

Cusso, R., L. R. Lerner, J. Cadefau, M. Gil, C. Prats, M. Gasparotto, and C. R. Krisman. 2003. 'Differences between glycogen biogenesis in fast- and slow-twitch rabbit muscle', *Biochim Biophys Acta*, 1620: 65-71.

Deacon, R. M. 2013. 'Measuring motor coordination in mice', *J Vis Exp*: e2609.

DePaoli-Roach, A. A., Z. Ahmad, M. Camici, J. C. Lawrence, Jr., and P. J. Roach. 1983. 'Multiple phosphorylation of rabbit skeletal muscle glycogen synthase. Evidence for interactions among phosphorylation sites and the resolution of electrophoretically distinct forms of the subunit', *J Biol Chem*, 258: 10702-9.

Drochmans, P. 1962. '[Morphology of glycogen. Electron microscopic study of the negative stains of particulate glycogen]', *J Ultrastruct Res*, 6: 141-63.

Etgen, G. J., Jr., C. M. Wilson, J. Jensen, S. W. Cushman, and J. L. Ivy. 1996. 'Glucose transport and cell surface GLUT-4 protein in skeletal muscle of the obese Zucker rat', *Am J Physiol*, 271: E294-301.

Fiol, C. J., A. M. Mahrenholz, Y. Wang, R. W. Roeske, and P. J. Roach. 1987. 'Formation of protein kinase recognition sites by covalent modification of the substrate. Molecular mechanism for the synergistic action of casein kinase II and glycogen synthase kinase 3', *J Biol Chem*, 262: 14042-8.

Flotow, H., and P. J. Roach. 1989. 'Synergistic phosphorylation of rabbit muscle glycogen synthase by cyclic AMP-dependent protein kinase and casein kinase I. Implications for hormonal regulation of glycogen synthase', *J Biol Chem*, 264: 9126-8.

Fontana, J. D. 1980. 'The presence of phosphate in glycogen', *FEBS Lett*, 109: 85-92.

Fox, J., L. D. Kennedy, J. S. Hawker, J. L. Ozbun, E. Greenberg, C. Lammel, and J. Preiss. 1973. 'De novo synthesis of bacterial glycogen and plant starch by ADPG: -glucan 4-glucosyl transferase', *Ann N Y Acad Sci*, 210: 90-103.

Freemont, P. S. 2000. 'RING for destruction?', *Curr Biol*, 10: R84-7.

Ganesh, S., K. L. Agarwala, K. Ueda, T. Akagi, K. Shoda, T. Usui, T. Hashikawa, H. Osada, A. V. Delgado-Escueta, and K. Yamakawa. 2000. 'Laforin, defective in the progressive myoclonus epilepsy of Lafora type, is a dual-specificity phosphatase associated with polyribosomes', *Hum Mol Genet*, 9: 2251-61.

Gibbons, B. J., P. J. Roach, and T. D. Hurley. 2002. 'Crystal structure of the autocatalytic initiator of glycogen biosynthesis, glycogenin', *J Mol Biol*, 319: 463-77.

Gould, G. W., and G. D. Holman. 1993. 'The glucose transporter family: structure, function and tissue-specific expression', *Biochem J*, 295 ( Pt 2): 329-41.

Gunja-Smith, Z., J. J. Marshall, C. Mercier, E. E. Smith, and W. J. Whelan. 1970. 'A revision of the Meyer-Bernfeld model of glycogen and amylopectin', *FEBS Lett*, 12: 101-04.

Handschin, C., S. Chin, P. Li, F. Liu, E. Maratos-Flier, N. K. Lebrasseur, Z. Yan, and B. M. Spiegelman. 2007. 'Skeletal muscle fiber-type switching, exercise intolerance, and myopathy in PGC-1alpha muscle-specific knock-out animals', *J Biol Chem*, 282: 30014-21.

Hansen, B. F., W. Derave, P. Jensen, and E. A. Richter. 2000. 'No limiting role for glycogenin in determining maximal attainable glycogen levels in rat skeletal muscle', *Am J Physiol Endocrinol Metab*, 278: E398-404.

Helander, I., H. Westerblad, and A. Katz. 2002. 'Effects of glucose on contractile function, [Ca2+]i, and glycogen in isolated mouse skeletal muscle', *Am J Physiol Cell Physiol*, 282: C1306-12.

Hermansen, L., E. Hultman, and B. Saltin. 1967. 'Muscle glycogen during prolonged severe exercise', *Acta Physiol Scand*, 71: 129-39.

Huang, K. P., and E. Cabib. 1972. 'Separation of the glucose-6-phosphate independent and dependent forms of glycogen synthetase from yeast', *Biochem Biophys Res Commun*, 49: 1610-6.

Jiang, S., B. Heller, V. S. Tagliabracci, L. Zhai, J. M. Irimia, A. A. DePaoli-Roach, C. D. Wells, A. V. Skurat, and P. J. Roach. 2010. 'Starch binding domain-containing protein 1/genethonin 1 is a novel participant in glycogen metabolism', *J Biol Chem*, 285: 34960-71.

Katzen, H. M., D. D. Soderman, and H. M. Nitowsky. 1965. 'Kinetic and Electrophoretic Evidence for Multiple Forms of Glucose-Atp Phosphotransferase Activity from Human Cell Cultures and Rat Liver', *Biochem Biophys Res Commun*, 19: 377-82.

Kraniou, Y., D. Cameron-Smith, M. Misso, G. Collier, and M. Hargreaves. 2000. 'Effects of exercise on GLUT-4 and glycogenin gene expression in human skeletal muscle', *J Appl Physiol (1985)*, 88: 794-6.

Krisman, C. R., and R. Barengo. 1975. 'A precursor of glycogen biosynthesis: alpha-1,4-glucan-protein', *Eur J Biochem*, 52: 117-23.

Kujoth, G. C., A. Hiona, T. D. Pugh, S. Someya, K. Panzer, S. E. Wohlgemuth, T. Hofer, A. Y. Seo, R. Sullivan, W. A. Jobling, J. D. Morrow, H. Van Remmen, J. M. Sedivy, T. Yamasoba, M. Tanokura, R. Weindruch, C. Leeuwenburgh, and T. A. Prolla. 2005. 'Mitochondrial DNA mutations, oxidative stress, and apoptosis in mammalian aging', *Science*, 309: 481-4.

Kuma, Y., D. G. Campbell, and A. Cuenda. 2004. 'Identification of glycogen synthase as a new substrate for stress-activated protein kinase 2b/p38beta', *Biochem J*, 379: 133-9.

Legros, F., F. Malka, P. Frachon, A. Lombes, and M. Rojo. 2004. 'Organization and dynamics of human mitochondrial DNA', *J Cell Sci*, 117: 2653-62.

Lin, J., H. Wu, P. T. Tarr, C. Y. Zhang, Z. Wu, O. Boss, L. F. Michael, P. Puigserver, E. Isotani, E. N. Olson, B. B. Lowell, R. Bassel-Duby, and B. M. Spiegelman. 2002. 'Transcriptional co-activator PGC-1 alpha drives the formation of slow-twitch muscle fibres', *Nature*, 418: 797-801.

Lomako, J., W. M. Lomako, and W. J. Whelan. 1990. 'The biogenesis of muscle glycogen: regulation of the activity of the autocatalytic primer protein', *Biofactors*, 2: 251-4.

Lomako, J., W. M. Lomako, W. J. Whelan, and R. B. Marchase. 1993. 'Glycogen contains phosphodiester groups that can be introduced by UDPglucose: glycogen glucose 1-phosphotransferase', *FEBS Lett*, 329: 263-7.

Luo, S., W. Zhu, D. Yue, J. Lin, Y. Wang, Z. Zhu, W. Qiu, J. Lu, C. Hedberg-Oldfors, A. Oldfors, and C. Zhao. 2015. 'Muscle pathology and whole-body MRI in a polyglucosan myopathy associated with a novel glycogenin-1 mutation', *Neuromuscul Disord*, 25: 780-5.

Maier, A., and D. Pette. 1987. 'The time course of glycogen depletion in single fibers of chronically stimulated rabbit fast-twitch muscle', *Pflugers Arch*, 408: 338-42.

Malfatti, E., J. Nilsson, C. Hedberg-Oldfors, A. Hernandez-Lain, F. Michel, C. Dominguez-Gonzalez, G. Viennet, H. O. Akman, C. Kornblum, P. Van den Bergh, N. B. Romero, A. G. Engel, S. DiMauro, and A. Oldfors. 2014. 'A new muscle glycogen storage disease associated with glycogenin-1 deficiency', *Ann Neurol*, 76: 891-8.

Melendez, R., E. Melendez-Hevia, and E. I. Canela. 1999. 'The fractal structure of glycogen: A clever solution to optimize cell metabolism', *Biophys J*, 77: 1327-32.

Meyer, F., L. M. Heilmeyer, Jr., R. H. Haschke, and E. H. Fischer. 1970. 'Control of phosphorylase activity in a muscle glycogen particle. I. Isolation and characterization of the protein-glycogen complex', *J Biol Chem*, 245: 6642-8.

Moslemi, A. R., C. Lindberg, J. Nilsson, H. Tajsharghi, B. Andersson, and A. Oldfors. 2010. 'Glycogenin-1 deficiency and inactivated priming of glycogen synthesis', *N Engl J Med*, 362: 1203-10.

Mu, J., A. V. Skurat, and P. J. Roach. 1997. 'Glycogenin-2, a novel self-glucosylating protein involved in liver glycogen biosynthesis', *J Biol Chem*, 272: 27589-97.

Murphy, R. M., H. Xu, H. Latchman, N. T. Larkins, P. R. Gooley, and D. I. Stapleton. 2012. 'Single fiber analyses of glycogen-related proteins reveal their differential association with glycogen in rat skeletal muscle', *Am J Physiol Cell Physiol*, 303: C1146-55.

Nielsen, J. N., and E. A. Richter. 2003. 'Regulation of glycogen synthase in skeletal muscle during exercise', *Acta Physiol Scand*, 178: 309-19.

Nielsen, J. N., and J. F. Wojtaszewski. 2004. 'Regulation of glycogen synthase activity and phosphorylation by exercise', *Proc Nutr Soc*, 63: 233-7.

Oishi, P. E., S. Cholsiripunlert, W. Gong, A. J. Baker, and H. S. Bernstein. 2011. 'Myo-mechanical analysis of isolated skeletal muscle', *J Vis Exp*.

Pederson, B. A., H. Chen, J. M. Schroeder, W. Shou, A. A. DePaoli-Roach, and P. J. Roach. 2004. 'Abnormal cardiac development in the absence of heart glycogen', *Mol Cell Biol*, 24: 7179-87.

Pederson, B. A., C. R. Cope, J. M. Schroeder, M. W. Smith, J. M. Irimia, B. L. Thurberg, A. A. DePaoli-Roach, and P. J. Roach. 2005. 'Exercise capacity of mice genetically lacking muscle glycogen synthase: in mice, muscle glycogen is not essential for exercise', *J Biol Chem*, 280: 17260-5.

Pederson, B. A., A. G. Csitkovits, R. Simon, J. M. Schroeder, W. Wang, A. V. Skurat, and P. J. Roach. 2003. 'Overexpression of glycogen synthase in mouse muscle results in less branched glycogen', *Biochem Biophys Res Commun*, 305: 826-30.

Pette, D. 1997. 'Functional and biochemical adaptations to low-frequency stimulation: possible applications to microgravity', *Int J Sports Med*, 18 Suppl 4: S302-4.

Pette, D. 1998. 'Training effects on the contractile apparatus', *Acta Physiol Scand*, 162: 367-76.

Picton, C., J. Woodgett, B. Hemmings, and P. Cohen. 1982. 'Multisite phosphorylation of glycogen synthase from rabbit skeletal muscle. Phosphorylation of site 5 by glycogen synthase kinase-5 (casein kinase-II) is a prerequisite for phosphorylation of sites 3 by glycogen synthase kinase-3', *FEBS Lett*, 150: 191-6.

Pitcher, J., C. Smythe, D. G. Campbell, and P. Cohen. 1987. 'Identification of the 38-kDa subunit of rabbit skeletal muscle glycogen synthase as glycogenin', *Eur J Biochem*, 169: 497-502.

Preiss, J., J. L. Ozbun, J. S. Hawker, E. Greenberg, and C. Lammel. 1973. 'ADPG synthetase and ADPG- -glucan 4-glucosyl transferase: enzymes involved in bacterial glycogen and plant starch synthesis', *Ann N Y Acad Sci*, 210: 265-78.

Roach, P. J. 2002. 'Glycogen and its metabolism', *Curr Mol Med*, 2: 101-20.

Roach, P. J., A. A. DePaoli-Roach, and J. Larner. 1978. 'Ca2+-stimulated phosphorylation of muscle glycogen synthase by phosphorylase b kinase', *J Cyclic Nucleotide Res*, 4: 245-57.

Roach, P. J., M. Rosell-Perez, and J. Larner. 1977. 'Muscle glycogen synthase in vivo state: Effects of insulin administration on the chemical and kinetic properties of the purified enzyme', *FEBS Lett*, 80: 95-8.

Rutter, G. A., and R. Rizzuto. 2000. 'Regulation of mitochondrial metabolism by ER Ca2+ release: an intimate connection', *Trends Biochem Sci*, 25: 215-21.

Ryu, J. H., J. Drain, J. H. Kim, S. McGee, A. Gray-Weale, L. Waddington, G. J. Parker, M. Hargreaves, S. H. Yoo, and D. Stapleton. 2009. 'Comparative structural analyses of purified glycogen particles from rat liver, human skeletal muscle and commercial preparations', *Int J Biol Macromol*, 45: 478-82.

Salmon, D. M., and J. P. Flatt. 1985. 'Effect of dietary fat content on the incidence of obesity among ad libitum fed mice', *Int J Obes*, 9: 443-9.

Salsas, E., and J. Larner. 1975. 'Action pattern of muscle glycogen synthase', *Mol Cell Biochem*, 7: 195-9.

Satoh, K. 1980b. 'Glycogen-binding protein components of rat tissues', *Biochem Biophys Res Commun*, 96: 28-33.

Schiaffino, S., and C. Reggiani. 2011. 'Fiber types in mammalian skeletal muscles', *Physiol Rev*, 91: 1447-531.

Simoneau, J. A., and C. Bouchard. 1995. 'Genetic determinism of fiber type proportion in human skeletal muscle', *FASEB J*, 9: 1091-5.

Simoneau, J. A., G. Lortie, M. R. Boulay, M. Marcotte, M. C. Thibault, and C. Bouchard. 1985. 'Human skeletal muscle fiber type alteration with high-intensity intermittent training', *Eur J Appl Physiol Occup Physiol*, 54: 250-3.

Skurat, A. V., and A. D. Dietrich. 2004. 'Phosphorylation of Ser640 in muscle glycogen synthase by DYRK family protein kinases', *J Biol Chem*, 279: 2490-8.

Skurat, A. V., A. D. Dietrich, and P. J. Roach. 2000. 'Glycogen synthase sensitivity to insulin and glucose-6-phosphate is mediated by both NH2- and COOH-terminal phosphorylation sites', *Diabetes*, 49: 1096-100.

Skurat, A. V. 2006. 'Interaction between glycogenin and glycogen synthase', *Arch Biochem Biophys*, 456: 93-7.

Skurat, A. V., S. S. Lim, and P. J. Roach. 1997. 'Glycogen biogenesis in rat 1 fibroblasts expressing rabbit muscle glycogenin', *Eur J Biochem*, 245: 147-55.

Smythe, C., and P. Cohen. 1991. 'The discovery of glycogenin and the priming mechanism for glycogen biogenesis', *Eur J Biochem*, 200: 625-31.

Smythe, C., P. Watt, and P. Cohen. 1990. 'Further studies on the role of glycogenin in glycogen biosynthesis', *Eur J Biochem*, 189: 199-204.

Stapleton, D., C. Nelson, K. Parsawar, D. McClain, R. Gilbert-Wilson, E. Barker, B. Rudd, K. Brown, W. Hendrix, P. O'Donnell, and G. Parker. 2010. 'Analysis of hepatic glycogen-associated proteins', *Proteomics*, 10: 2320-9.

Sullivan, M. A., J. Li, C. Li, F. Vilaplana, D. Stapleton, A. A. Gray-Weale, S. Bowen, L. Zheng, and R. G. Gilbert. 2011. 'Molecular structural differences between type-2-diabetic and healthy glycogen', *Biomacromolecules*, 12: 1983-6.

Szydlowski, N., P. Ragel, S. Raynaud, M. M. Lucas, I. Roldan, M. Montero, F. J. Munoz, M. Ovecka, A. Bahaji, V. Planchot, J. Pozueta-Romero, C. D'Hulst, and A. Merida. 2009. 'Starch granule initiation in Arabidopsis requires the presence of either class IV or class III starch synthases', *Plant Cell*, 21: 2443-57.

Tagliabracci, V. S., J. M. Girard, D. Segvich, C. Meyer, J. Turnbull, X. Zhao, B. A. Minassian, A. A. Depaoli-Roach, and P. J. Roach. 2008. 'Abnormal metabolism of glycogen phosphate as a cause for Lafora disease', *J Biol Chem*, 283: 33816-25.

Tagliabracci, V. S., C. Heiss, C. Karthik, C. J. Contreras, J. Glushka, M. Ishihara, P. Azadi, T. D. Hurley, A. A. DePaoli-Roach, and P. J. Roach. 2011. 'Phosphate incorporation during glycogen synthesis and Lafora disease', *Cell Metab*, 13: 274-82.

Tagliabracci, V. S., J. Turnbull, W. Wang, J. M. Girard, X. Zhao, A. V. Skurat, A. V. Delgado-Escueta, B. A. Minassian, A. A. Depaoli-Roach, and P. J. Roach. 2007. 'Laforin is a glycogen phosphatase, deficiency of which leads to elevated phosphorylation of glycogen in vivo', *Proc Natl Acad Sci U S A*, 104: 19262-6.

Torija, M. J., M. Novo, A. Lemassu, W. Wilson, P. J. Roach, J. Francois, and J. L. Parrou. 2005. 'Glycogen synthesis in the absence of glycogenin in the yeast Saccharomyces cerevisiae', *FEBS Lett*, 579: 3999-4004.

Valles-Ortega, J., J. Duran, M. Garcia-Rocha, C. Bosch, I. Saez, L. Pujadas, A. Serafin, X. Canas, E. Soriano, J. M. Delgado-Garcia, A. Gruart, and J. J. Guinovart. 2011. 'Neurodegeneration and functional impairments associated

with glycogen synthase accumulation in a mouse model of Lafora disease', *EMBO Mol Med*, 3: 667-81.

Vardanis, A. 1990. 'Fractionation of particulate glycogen and bound enzymes using high-performance liquid chromatography', *Anal Biochem*, 187: 115-9.

Verhoeven, K., K. G. Claeys, S. Zuchner, J. M. Schroder, J. Weis, C. Ceuterick, A. Jordanova, E. Nelis, E. De Vriendt, M. Van Hul, P. Seeman, R. Mazanec, G. M. Saifi, K. Szigeti, P. Mancias, I. J. Butler, A. Kochanski, B. Ryniewicz, J. De Bleecker, P. Van den Bergh, C. Verellen, R. Van Coster, N. Goemans, M. Auer-Grumbach, W. Robberecht, V. Milic Rasic, Y. Nevo, I. Tournev, V. Guergueltcheva, F. Roelens, P. Vieregge, P. Vinci, M. T. Moreno, H. J. Christen, M. E. Shy, J. R. Lupski, J. M. Vance, P. De Jonghe, and V. Timmerman. 2006. 'MFN2 mutation distribution and genotype/phenotype correlation in Charcot-Marie-Tooth type 2', *Brain*, 129: 2093-102.

Vilchez, D., S. Ros, D. Cifuentes, L. Pujadas, J. Valles, B. Garcia-Fojeda, O. Criado-Garcia, E. Fernandez-Sanchez, I. Medrano-Fernandez, J. Dominguez, M. Garcia-Rocha, E. Soriano, S. Rodriguez de Cordoba, and J. J. Guinovart. 2007. 'Mechanism suppressing glycogen synthesis in neurons and its demise in progressive myoclonus epilepsy', *Nat Neurosci*, 10: 1407-13.

Wang, S. J., H. Li, B. E. Shan, Q. W. Cong, and L. N. Liu. 2002. '[Changes of glycogen or sacchariferous materials in esophageal epithelium tissue]', *Ai Zheng*, 21: 790-3.

Whelan, W. J. 1986. 'The initiation of glycogen synthesis', *Bioessays*, 5: 136-40.

Wilson, W. A., A. V. Skurat, B. Probst, A. de Paoli-Roach, P. J. Roach, and J. Rutter. 2005. 'Control of mammalian glycogen synthase by PAS kinase', *Proc Natl Acad Sci U S A*, 102: 16596-601.

Worby, C. A., M. S. Gentry, and J. E. Dixon. 2006. 'Laforin, a dual specificity phosphatase that dephosphorylates complex carbohydrates', *J Biol Chem*, 281: 30412-8.

Zeqiraj, E., X. Tang, R. W. Hunter, M. Garcia-Rocha, A. Judd, M. Deak, A. von Wilamowitz-Moellendorff, I. Kurinov, J. J. Guinovart, M. Tyers, K. Sakamoto, and F. Sicheri. 2014. 'Structural basis for the recruitment of glycogen synthase by glycogenin', *Proc Natl Acad Sci U S A*, 111: E2831-40.